PACIFIC EARTHQUAKE ENGINEERING
RESEARCH CENTER

Seismic Performance of Pile-Wharf Connections

Charles W. Roeder
Robert Graff
Jennifer L. Soderstrom
Jung Han Yoo
University of Washington

PEER 2002/07
DECEMBER 2001

Seismic Performance of Pile-Wharf Connections

Charles W. Roeder
Professor
Department of Civil and Environmental Engineering
University of Washington

Robert Graff
Graduate Student Researcher

Jennifer L. Soderstrom
Graduate Student Researcher

Jung Han Yoo
Graduate Student Researcher

PEER Report 2002/07
Pacific Earthquake Engineering Research Center
College of Engineering
University of California, Berkeley
December 2001

Abstract

Ports represent a large economic investment for society. When shipping is interrupted due to earthquake damage, the resulting unemployment and other social costs are significant. Wharfs are essential to shipping, and these structures are susceptible to earthquake damage. Because wharfs are supported on piles, the pile-wharf connection is an important part of the seismic resistance and structural integrity of the system. However, the seismic performance of pile-wharf connections is not well understood.

The seismic performance of pile-wharf connections is examined. The types of piles and pile connections used in past seismic design of wharf construction are reviewed. Past research related to these connections is noted. An experimental study of the seismic performance of moment-resisting connections used with prestressed concrete piles is described. Eight typical connections were tested, and the performance of these connections is evaluated. The test specimens included a range of typical connections and several recent connection innovations that were employed to reduce wharf construction costs. Both precast pile connections and connections with pile extensions are examined. The connections were tested under cyclic inelastic loading, and the effects of axial load are considered. The connections had relatively large inelastic rotational capacity but also had significant deterioration in resistance and stiffness. The consequences of this behavior are examined in typical wharf structures through inelastic analysis of the complete structural system.

Keywords: ductility, earthquakes, experiments, inelastic analysis, pile connections, precast concrete piles, ports

Acknowledgments

This work was supported in part by the Pacific Earthquake Engineering Research Center through the Earthquake Engineering Research Centers Program of the National Science Foundation under award number EEC-9701568.

Additional funding was provided by the University of Washington and the State of Washington. This financial support is gratefully acknowledged.

The authors also want to thank engineers from the ports of Los Angeles, Oakland, and Seattle for providing design drawings and other information regarding methods used for the seismic design and construction of past wharf structures at their facilities.

Contents

List of Figures

List of Tables

1 Introduction

1.1 PILE-WHARF CONNECTIONS

Ports represent a large economic investment for society, and the economic loss when shipping is discontinued can be huge. Port facilities are very susceptible to earthquake damage. It was estimated that direct damage to the Port of Kobe, Japan, during the 1995 earthquake exceeded U.S. $11 billion [EQE, 1995]. However, the actual financial loss greatly exceeded this amount through lost economic activity. By the year 2000, the Port of Kobe had recovered only about 80% of its 1994 container traffic volume [Landers, 2001], while surrounding ports in Japan and Asia increased their volume by 40% to 100%. This represents a large economic loss to the region. In view of the importance of port facilities, it is worthwhile to evaluate their seismic performance, but very little research has been devoted to this topic. The Pacific Earthquake Engineering Research (PEER) Center's second and third year research programs included several studies to evaluate the seismic performance of port facilities under a wide range of seismic occurrences. The behavior of the system was to be evaluated and improvements to its performance were to be developed where necessary. The seismic occurrences of interest to these studies include strong shaking due to ground motion, deformations due to liquefaction or lateral spread of the soil, movements or loads due to slope stability failures, or a combination of the foregoing.

Wharfs support very large gravity loads on both a short-term and long-term basis. Therefore, the seismic inertial forces on these structures can be quite large. The pile-wharf deck connection is important to this evaluation because the piles are the sole support for the large gravity loads, and they are needed to assure the lateral stability of the structural system. If the piles or connections are unable to sustain the seismic movements without losing their gravity-load resistance, the piers or wharfs may collapse or lose the ability to perform their service function.

A typical wharf section is illustrated in Figure 1.1. It comprises a soil or rock dike or embankment, a concrete deck, and prestressed concrete piles that support the deck loads and

resist lateral seismic forces. The vertical piles used in modern West Coast construction are usually 24 in. (610 mm) diameter octagonal precast prestressed piles made from 6000 psi (41.4 MPa) concrete. Many wharf decks are constructed of cast-in-place concrete, but some are a combination of cast-in-place concrete with precast concrete elements that support the concrete during construction. Before the deck is cast, the pile heads are cut approximately 2 in. (50 mm) above the surface of the deck or girder formwork. If a pile is driven below deck level, an extension must be added to the end of the pile. If the pile encounters its maximum driving resistance while the head of the pile is above this height, the top portion of the pile is cut off.

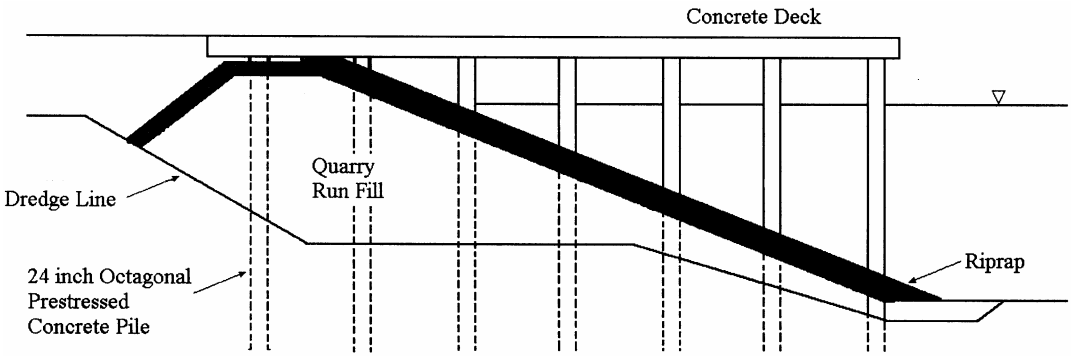

Fig. 1.1 Schematic of Typical Wharf Section with Prestressed Concrete Piles

The general design hypothesis for these wharf structures [Birdy, 1999] is that the pile and wharf deck be designed as a ductile frame with plastic hinges forming in the piles under seismic loading. Detailing of the pile-deck connection must then be sufficient to develop these pile forces and to assure adequate inelastic deformation during large earthquakes. It is also desirable that the connection remains undamaged (other than minor flexural cracking) under small or moderate seismic events because it is necessary that the port remain in service under these conditions. Further, the connections are difficult to inspect and repair, and so premature damage may go undetected. Common connection details used in California and Washington wharfs are described in Chapter 2.

Alternative structural configurations have been used for seismic resistant design of wharfs. Steel batter piles are sometimes used to provide lateral resistance as illustrated in Figure 1.2. The steel piles have been H-piles, tubes, and tubular steel piles filled with concrete. Vertical precast concrete piles are still used to support most of the gravity load as shown in the figure. Precast concrete batter piles were used in some older wharfs, but have not been used in

recent construction. Connection details for these steel batter piles are briefly discussed in Chapter 2, but none of these connections were evaluated in the experimental study described in this report. The use of batter piles in seismic regions has decreased because of perceived difficulty in achieving ductile behavior [Ports, 1992]. However, as will be noted in Chapter 2, there is disagreement among engineers who design these facilities, and some ports retain a strong preference for steel batter pile construction.

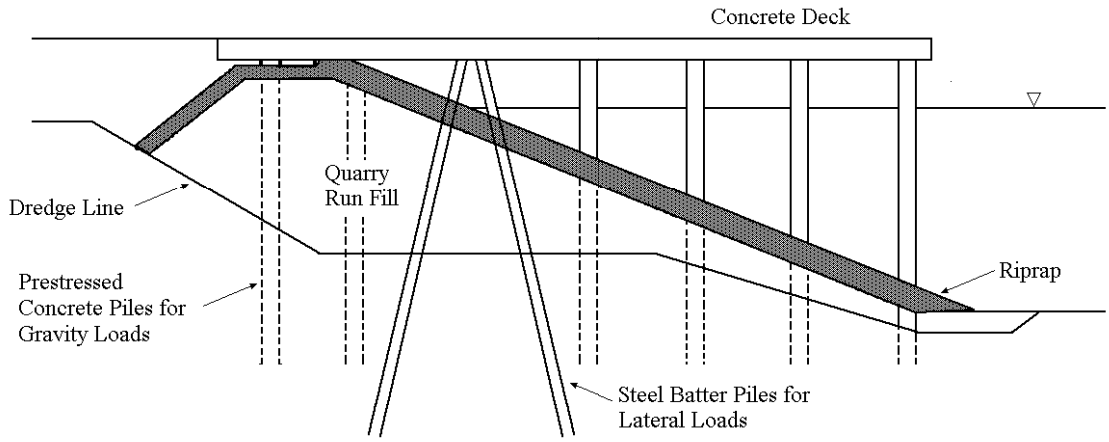

Fig. 1.2 Schematic of Typical Wharf Section with Steel Batter Piles

There is wide variation in the way wharfs are designed and constructed, but there is currently no national unified code for the analysis and design of these structures. Different aspects of design are addressed in the Uniform Building Code, ACI 318, Mil-Handbook 1025/1, and AASHTO Bridge Design Specifications.

1.2 PAST RESEARCH

The seismic performance of pile-wharf deck connections is an essential element in understanding the seismic performance of port facilities, but only a very few studies have investigated the seismic performance of pile connections. The behavior of several prestressed concrete pile connections was examined at the University of Washington [Pizzano, 1984]. In this study, 14 in. (350 mm) diameter octagonal pile sections were embedded 1.5 pile diameters into relatively small pile caps. Connection details included

- embedding the piles in the pile cap for up to 1.5 diameters,
- extending the prestressing strands 5 ft (1.52 m) beyond the end of the pile,
- grouting six #6 dowels 18 in. (450 mm) into ducts in the pile, and

- grouting six #8 dowels 24 in. (600 mm) into ducts in the pile.

One connection was loaded monotonically, and the rest were subjected to cyclic lateral loading until failure. Figure 1.3 shows the load-deflection history for the pile-cap specimen with six #6 grouted bars and with medium axial load. This specimen provided intermediate performance to the various connections tested. The specimen failed explosively at a location approximately one-half pile diameter from the pile-cap face after reaching a maximum curvature of approximately .0007 rad/in. and a maximum load of 40 kips (178 kN). This brittle failure occurred because the pile had relatively light spiral reinforcement. The maximum bending moment reached prior to failure was 1850 kip-in. (209 kN-m). The performance achieved by extended strand connections in this study was mixed. Some of these specimens provided the poorest performance noted in this research, while others were among the best. Pile pullout was not observed in the study, even in the pile cap where no connecting steel was used. These connection tests are of limited value in understanding the seismic performance of present day pile-wharf connections because pile and connection details are quite different than those used for seismic design today.

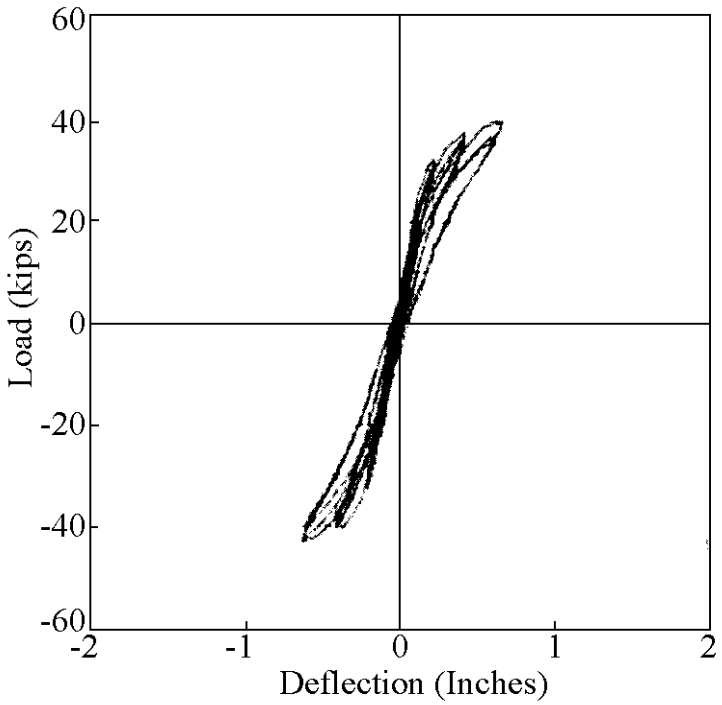

Fig. 1.3 Load-Deflection History for Pile-Cap Connections Tested by Pizzano [1984]

Pam and Park [1990] conducted tests in New Zealand to investigate the strength and ductility of prestressed concrete piles and cast-in-place concrete pile caps. Six pile-cap

connections were constructed by embedding 15.7 in. (400 mm) diameter octagonal piles in 36.5 x 36.5 x 78.8-in. (928 x 928 x 2000 mm) pile caps. For the first two tests, the end of the pile was embedded 31.5 in. (800 mm) into the pile cap (other specimens were set 2 in. into the cap). In three specimens, the pile prestressing steel was exposed and embedded in the pile cap with the addition of spiral reinforcement. The sixth connection is shown in Figure 1.4 and was made by grouting four D20 dowels into 20.9 in. (530 mm) ducts in the pile. The dowels extended 9.85 in. (250 mm) into the cap and formed 90º crossing hooks.

An axial load was applied to the specimens as they were subjected to simulated seismic loading. Pam and Park found that all of the connection details allowed the flexural strength of the pile to be reached while exhibiting satisfactory ductile behavior. They concluded that the preferred type of connection was embedding the pile deep into the cast-in-place concrete pile cap. This type of connection was the easiest to construct and resulted in the least damage to the pile cap. The connection using dowel bars, Figure 1.4, was considered the least desirable. It was more flexible than the other connections, but the damage during inelastic cyclic loading concentrated in a wide crack at the end of the pile. Figure 1.5 shows its load-deflection hysteresis. The maximum experimental moment was approximately 2000 kip-in. (227 kN-m), significantly less than the other connections tested. It is illustrated here because it has limited similarity to connections presently used in the U.S. Plastic hinging in the connection of Figure 1.4 did not occur along the pile as in the other units, but at the interface. Pam and Park also recommended that spiral steel be provided within the pile-cap region.

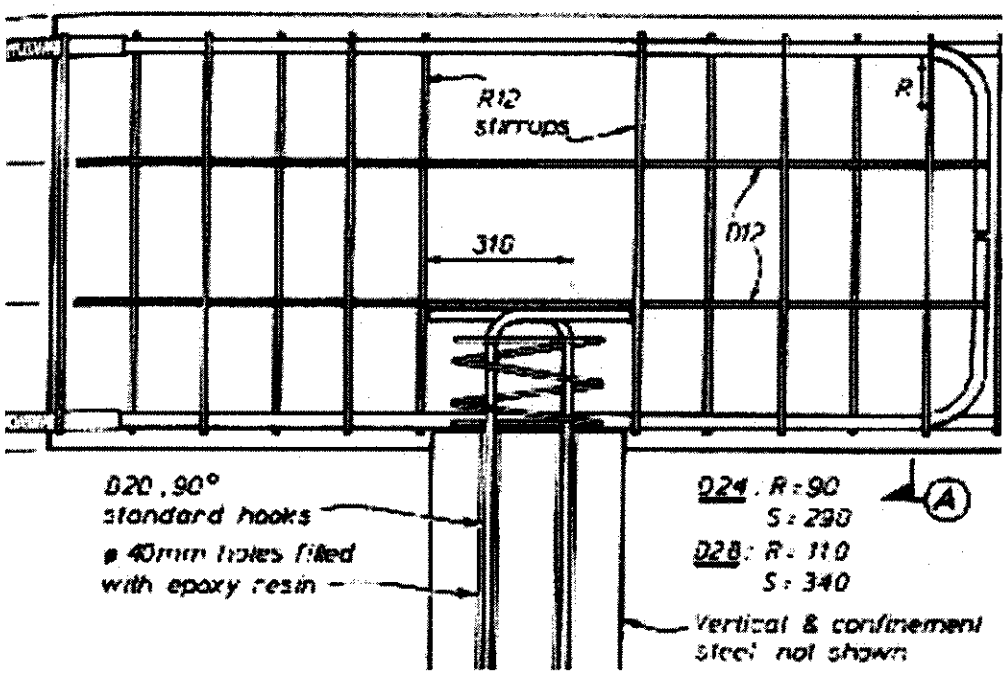

Fig. 1.4 Detail of Pile–Pile Cap Unit Tested by Pam and Park [1990]

A new pile-deck connection that utilized headed reinforcement and bond bars in the joint region was tested for the Port of Los Angeles [Sritharan and Priestley, 1998]. Eight #10 dowel bars were placed in the longitudinal direction with #9 T-headed bars and bond bars in the connection. Spiral reinforcement was added to the joint region within the deck. The precast prestressed pile was replaced with an in-situ concrete construction, and the dowels were placed prior to pouring concrete.

The connection was subjected to a simulated seismic loading, with drift levels reaching 6.7%. No axial load was applied. Figure 1.6 shows the measured load-deflection history of the connection. Sritharan and Priestley concluded that the design using headed reinforcement in the joint region was sufficient to develop a desirable level of ductility in the pile-deck system. They also concluded that the bond bars need not be placed in close contact with the dowels to perform satisfactorily.

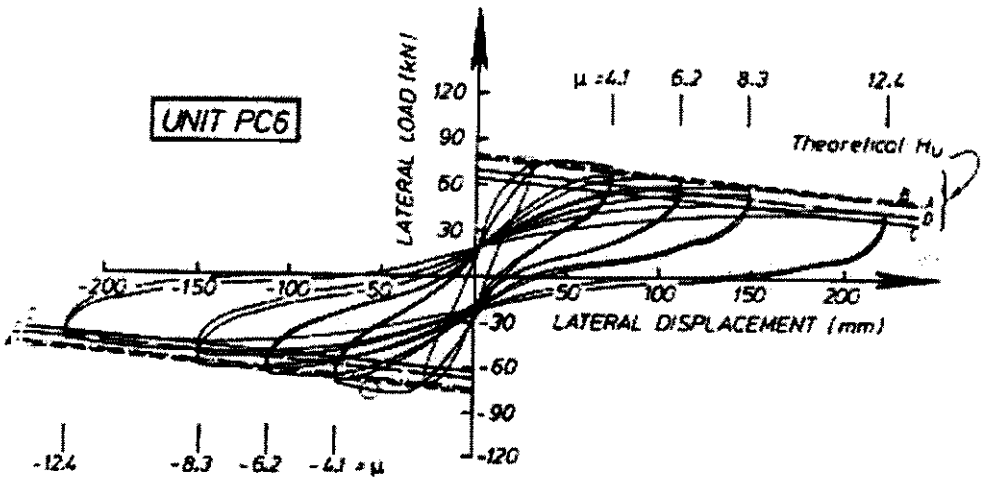

Fig. 1.5 Load-Deflection History for Connection of Fig. 1.3

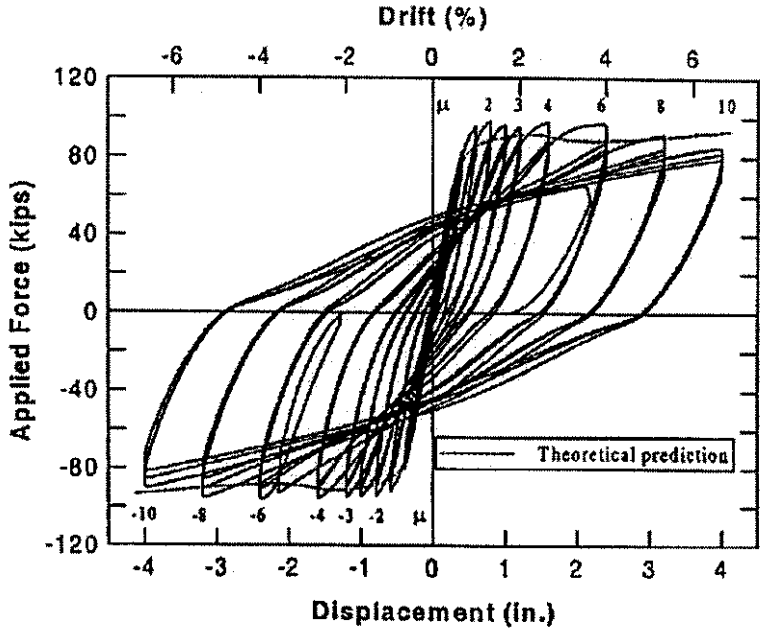

Fig. 1.6 Load-Deflection History for Sritharan and Priestley Test

The seismic performance of steel H-piles connected to reinforced concrete pile caps was also investigated [Xiao et al., 1999]. A relatively simple anchorage detail was used as was commonly employed in California bridge construction. The piles were anchored approximately one half a pile depth, and hairpin shaped rebars were inserted through holes in the piles to provide additional anchorage. This was postulated as a pin connection, which could transfer

relatively little bending moment. The piles were loaded with monotonic lateral load, cyclic axial tensile and compressive load, cyclic lateral load, and combined cyclic axial and lateral load. The ultimate tensile capacity of the piles could not be developed with this detail, but significant bending moment with significant ductility was noted. Figure 1.7 shows a moment-rotation curve for one of the specimens with cyclic lateral load and constant axial load.

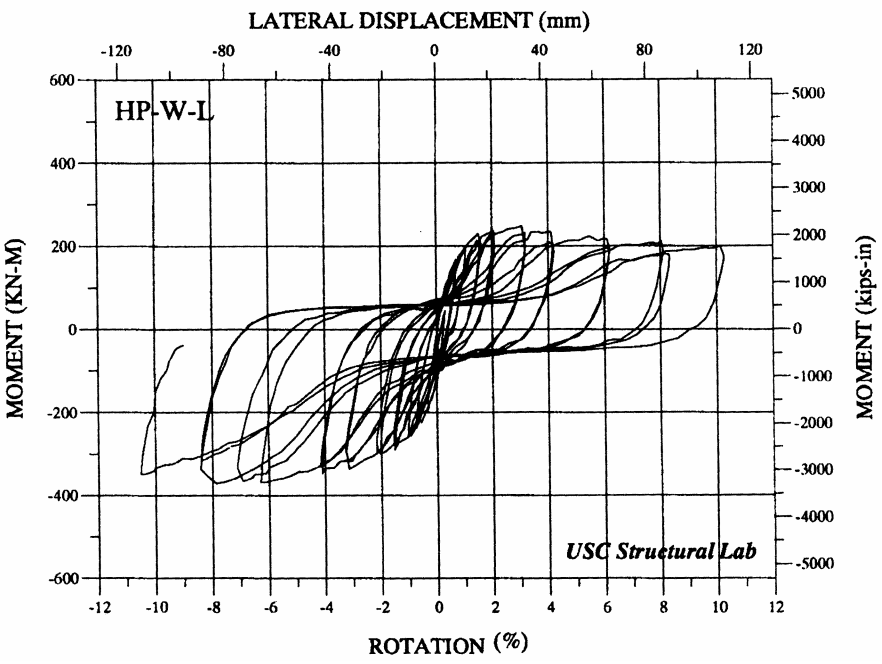

Fig. 1.7 Moment-Rotation History for Steel H-Pile by Xiao and Others

2 Review of Design Practice

2.1 INTRODUCTION

The design practice was reviewed to better understand the variations in pile-wharf connection design and to evaluate the consequences for this research study. The review started with systematic interviews with engineers who design and maintain these facilities. Some interviews were conducted by phone, but others consisted of personal visits by researchers with senior engineers of the ports of Los Angeles, Seattle, and other facilities. The goals of these interviews were

- to understand the design practice used by various port authorities including the history and evolution of the practice,
- to determine the rationale or justification for this practice, and
- to obtain design drawings and documentation that could be used to better understand the connection design details and design procedures.

The results of these interviews provided a good understanding of the variation in the design practice and the evolution of this practice in the major port facilities of Oakland, Long Beach, and Los Angeles, California, as well as Seattle and Tacoma of Washington state. Design drawings were obtained for more than 30 different wharfs at these ports. These drawings were adequate to provide the details of pile-wharf connections and the major member sizes and global geometry of each structure. The information search emphasized newer port facilities (those facilities constructed within the past 15 years), but drawings for several older facilities were obtained, since they aided in understanding the progression of the present design philosophy.

This chapter will provide an overview of the practice observed from these interviews and the results of initial analysis of the various connection options and design philosophies.

2.2 VARIATION IN DESIGN PRACTICE

The interviews and the design drawings showed a very wide variation in the design practice for pile-wharf connections, and the connections that have been designed appear to be

unique for almost every port structure. Part of the variation is driven by uncertainty among engineers as to the performance of various connection types, but a substantial part of the variation is caused by the need to produce economical structural designs and the need to improve the economy of port construction. At the same time, there are very clear trends in the practice. The connections may be unique in most structures, but clear similarities exist in most of the designs that have been produced by this practice. In addition, the interviews showed that despite the wide variation in practice, opinions are very strong and widely divergent as to what constitutes a good pile-wharf connection detail.

One clear divergence in opinion occurs over the use of vertical precast concrete piles with moment-resisting connections and steel batter piles for lateral load resistance. This divergence is schematically illustrated in Figures 1.1 and 1.2. The ports of Los Angeles and Oakland employed batter piles in older wharf structures. These older ports employed precast concrete batter piles, and a cursory examination of the pile-wharf connection used with these older connections shows that the connections did not have adequate resistance to develop the tensile capacity of the pile. Some of these precast concrete batter piles performed poorly in the 1989 Loma Prieta earthquake [EERI, 1990] , and the ports of Los Angeles and Oakland do not employ batter piles in present day port construction. These engineers have strong preferences toward moment-resisting connections of precast concrete piles to the wharf superstructure. They have developed an evolving line of reasoning and design practice, and this practice is summarized in the Section 2.2.1.

Other ports have a different attitude toward batter pile construction. These ports may still employ moment-type connections with vertical precast concrete piles as illustrated in Figure 1.1, but they also prefer steel batter piles for many applications. Steel batter piles are used because their behavior is similar to that of braced frame construction. That is, the tensile yield capacity of the pile, the pile pull-out capacity, and the buckling capacity define the connection and seismic design requirements. Batter piles are believed to more economically provide larger lateral stiffness and resistance than the precast piles in a moment-frame configuration, and they are thought to provide better resistance to structural damage during smaller seismic movements of the soil embankment. These batter pile connections provide very different connection design strategies, and some of these connection details are discussed briefly in Section 2.2.2.

2.2.1 Precast Piles with Moment-Resisting Connections

Precast piles with moment-resisting connections are commonly used in wharf structures with the general structural configuration as illustrated in Figure 1.1. Early connections of this type were designed by one of two general design concepts illustrated in Figure 2.1. One of these concepts employs outward bent dowel bars as illustrated in Figures 2.1a and 2.1b. The other concept employed extended prestress strand connections as shown in Figure 2.1c. Figure 2.1a shows a detail where dowel bars are bonded into corrugated tubes in the ends of precast piles, and the bars are bent outward into the top of the wharf deck. The bent bars are oriented in a radial or orthogonal pattern. In this report, this detail will be identified as the "outward bent dowel" connection. Variations of this detail have been used more than other connections in past construction, and are still used today. This variation occurs in

- the number and size of the dowel bars,
- the relative size of the bars as compared to the prestressed pile reinforcement,
- the length of the bar embedment into the wharf deck and into the end of the pile,
- the use of spiral steel to confine the concrete within the connection zone of the wharf deck,
- the use of duct tubes or drilled holes for dowel embedment,
- the pattern with which the bars fan out into the wharf deck, and
- the placement of the embedded bars relative to the top layer of flexural reinforcement in the wharf deck.

There are no known experiments to evaluate the seismic performance of these connections. The tests by Pizzano [1984] don't accurately reflect the pile reinforcement (particularly the spiral reinforcement) and dowel bar size and orientation used in present day wharf construction. The tests by Pam and Park [1990] employ a much shallower deck embedment than used in wharf construction. However, as noted earlier, the connection is widely used with quite wide variation in the details of its application. Spiral steel is infrequently used to confine the concrete within the connection zone of the wharf deck (not shown in Fig. 2.1a), and some engineers expressed concern about the performance of the connection because of the tendency of the dowels to pull the connection apart without this added reinforcement. They suggested that the lack of confining steel may lead to early deterioration of the connection

performance. Spirals have seldom been used for this confinement because they inhibit anchorage of the dowels into the pile and placement of the wharf deck flexural reinforcement. The outward radial fan pattern of the dowel bars also inhibit placement of the wharf deck flexural reinforcement, the bars are often oriented in the longitudinal and transverse directions of the supporting frame to minimize this interference. This later variation results in crowding of the reinforcement and difficulty in concrete placement. These concerns increase the cost and complexity of construction for this connection detail, and force engineers to balance their desire for improved connection performance with construction economy.

The outward bent dowel connection must be bonded within the corrugated steel tubes in the ends of the precast piles. However, piles are normally driven to the point where they achieve the required driving or bearing resistance. This pile bearing resistance is unlikely to be achieved when the top of the pile is precisely a few inches above the lower surface of the wharf deck. In some cases, the pile will extend above this point, and under these conditions the pile is cut off, and the connection shown in Figure 2.1a is employed at the end of the pile cutoff. The corrugated dowel ducts are made sufficiently long to account for this contingency. In other cases, the pile must be driven to an elevation well below the bottom of the wharf deck. Under these conditions, the connection illustrated in Figure 2.1b is used, and this connection is identified as the "extended outward bent dowel" connection in this report. The pile extension serves as a reinforced concrete column. Spiral reinforcement is employed in the extension to confine the concrete and provide shear resistance, but it is not normally extended into the wharf deck concrete for the construction problems noted earlier. There are fundamental differences in ductility that can be achieved with reinforced concrete column connections and precast pile connections, and so the extended outward bent dowel connections are treated as a different connection type. However, other factors are identical to the connection of Figure 2.1a.

Pile extensions are also used for all of the connections included in Figure 2.2. However, they are not discussed separately for those connections because the effect of the extension on connection performance should be similar for all precast pile connection types. That is, if the effect of the pile extension on the outward bent dowel connection performance is understood, the effect should be similar for other connection types.

A number of older wharf structures utilized a second design concept as illustrated in Figure 2.1c. With this detail, the goal was to use a slightly longer pile that commonly extended well above the bottom of the wharf deck. In some cases strand extensions were left at the pile

driving end to facilitate this connection, but these extensions interfere with pile driving. If the pile was driven to an elevation higher than the bottom of the wharf deck, the concrete above the bottom line of the deck was crunched after the pile was driven with a pincher device. The prestressing strands of the pile were then fanned out into the wharf deck to provide the moment transfer as required. This detail has been used in several older wharf structures but is not employed today. Tests on similar details have been completed [Pizzano, 1984], and the performance of these connections was mixed. Port engineers expressed further concern about this connection. They note that extended strands interfered with pile driving. They note that the concrete crushing device commonly pinches the prestressing strand, and this may nick and cut the prestressing strand extensions. The reinforcing strand is high-strength steel with limited ductility, and nicks and cuts may cause early fracture of the reinforcement and may adversely affect the connection performance. Thus, while there is limited information on the seismic performance of this connection detail, there was generally an opinion that this connection does not provide the desired performance for present seismic design standards.

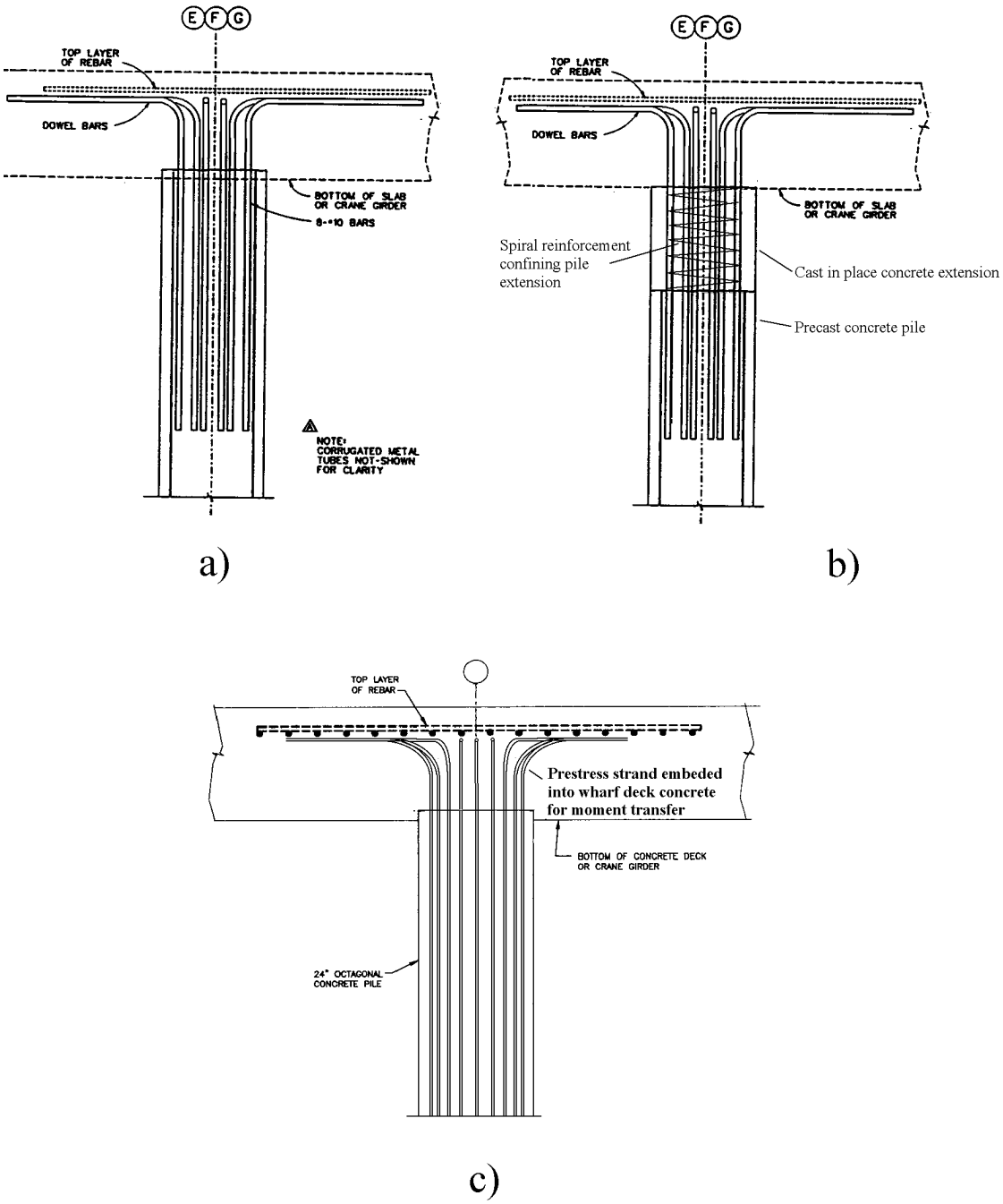

Fig. 2.1 Typical Prestressed Concrete Pile Moment Connections; (a) Outward Bent Dowel Connection; (b) Extended Outward Bent Dowel Connection; and (c) Extended Strand Connections

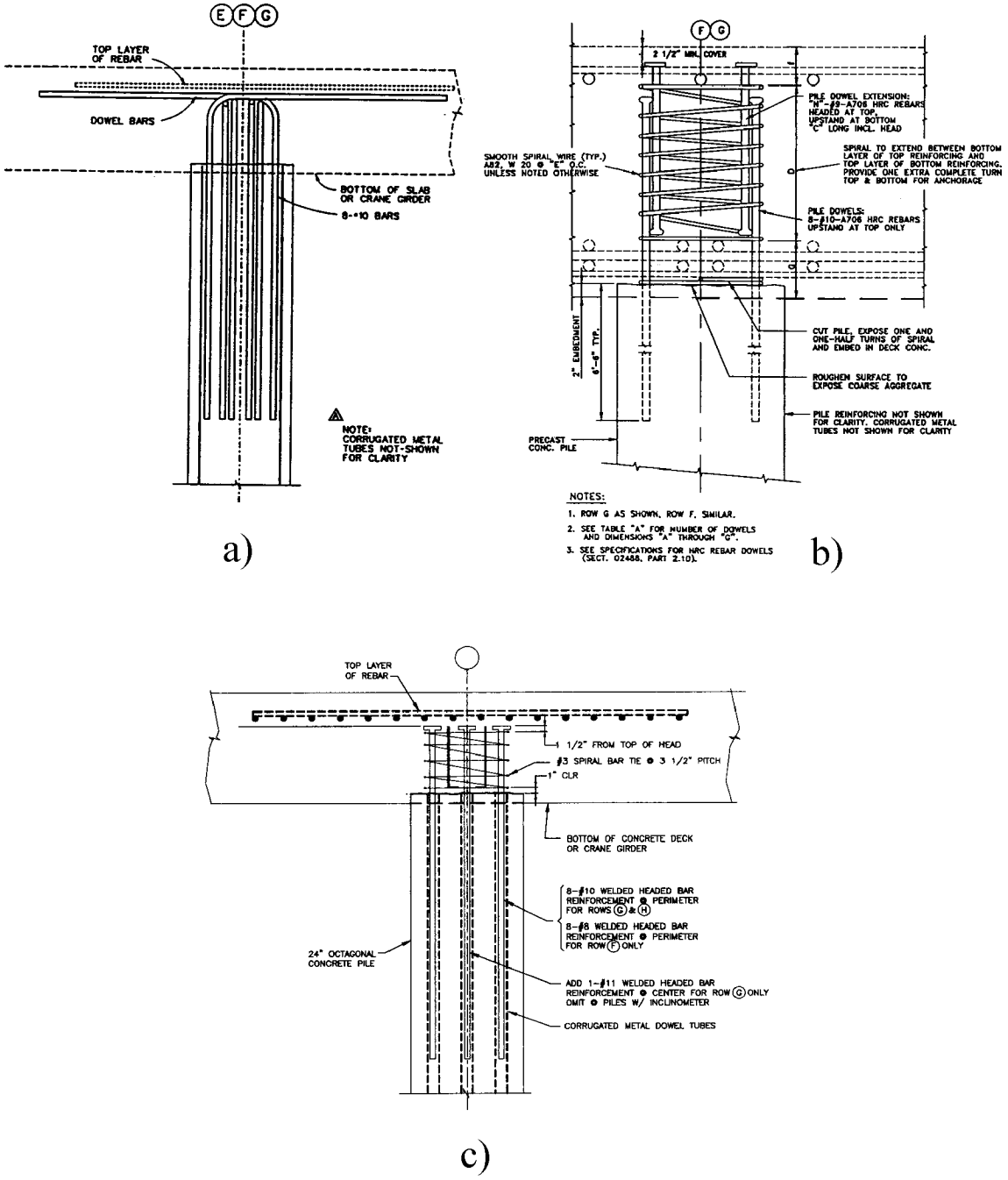

Fig. 2.2 Typical Prestressed Concrete Pile Moment Connections; (a) Inward Bent Dowel Connection; (b) Bond Bar Connection; (c) T-Headed Dowel Bar Connections

The prior discussion has noted that the outward bent dowel connection is commonly used, but there are concerns about the confinement of the concrete in the connection zone of the

wharf deck concrete. As a result, a few wharfs have employed the connection detail illustrated in Figure 2.2a. This detail is similar to the outward bent dowel detail, but the bars are bent inward as is sometimes done in building construction at exterior column connections. This detail is identified as the "inward bent dowel" connection in this report, and some engineers believe that this connection provides better confinement of the concrete in the connection zone. However, it is otherwise similar to the outward bent dowel detail.

The bent dowel bar details described above all cause considerable interference for placement of the flexural reinforcement in the wharf deck. As a result, the connection shown in Figure 2.2b has been used to overcome this economic concern. This connection will be identified as the "bond bar connection" in this report. Reinforcing bars are bonded into corrugated steel ducts as with the previous details, but the bars are not bent to provide moment transfer into the wharf deck. Instead bond bars and T-headed bars are employed to develop the tensile force in the dowels and to transfer moment to the wharf deck. Bond bars have bulbous ends that facilitate transfer of force from one bar to another as shown in Figure 2.2b. T-headed bars have small flat plates welded to the end of the bar sections as seen in Figures. 2.2b and 2.2c. These connections concentrate the reinforcing bars into the connection zone and reduce the interference to the deck flexural reinforcement. In addition, it is easier to employ spiral reinforcement about the connection zone with this connection. This connection has been tested [Sritharan and Priestley, 1998] as an extended connection, and good seismic performance was noted. Figure 1.6 shows the load-deflection performance observed from this test, but it should be emphasized that this test was effectively a normal reinforced concrete pile rather than a prestressed concrete pile and no axial load was employed in the test. This connection has been used in recent port structures in Los Angeles and Oakland.

The bond bar detail avoids interference with the flexural reinforcement of the wharf deck. It permits use of the spiral reinforcement within the joint, but it results in considerable crowding of the connection region because both bond bars and T-headed bars are required. As a result, the connection shown in Figure 2.2c was used to reduce this crowding. This detail eliminates the bond bar and simply employs T-headed bars as shown in the sketch. This detail has been also been used in several recent wharf structures, but no tests of this have been completed. In this report, this connection is identified as the T-headed dowel connection.

It should be recognized that these details are commonly used at all pile-wharf connections. However, the vast majority of the lateral stiffness and resistance is provided by the

shortest piles because of the differential pile length, illustrated in Figure 1.1. This differential length also affects the distribution of ductility demands, and the shortest piles also clearly have the largest ductility demands under seismic excitation.

2.2.2 Batter Piles

As noted earlier, steel batter piles are preferred by some engineers, and have been used in a number of recent seismic resistant wharf construction projects. Precast concrete batter piles have been used in the past, but they have not been used recently. A number of connection details have been used for steel batter piles, and some are illustrated in Figure 2.3. Figure 2.3a shows a detail where H-piles are embedded into the cap beam of the wharf deck. The H-pile has a cap plate to provide end bearing and a limited pullout cone for tensile resistance. However, the embedment length is relatively short. Eight dowel bars are welded to the pile flange and anchored into the concrete with a bent bar detail.

Figure 2.3b shows a relatively complex anchorage arrangement where the tubular steel pile is cast into the concrete wharf deck beams, and the pile bears on the concrete through an internal steel plate. The internal steel seat plate is anchored into the concrete wharf deck girder by high-strength steel bars for tensile resistance. Figure 2.3c shows another detail that utilizes shear connectors and bent bars to transfer the nominal shear force and resultant tensile force into the wharf deck. The pile connection directly balances the bulk of the axial pile force by direct connection of the two batter piles.

It should be noted that the steel batter piles were always used in combination with precast concrete piles for gravity load support. The precast piles normally had a outward bent dowel detail such as illustrated in Figures 2.1a and 2.1b. Other details have been employed for steel batter pile connections. In all cases, the steel batter pile-wharf connections were surprisingly complex, when it would appear that simpler connections may provide improved connection performance.

2.3 SIMPLIFIED ANALYSIS OF CONNECTION PERFORMANCE

Simplified analyses were performed on each of the connection variations to establish the resistance and expected ductility of the pile and the connection. Basic concepts of force path, equilibrium and elementary mechanics were used in these calculations, and the models and equations used in these predictions were typical of those employed by design engineers. With

these estimates, the controlling yield mechanism and controlling failure mode for each connection were estimated. The inelastic deformation capacity for each connection type was estimated for the various yield mechanisms and failure modes noted in the simplified analysis. The resulting predictions were used as an aid in establishing a test program for the experimental research that follows. Individual evaluation sheets were prepared for each connection to illustrate the weak links and concerns for that connection type. Figure 2.4 illustrates one of these evaluation sheets.

The results of these analyses are repetitive. They are specific to individual wharf designs and too numerous to individually list here. However, several general observations are worthy of note. First, all connections with steel batter piles and precast prestressed concrete piles were weaker than the piles themselves. This meant that the primary yielding and failure was expected within the connection and at the interface between the pile and the wharf deck. With the steel batter piles, this occurred because of the short embedment lengths used and the rather tenuous details used to attach the steel to the concrete. With the precast concrete piles used in moment-type connections, the connection was significantly weaker than the pile because the dowel bars were placed at a much smaller radius than the normal pile prestressing strand. In addition, both dowel bars and prestressing strands at the pile-deck interface reinforced the pile section. Prestressing strands are not fully developed at the end of the pile, but they still provide some reinforcement at this region. As a result, moment connections with precast concrete piles must likely develop their ductility and inelastic deformation within the small region adjacent to the interface between the end of the pile and the bottom of the wharf deck. That is, the simplified analysis suggests that the precast pile connections cannot develop a plastic hinge extending over a significant length of the pile. Connections with reinforced concrete pile extensions genuinely had columns that were weaker than the connection zone, and the simplified analyses suggested that plastic hinges could develop in the column member. The simplified calculations suggested that axial load exacerbated this effect. These observations are quite important because many past pile connection tests employed pile extension connections such as shown in Figure 2.1b with no axial load. These factors suggest that these past tests may not reflect the performance expected from precast pile connections because the pile extension behaves more like a reinforced concrete column and distributes the inelastic deformation over a significant length of the member rather than concentrating it at the connection interface.

These simplified analyses were used to further plan an experimental research program that followed. A given requirement of the research funding was that the focus of the experimental research would be upon moment-resisting precast concrete connections. Therefore, batter pile details were excluded from the research program. However, a range of precast concrete connections was included in the study based upon the variability in design described here.

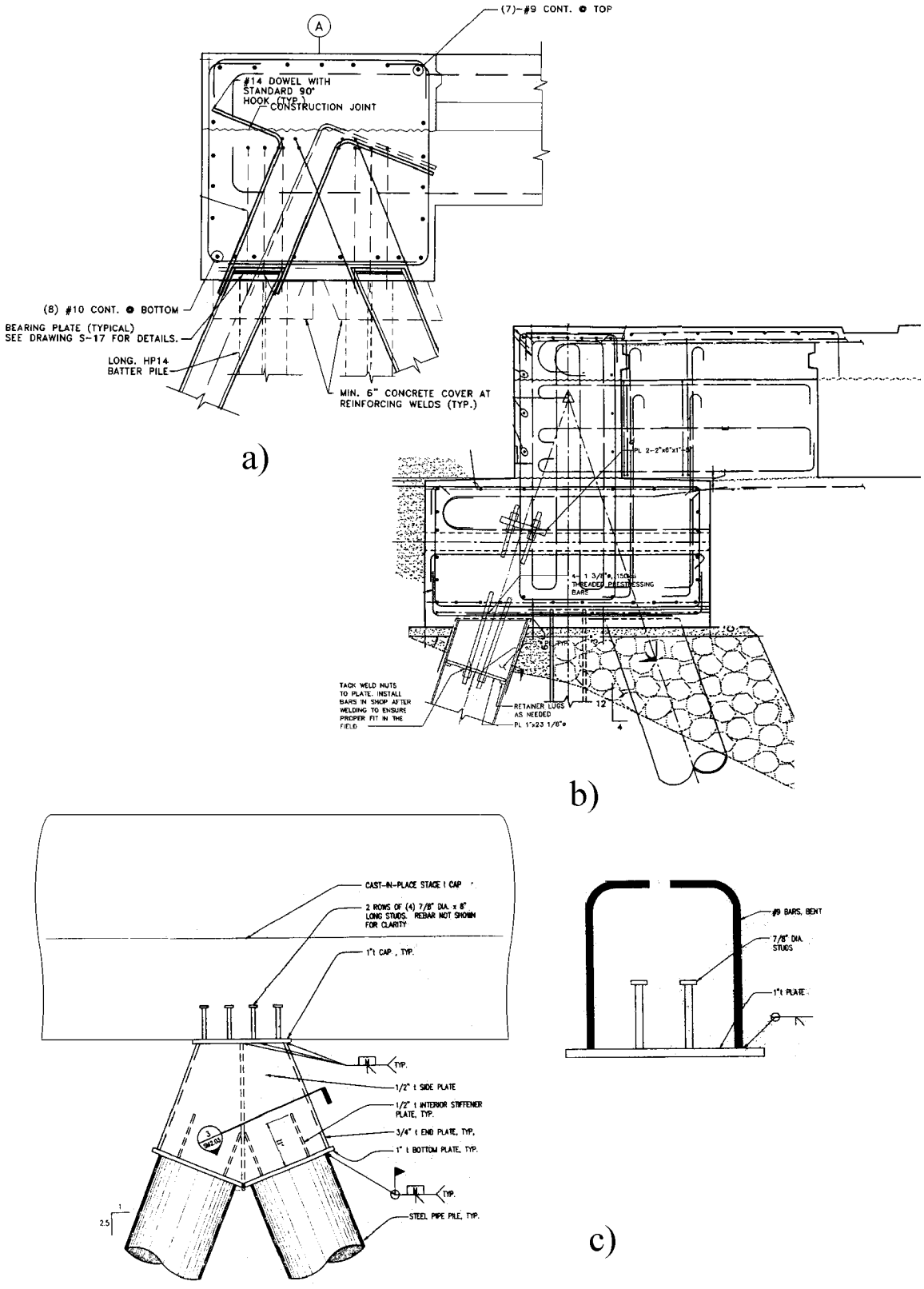

Fig. 2.3 Typical Steel Batter Pile Connections

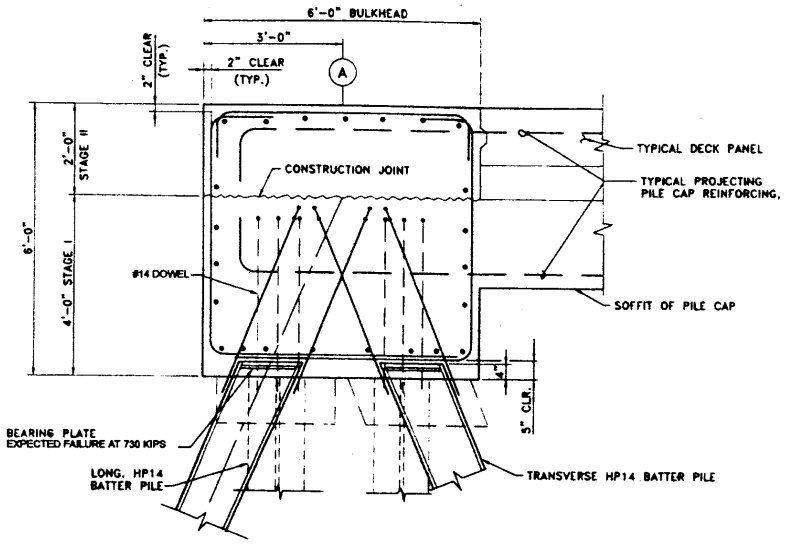

This structure is composed of two types of piles: steel batter piles and prestressed concrete piles. In the following analysis it was assumed that a horizontal force acts on the deck, which then transmits the force to the piles.

The batter piles exist in pairs. There are, in general, two sets of batter piles per bent: two oriented at a 5:12 angle N-S (one in each direction) and two oriented at a 5:12 angle E-W. As the system is loaded, one batter pile will be in compression while its mate is in tension. Tensile forces are transferred from the concrete deck to the steel HP14 section by #14 dowels, which are welded to the section flange. Compression is achieved through the bearing of the concrete on the HP section itself, and on bearing plates welded to the top of the section.

Analysis of the batter pile connection indicates that it will likely fail in compression after the welds attaching the bearing plates yield. A second failure mode could occur when the dowels yield in tension. Also of concern is cone pullout, as a rough calculation estimated this capacity at 440 kips. The actual capacity should be significantly greater than this value, though, because reinforcing steel in the bulkhead was not considered in its calculation. A summary of estimated capacities follows.

Failure mode	Estimated capacity (kips)
Weld of bearing plate to HP section	730
Rebar yielding	810
HP section yielding	1070
Punching shear	1070
Bearing of concrete	1410
Weld of rebar to HP section	1560
Cone pull-out	>440

Several assumptions were made in this analysis: (1) The batter piles are completely fixed in the soil, (2) A typical HP14x89 section with six #14 dowels, (3) The fillet weld strength = 1.4 * [0.6Fexx] normal to weld, (4) Fexx = 70 ksi for all welds, (5) Normal weight concrete with f'c = 6000 psi in the bulkhead and deck. Additional assumptions are stated in the attached calculations.

Fig. 2.4 Typical Connection Data Sheet

3 Experimental Program

3.1 INTRODUCTION

Eight pile-wharf connections were tested at the University of Washington Structural Research Laboratory to evaluate their resistance, stiffness, and ductility. The test specimens all simulate moment-resisting connections of prototype structures of the types discussed in Chapter 2 and illustrated in Figures 2.1 and 2.2. Table 3.1 summarizes the 8 specimens and the specific goals of each test. Various wharfs from the ports of Los Angeles and Oakland were used as the prototype structures for these test specimens. Reinforced concrete piles were used in Specimens 1 and 2 to evaluate connections with pile extensions. Precast prestressed concrete piles were used in Specimens 3–8, and reinforced concrete was used for the decks of all eight specimens. The first four specimens are described and evaluated in detail by Soderstrom [2001], and the last four specimens are described and evaluated by Graff [2001].

Specimens 1 and 2 were based on pile extensions from Oakland and Los Angeles wharfs, which are used to extend the length of a precast pile driven below the deck level. A detail taken from the plans of Oakland's berth 30 wharf is shown in Figure 2.1. This was the prototype for these two test specimens, but most other pile extensions were similar in design. If the extension length was less than 6 in., the extension and deck were cast monolithically; otherwise the pile extension was cast prior to the deck or girder. The pile extensions contained either eight #9 dowels or eight #10 dowels grouted into the precast sections and extending into the deck. Some dowels were epoxy-coated, but others were not. The hook length of the bent dowels varied depending on the plan and pile placement.

Table 3.1 Summary of Test Specimens

Specimen	Connection Type	Special Conditions	Goals of Test
1	Extended Outward Bent Dowel (Fig. 2.1b)	No axial load.	Comparison with Specimen 3 shows the behavior of extended pile connections as compared to precast pile connections.
2	Extended Outward Bent Dowel with spiral reinforcement	No axial load. Spirals around dowels in deck.	Comparison with Specimen 1 shows the effect of spiral reinforcement in connection zone.
3	Outward Bent Dowel (Fig. 2.1a)	No axial load.	Baseline connection for most comparisons.
4	Outward Bent Dowel (Fig. 2.1a)	With axial load.	Comparison with Specimen 3 shows the effect of axial load on connection performance.
5	Inward Bent Dowel (Fig. 2.2a)	With axial load.	Comparison with Specimen 4 shows the difference in between outward and inward bent details.
6	T-Headed Dowel Bar (Fig. 2.1c)	With axial load.	Comparisons with Specimens 4 and 5 show the difference between bent dowel and T-Headed dowel details.
7	Bond Bar (Fig. 2.1c)	With axial load.	Comparisons with Specimens 4 and 5 show the difference between bent dowel and Bond Bar details.
8	Outward Bent Dowel but lighter deck reinforcement	With axial load.	Comparisons with Specimens 3 and 4 show the effect of the substantial shear reinforcement in the deck.

Specimens 3–8 were also modeled on pile-wharf deck connections used in Oakland and Los Angeles ports. The prototype connections used precast prestressed concrete piles that were embedded 2 in. (50 mm) into the deck slab or girder, as shown in Figure 3.2 for these specimens. Figure 3.2 indicates a 1 ft (305 mm) length for the dowel bars beyond their bend into the wharf deck, but most newer structures employed a longer length. The dowel bar size and orientations were similar to those noted with extended pile connections. The embedment length of the

dowels into the pile varied from 48 in. to as much as 96 in. (1.22 to 2.44 m), depending on the plan and the location of the pile. Sixty inches was the most common embedment length. In Oakland wharfs, spiral reinforcement was often placed around the dowels in the connection zone of crane girder connections as shown in Figure 3.1. These connections bear the added weight of large container cranes common in most port facilities.

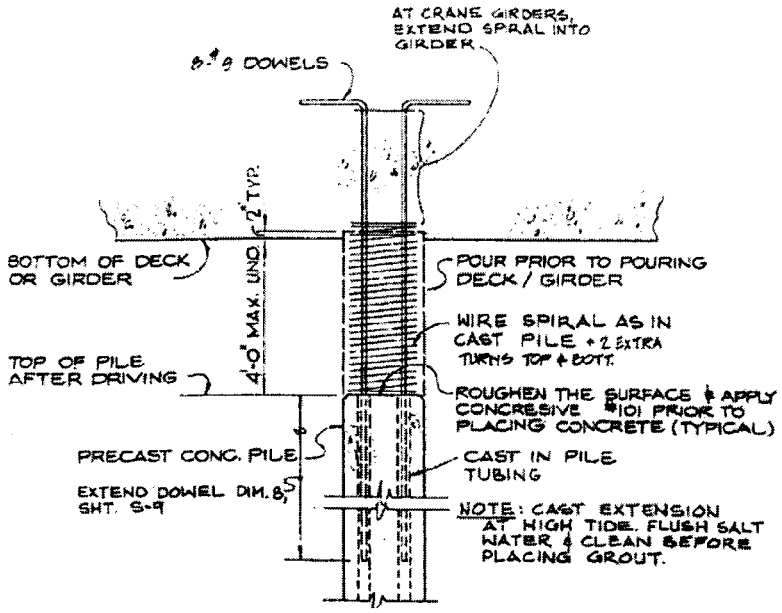

Fig. 3.1 Typical Pile Extension Detail from Port of Oakland Wharf, Berth 30

Prototype pile sections were normally solid octagonal precast prestressed piles that were 24 in. (610 mm) in diameter. All contained spiral reinforcement of varying size and pitch, and prestressing strands arranged in a circular pattern within the spiral. The size and number of prestressing strands also varied, as did the design prestress force. Most 24-in. piles had corrugated ducts for the dowels set in a 12 or 13 in. (305 or 330 mm) diameter circle, but some were drilled holes as shown in Figure 3.3. Some piles contained additional reinforcing steel. Some piles contained internal jet pipes to facilitate driving if they encountered premature resistance. Hollow octagonal piles were used in a few prototype structures, but these are generally believed to provide inferior performance. The test specimens were designed based upon these and similar prototype structures, but because of the specimen cost, the specimens attempted to be as generic and broadly based as possible.

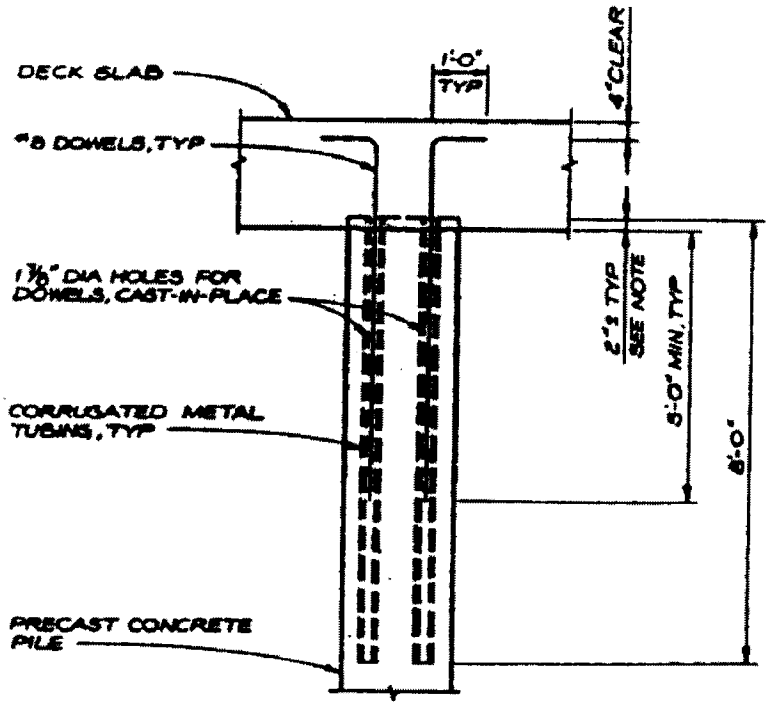

Fig. 3.2 Typical Connection Detail from Port of Los Angeles Wharf, Berths 226–229

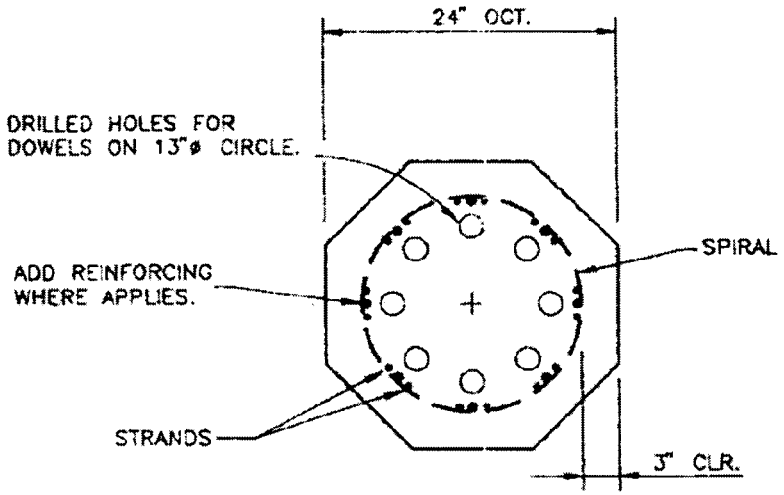

Fig. 3.3 Typical Pile Section from Port of Oakland Wharf, Berth 68

3.2 TEST SPECIMENS

The test specimens were designed to model these typical prototype structural details as closely as possible. The test specimens were all approximately 69% scale of the prototype structures. This scale factor was chosen due to the limited availability of diameters of

prestressed octagonal piles. Piles are frequently manufactured in 24, 18, and 16-½-in. (610, 460, and 420 mm) diameters. The 16-½-in. (460 mm) diameter pile was selected because it was the largest pile that could be economically obtained at the time the test specimens were built. This scaling also readily fit the laboratory equipment and maximized the research results that could be obtained with the available time and funding. The piles were purchased from Concrete Technology Corporation of Tacoma, Washington, and were manufactured on the ends of forming beds used for a large construction project in progress at that time. The piles were manufactured as normal commercial piles including steel rings that are installed at the driving end to facilitate pile driving. Analysis of the prototype structures shows that the piles with shorter clear length provide the vast majority of the lateral stiffness and resistance for wharf structures. However, the clear length of the piles is not a good indicator of the effective length for flexure, because some bending deformation occurs below the soil line. The length used in the test specimens as shown in Figure 3.4 is quite short, but it represents an approximate scaling of an intermediate short pile length estimated for the various prototype structures. Some prototype piles almost certainly have shorter pile lengths to their inflection points than the lengths used in these experiments. Shorter lengths will affect the connection performance as discussed later in this report.

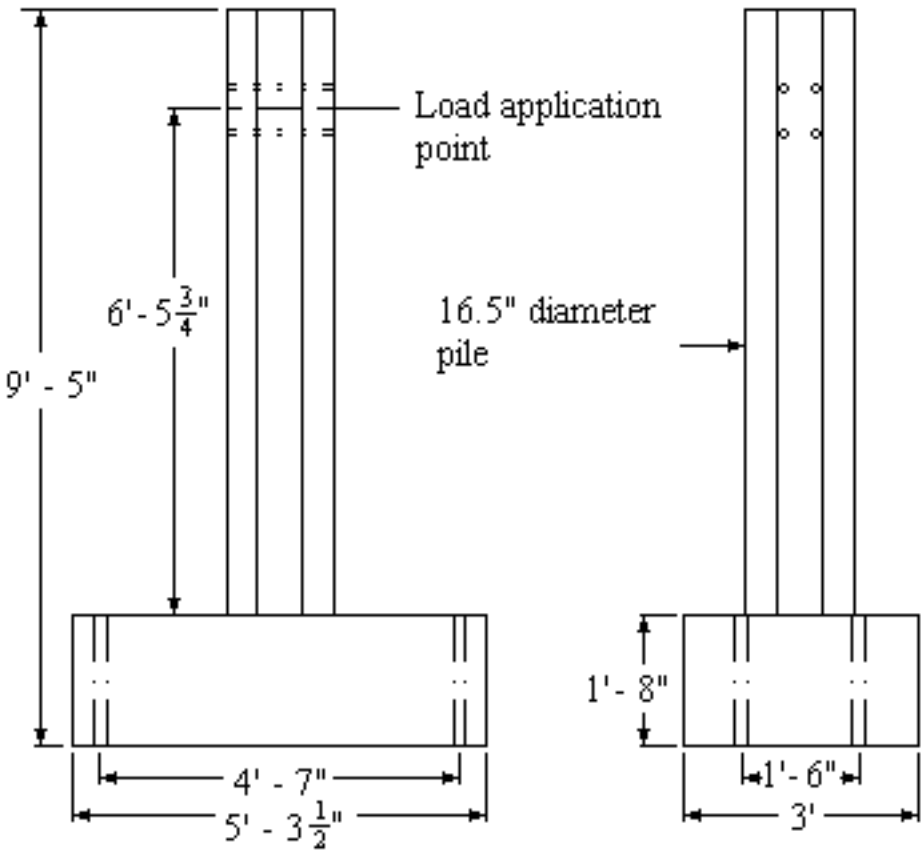

Fig. 3.4 Geometry of Test Specimens

Figure 3.4 shows the general geometry of the test specimens. The specimens were designed and constructed in the normal upright position, but they were tested in the inverted position as suggested in the figure. This permitted anchorage of the specimen deck to the laboratory strong floor at existing tie downs. Prototype deck depth or thickness varied widely in different structures. It was commonly about 30 in. (760 mm) deep for connections without girder framing. The greatest depths occurred when piles connected to a crane support girder. The test specimen deck section thickness was an approximate 69% scaling of the 30 in. (760 mm) typical thickness. This deck section was designed to be large enough to permit complete transfer of the pile shear and moment to the deck structure without causing excessive interference from the tie downs. The size of the deck slab section was also minimized to avoid excessive specimen cost or weight. A 63.5 x 36 x 20 in. (1.61 x .92 x .52 m) deck slab section was employed, since this satisfied the diverse objectives.

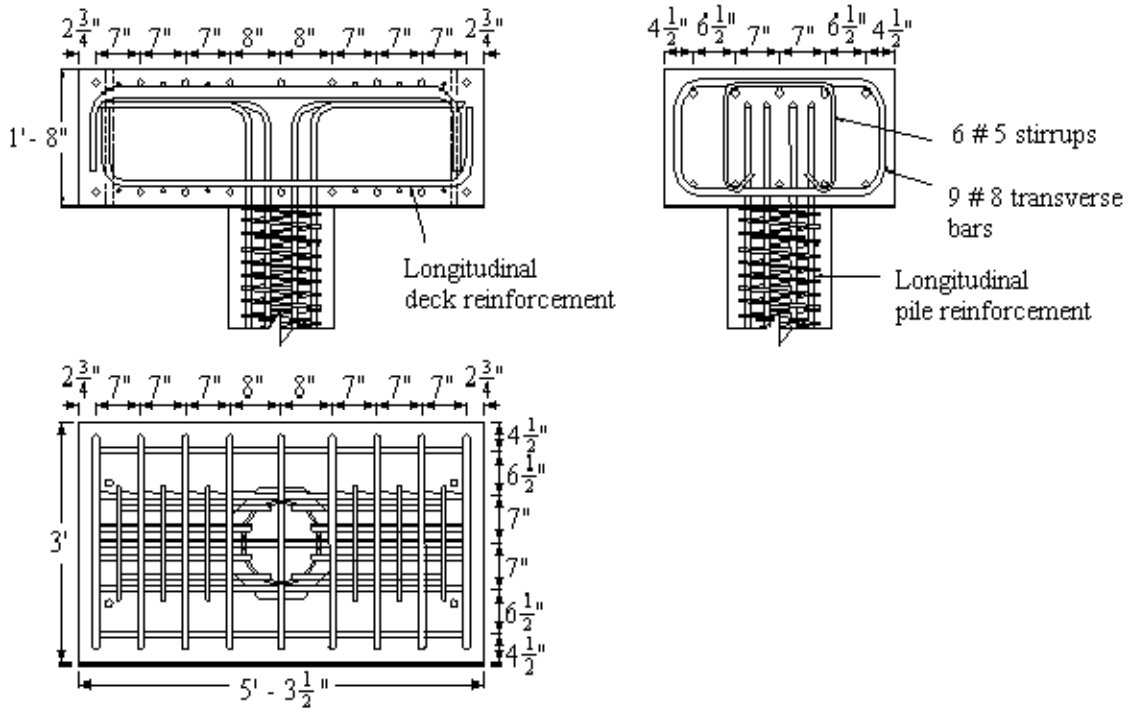

Fig. 3.5 Deck Slab Section Reinforcement for Specimens 1–7

The flexural reinforcement of the deck was also scaled from prototype structures, and Figure 3.5 shows reinforcement used for Specimens 1–7. In the prototype structure, the development of the tensile capacity of these large reinforcing bars is easily achieved because of the large plan dimensions of the prototype structure. However, the limited dimensions of the specimen deck slab section required that the bars be bent at the ends of the slab section if they were to develop their required stiffness and resistance. The bent rebar effectively provides confinement and shear reinforcement to the deck section that is greater than that expected in the prototype structure. Further, the tie downs themselves aid in confining the concrete within the deck slab section. As a result, the deck reinforcement of Specimen 8 was modified to significantly reduce this confinement and shear reinforcement as shown in Figure 3.6. Comparison of the results of this test with the results of Specimens 1–7 permitted quantification of the effect of this added confinement. Specimen 8 had the same flexural reinforcement in the deck section as used for the other specimens, but the bent bars were cut to significantly reduce their confinement of the connection. In addition, supplemental shear stirrups that are frequently used in crane rail girders or other stiffening elements were eliminated in Specimen 8.

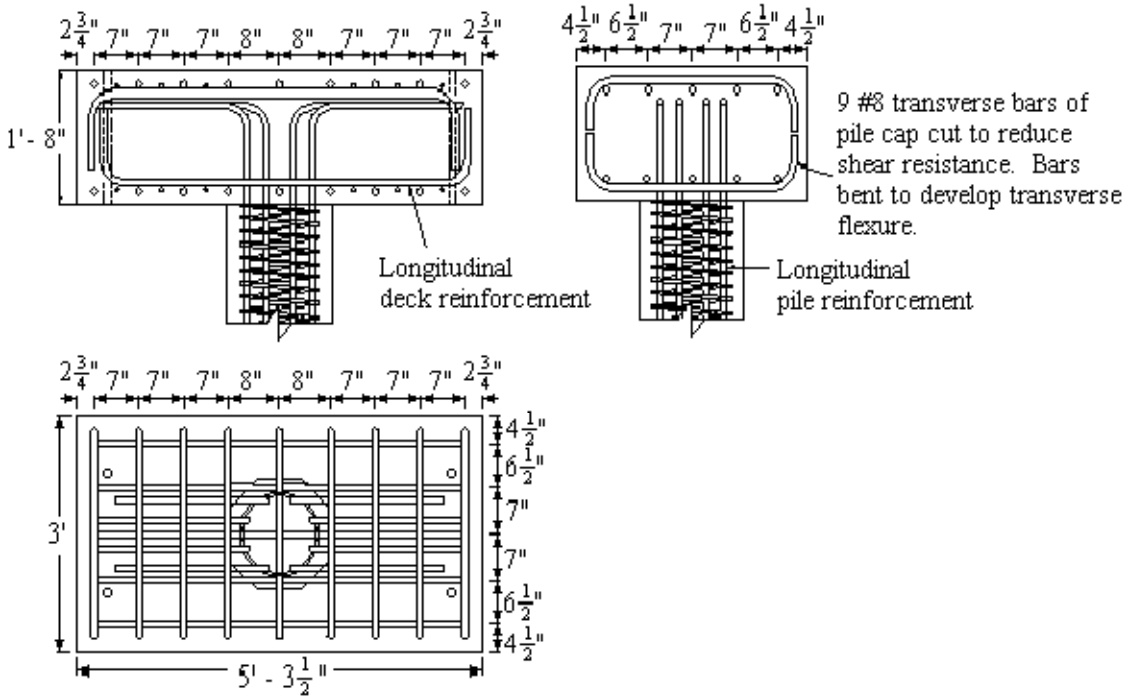

Fig. 3.6 Deck Slab Section Reinforcement for Specimen 8

Specimens 1 and 2 were reinforced concrete cast-in-place pile extensions with the outward bent dowel connection. The pile extension was cast simultaneously with the deck, creating a monolithic structure. This was done for more rapid construction and reduced construction cost. In practice, the extension might be placed only with the deck if the length does not exceed 6 in. (150 mm). Eight #7 reinforcing bars extended from the piles and were hooked to run parallel with the deck reinforcement as shown in Figures 3.5 and 3.7. These dowels were again a 69% scale of the eight #10 bars commonly used in the prototype structures. In the Los Angeles and Oakland structures, the hooks from the bent dowel bars were aligned in a radial pattern in the wharf deck, but this configuration was not practical in the small deck slabs used in these tests. Instead, all eight hooks were positioned parallel to the direction of load application. The pile sections contained #3 spiral reinforcement at 2 in. (50 mm) pitch, which ended at the pile-deck interface. Specimen 2 was identical to Specimen 1 except that spiral reinforcement extended into the joint region of Specimen 2 as illustrated in Figure 3.8. This permitted evaluation of the effect of this supplemental confinement on connection performance.

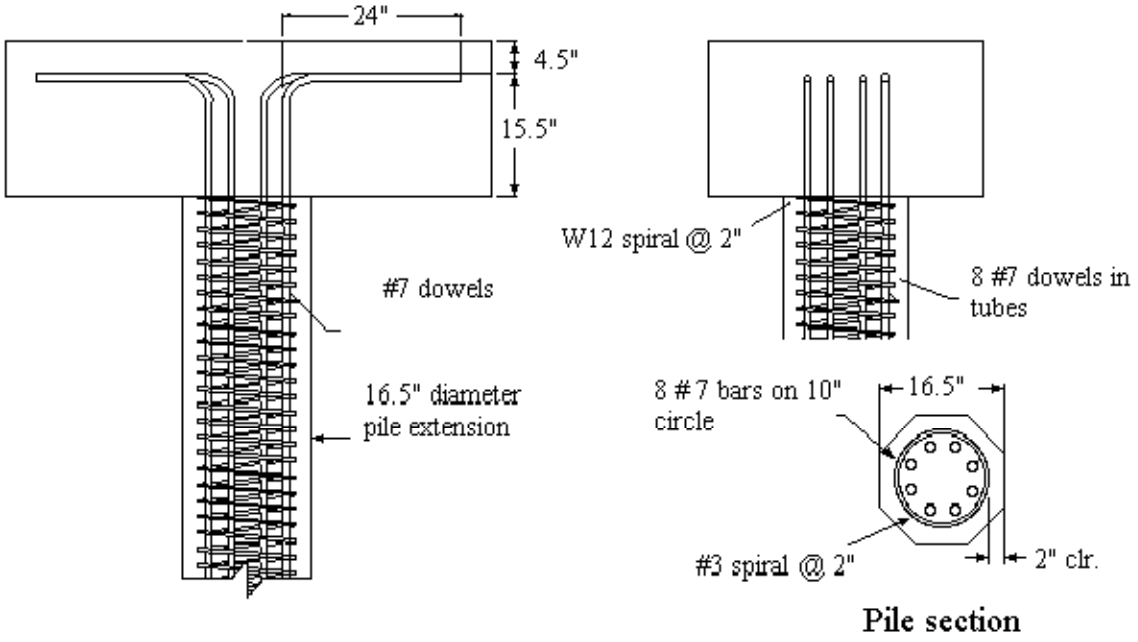

Fig. 3.7 Specimen 1 Reinforcement Details

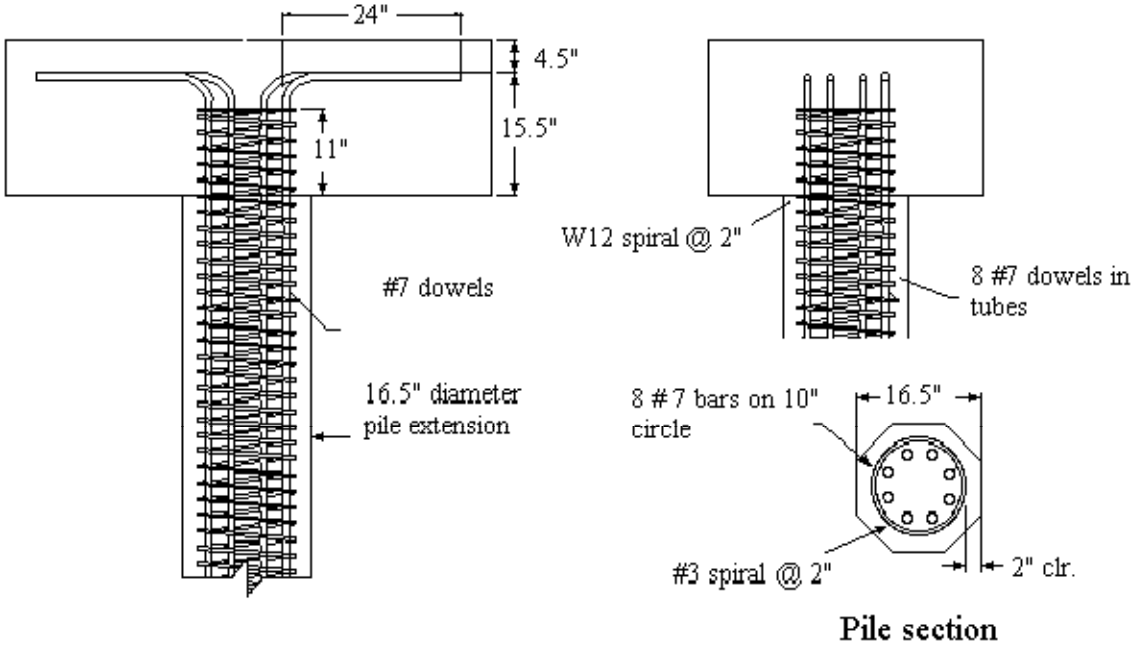

Fig. 3.8 Specimen 2 Reinforcement Details

Specimens 3, 4, and 8 were outward bent dowel connections with precast prestressed concrete piles. The piles were set 2 in. (50 mm) into the deck. As shown in Figure 3.9, prestressing was provided by eleven 0.5 in. (12.5 mm) diameter grade 270 strands with an

applied prestress of 203 ksi (1400 MPa or 75% gross ultimate tensile strength). After losses, the actual prestress would be less. The prestressing effect would also be reduced near the ends because of the requirements for development of the tensile stress, and the short piles are likely to experience some reduction over most of their length. In addition to prestressing strands, the specimens contained eight #7 dowels grouted into the pile ducts and hooked 90 degrees in the deck as shown in Figure 3.9.

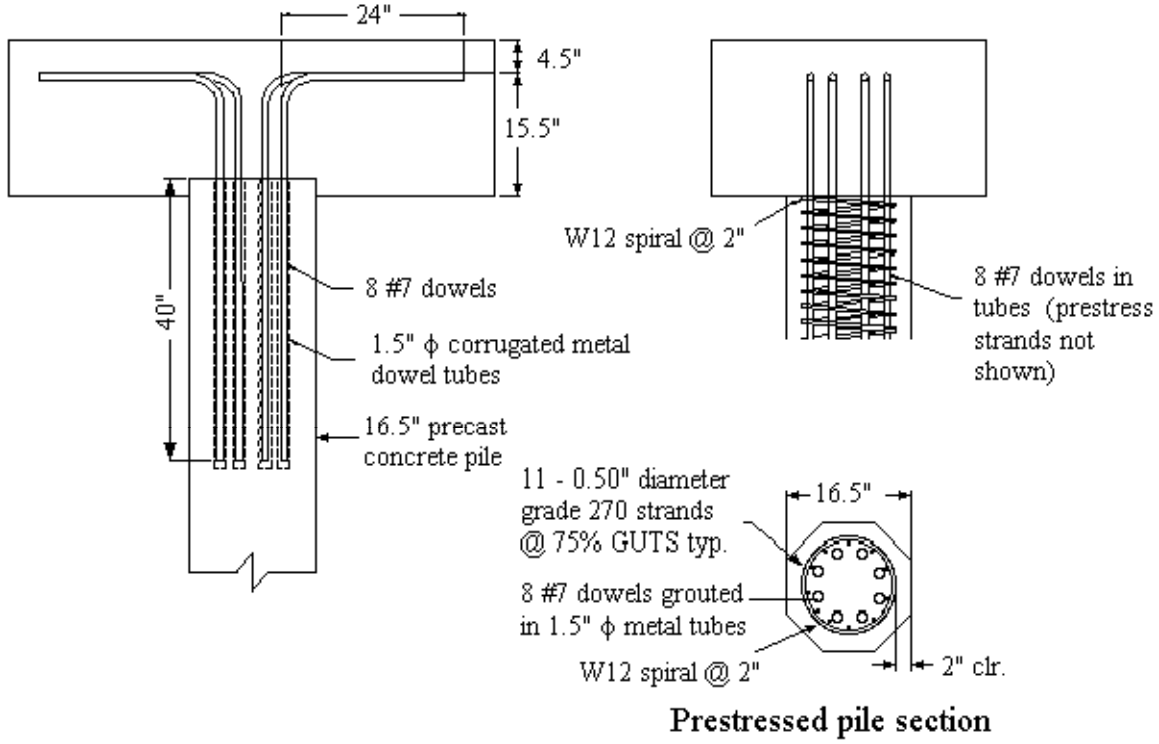

Fig. 3.9 Specimens 3, 4, and 8 Reinforcement Details

Specimen 5 was identical to Specimens 3 and 4 except that the inward bent dowel connection was employed. This detail forced the bars to cross over the head of the pile from both sides as illustrated in Figure 3.10, and the crossed bars create a confined pocket of concrete over the head of the pile. Some engineers expressed the opinion that this configuration may improve the connection performance, and the detail has been used in several prototype structures.

Specimen 6 used the T-headed dowel bar connection with the connection details shown in Figure 3.11. This detail has been used in several recent port facilities as a means of improving the economy and constructability of the structure. The Type 120 T-headed bars were provided by Headed Reinforcement Corporation as a 69% scale of the prototype structure. These headed

bars consisted of a reinforcing bar with the addition of a 2.5 x 2.5 in. (100 x 100 mm) square steel plate welded to the end of the bar. The end plate is intended to anchor the reinforcement and eliminate the need for a bent dowel bar. This pile-deck detail was used in wharfs in Oakland, California.

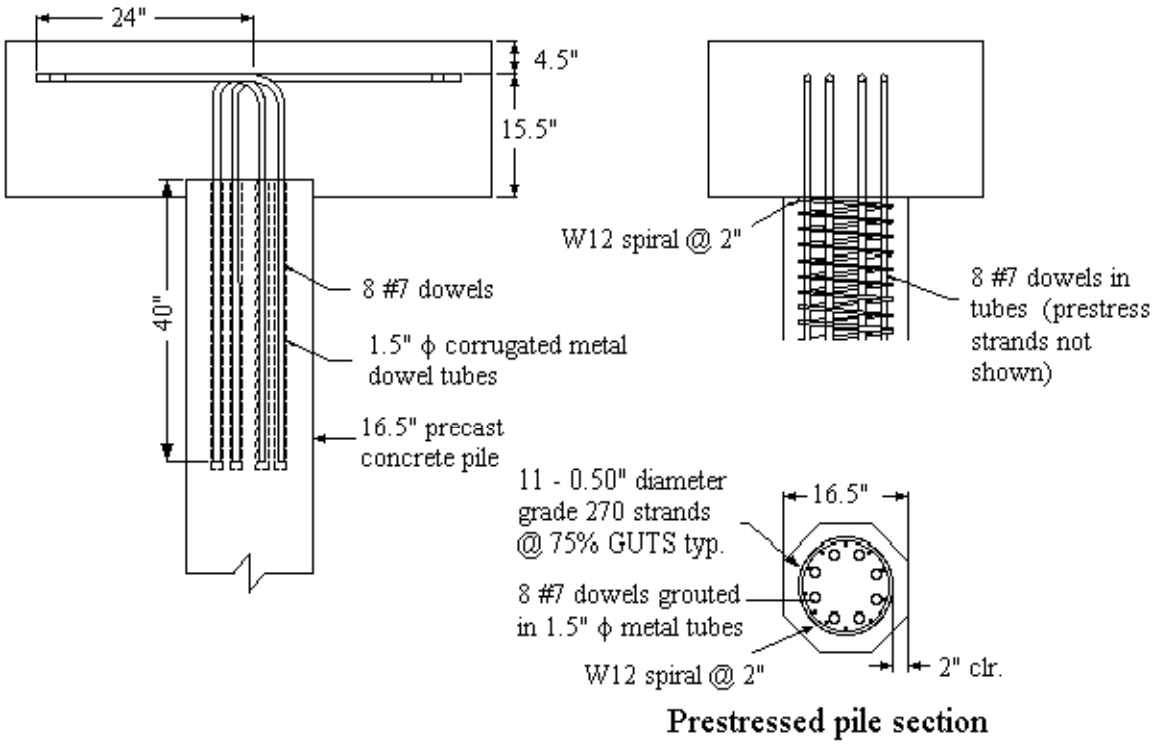

Fig. 3.10 Specimen 5 Reinforcement Details

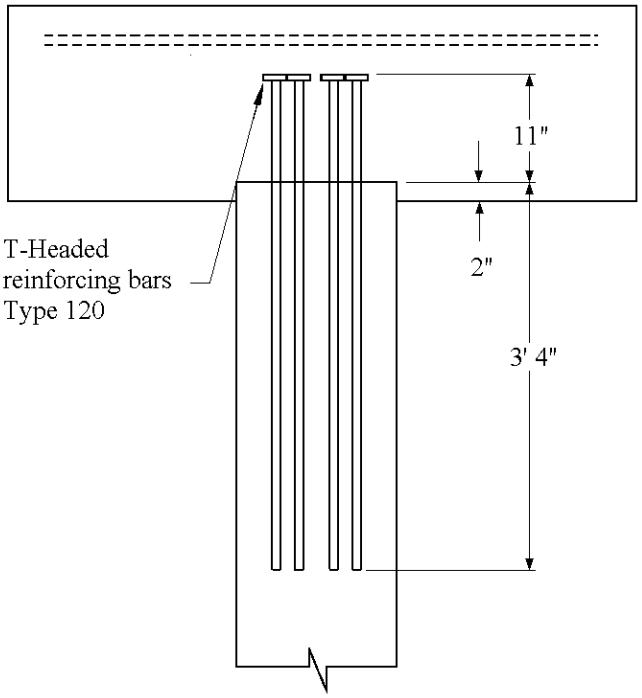

Fig. 3.11 Specimen 6 Reinforcement Details

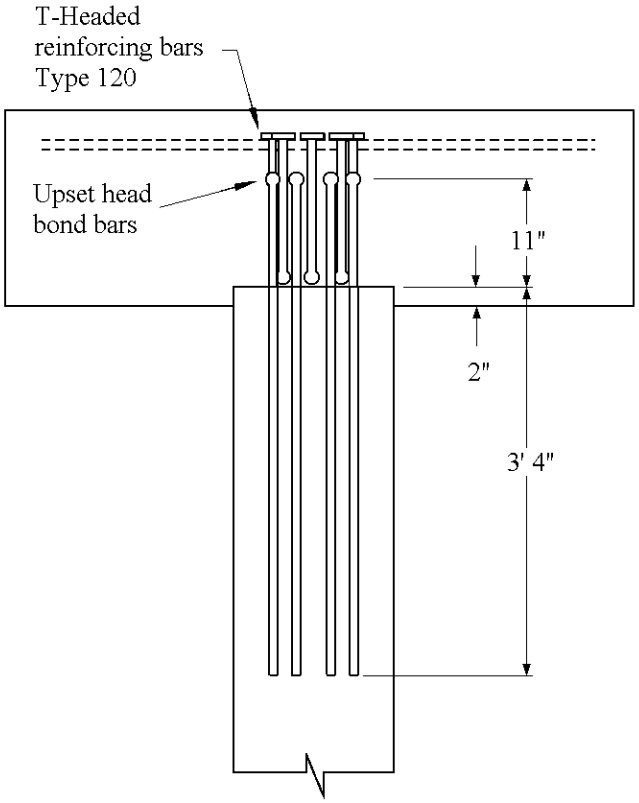

Fig. 3.12 Specimen 7 Reinforcement Details

Specimen 7 also used bars from the Headed Reinforcement Corporation and utilized the bond bar connection described in Chapter 2. This connection detail was also proposed to improve the connection by reducing bar interference, but it is more cumbersome than the detail used in Specimen 6. Bars that the manufacturer refers to as "bond bars" were used in this detail. The bond bars consisted of reinforcing bars 15 in. in length formed at one end into a semi-conical end, which the manufacturer refers to as an "upset head." On the opposite end of the bond bar a Type 120 T-head was used. In addition bars with upset heads were grouted into the prestressed pile section. This detail was used in a Los Angeles port facility, and the detail was tested using a reinforced concrete pile (that is, an extended pile connection without axial load) in a previous study [Sritharan and Priestley, 1998]. However, the spiral reinforcement was not placed around the dowel bars in Specimen 7, because some engineers believe it interferes with construction. Further, this spiral reinforcement has not been used on some prototype structures.

Specimen 8 used the same connection detail as Specimens 3 and 4 because it is the most commonly used detail in existing port facilities. However, a variation in the deck reinforcement was used as shown in Figure 3.6, and discussed earlier in this section.

3.3 SPECIMEN CONSTRUCTION

The construction methods used for the test specimens were designed to simulate the methods used in the field for the prototype structures as closely as possible. For this reason the test specimens were constructed in an upright position, as they would be in the field. In this position, any effects of aggregate settlement or increased water cement ratio at the upper surface would be similar to those expected for the prototype structures. This required strong formwork for supporting the wet concrete during construction. The specimens were cast in pairs to facilitate this support. The formwork and support falsework was designed using the 1997 National Design Specification wood design manual, and it is illustrate in the photo of Figure 3.13. Specimens 1 and 2 were constructed using reinforced concrete pile extensions as opposed to the prestressed concrete pile sections, which were used in Specimens 3–8. Therefore, Specimens 1 and 2 also required formwork for the pile extensions as shown in the photo.

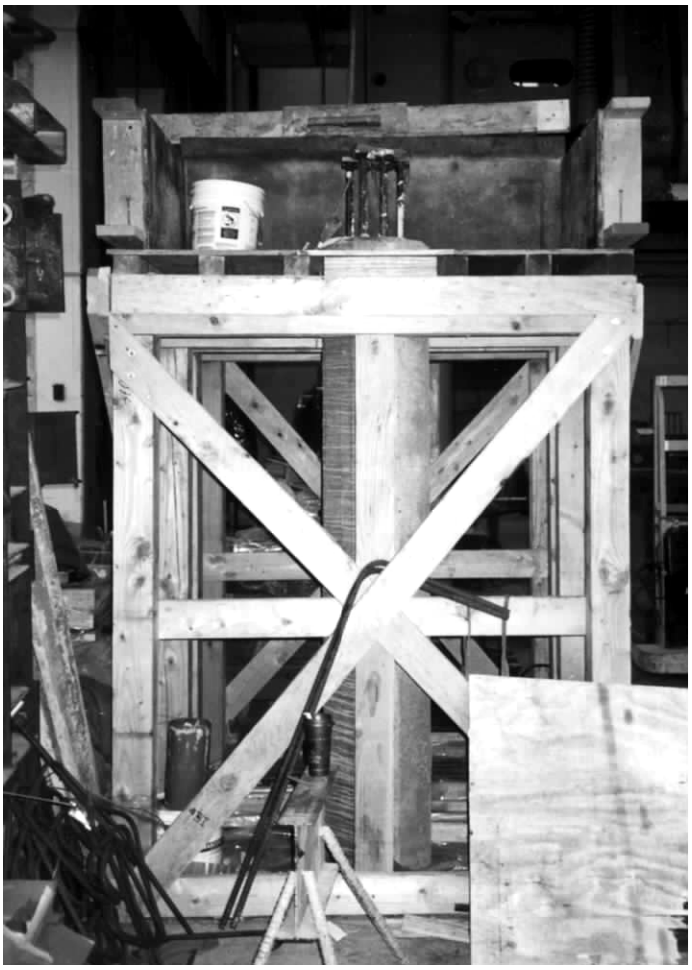

Fig. 3.13 Photo of Formwork Support Structure and Piles during Construction

Construction of the specimens began with cutting grooves along the length of selected dowel reinforcing bars and mounting strain gauges to the bars. In the cases of Specimens 1 and 2, the pile extension reinforcing bars were tied and placed in the forms. Specimens 3–8 utilized prestressed pile sections, and reinforcing bars (dowels) were grouted into each of the eight corrugated ducts provided in the prestressed pile. Once the grout was sufficiently cured the pile sections were lifted using an overhead crane and placed into the formwork. Then the remaining reinforcing bars were placed into the deck slab section formwork and tied around the head of the pile.

The concrete was placed after the reinforcing bars were tied in position. The concrete for the test specimens was mixed and delivered by a local commercial supplier. It was a pea gravel mix designed to achieve a 6000 psi (41.4 MPa) 28-day strength and to facilitate placement between the closely spaced bars. The slump was between 5 and 7 in. (125 to 175 mm). This

free-flowing mix was used to overcome the amount of bar congestion that occurred in the specimens. The concrete was placed so that it had no more than 4 ft (1.2 m) of free-fall before reaching its final position to avoid separation of the aggregate. In addition, the concrete was vibrated periodically throughout placement to remove any air voids in the specimens. Concrete test cylinders were taken for material property tests. The specimens and cylinders were cured for at least 28 days prior to testing. During early days of curing, the specimens and some test cylinders were moistened periodically and covered to reduce evaporation. They were then exposed to the open air during the remainder of their curing period. These test cylinders dried out more quickly than the test specimens, and the cylinders are believed to be a lower bound on the true concrete strength. A few other test cylinders were cured in a fog room to provide an upper-bound estimate of the concrete strength. Only lower-bound estimates are provided in this report. Cylinders were tested on the day of each connection experiment and on several days prior to those dates so that the concrete strength was accurately known during and in preparation for testing.

3.4 TEST SETUP

As noted earlier, the test specimens were tested in an inverted position as depicted in Figures 3.4 and 3.14. This configuration allows the specimens to be fixed to the strong floor while mounting a hydraulic actuator to the laboratory reaction wall to displace the top of the pile as illustrated in Figure 3.14. In actual wharfs the deck moves during a seismic event relative to the pile base. In the tests the pile is displaced relative to the deck section. This is the same condition for the pile connection as seen in the actual wharf except that the pile length for the test specimen was based upon the length to the estimated inflection point of the prototype structure. An MTS hydraulic actuator with $\pm$10 in. ($\pm$250 mm) stroke was used to displace the top of the pile as shown in the figure. The actuator capacity was 83 kips (370 kN) in compression and 55 kips (245 kN) in tension. The actuator was secured to the top of the specimen using four 5/8 in. (15.9 mm) B-7 threaded rods. Each rod passed through the pile and a 3/8 in. (9.5 mm) steel plate jacketing the pile. The steel jacket distributes the force of the actuator to the pile without damaging the pile in this region. The jacket was placed around the pile and hydrostone was poured between it and the pile to provide a smooth surface for the plate bearing. These rods were then stressed to a minimum of 10 kips (44.5 kN) each to avoid any looseness in the load apparatus during testing.

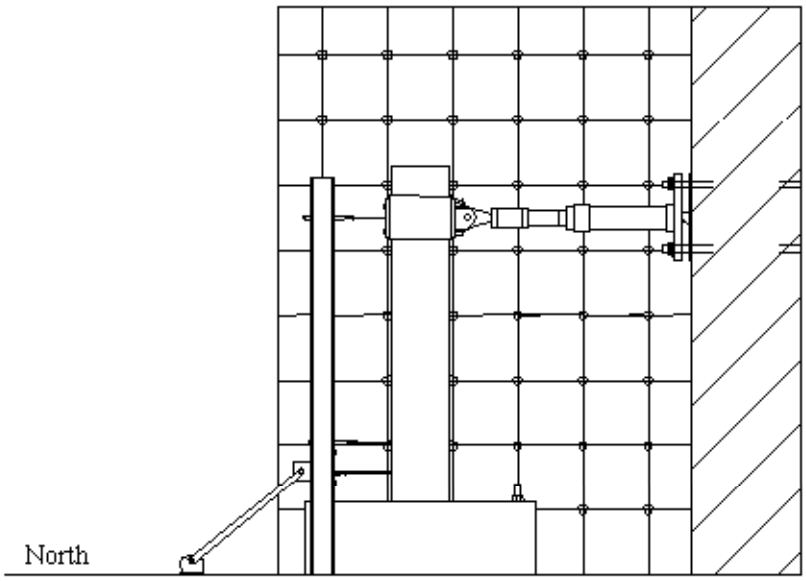

Fig. 3.14 General Test Setup

The actuator was attached to a 24 x 24 x 3 in. (610 x 610x 75 mm) plate. The plate was bearing on a pivot on the reaction wall that allowed end rotation of the actuator. The specimens were clamped to the laboratory strong floor using four 1-½ in. (38 mm) B-7 threaded rod through ducts illustrated in Figure 3.4. Hydrostone was placed between the specimen and the floor. The threaded rods were each stressed to a minimum load of 60 kips (267 kN) to avoid any rigid body movement or slip of the test specimen. Out-of-plane displacement of the pile and the actuator was controlled using a guide and bearing system that was attached to the steel jacket through a C-shaped bracket as illustrated in Figure 3.15. Two 2 in. (50 mm) diameter roller bearings were attached to the bracket, and they traveled in a track mounted to the reaction wall. The roller bearings restrained out-of-plane movement of the end of the pile, but the bearings permitted movement in the plane of loading with little resistance. Restraint of out-of-plane movement limited undue stress on the actuator and stabilized the test specimen.

Fig. 3.15 Out-of-Plane Restraint

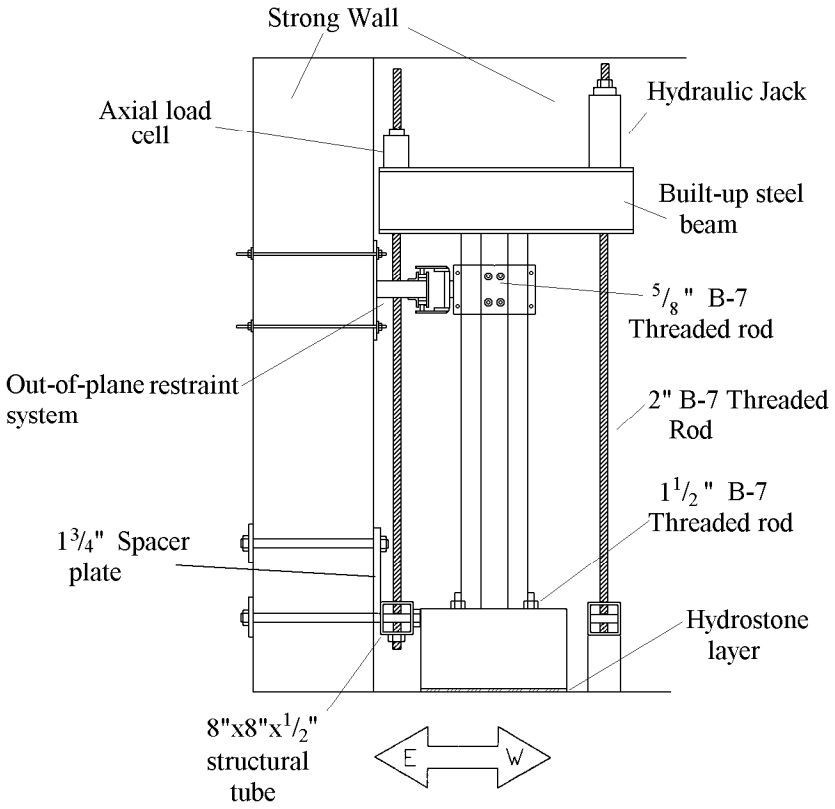

Fig. 3.16 Axial Load Apparatus

Specimens 3–8 were subject to an axial load as well as a cyclic lateral load. The axial load in the piles was accomplished by placing a built-up steel beam over the top of the pile and pulling down on either side with two 2 in. (50 mm) B-7 threaded rods as shown in Figure 3.16. On top of the built-up beam, a center hole load cell was placed over one threaded rod, while the

other threaded rod passed through a center hole hydraulic jack. The other end of the two threaded rods passed through a slotted 8 x 8 x 1/2 in. (200 x 200 x 12.5 mm) structural tube that was secured to the strong wall on the east side of the specimen and to the strong floor on the west side. Each of the rods was fitted with a conical washer on the underside of the structural tube which allowed the rods to rotate. This rotation was needed to avoid bending of the threaded rods during the test. This helped to keep the axial load as stable as possible during the test.

3.5 INSTRUMENTATION

The data acquisition system used a Pentium II 266 MHz PC running Windows 98 and LabView software. The LabView system included one potentiometer module and four strain gauge / load cell modules which provided digital data to the PC.

An MTS 100 kip (445 kN) capacity load cell was used to measure the load produced by the actuator. In addition a 200 kip (290 kN) capacity load cell was built to measure the axial load being exerted on the pile. This 200 kip load cell was capable of measuring the axial load of 222 kips (988 kN), because it was only measuring approximately one half the axial load placed on the pile due to the lever arm action of the built up steel beam seen in Figure 3.16.

Ten YFLA-2-5L 120-ohm high elongation strain gauges from Tokyo Sokki Kenkyujo Co. LTD were used in the 1/4 bridge configuration in each test specimen. The strain gauges were placed along two opposite reinforcing bars as shown in Figure 3.17. These bars were expected to experience the highest strains during testing, and the strain gauges showed the variation in strain along the bar length. This information ultimately aided in determining the transfer of moment between the pile and the wharf deck.

Both linear-variable differential transformers (LVDTs) and potentiometers were used to record displacements along the pile and the deck section as shown in Figure 3.18. Four potentiometers were used to record slip of the specimen relative to the floor. Two of these potentiometers recorded slip in the direction of the actuator force, and two recorded slip perpendicular to this direction. No slip occurred in any of the connection experiments. Four LVDTs with stroke lengths of 6 in. (150 mm) were used to measure average curvature in the pile near the pile-wharf interface. The curvature measurements were taken between threaded rods embedded in the pile at the 1/2 and 1 diameter points along the pile length and the surface of the deck section. Three LVDTs with stroke lengths of 12 in. (300 mm) were used to record horizontal deflections of the pile. The first of which recorded the deflection of the pile at the

height of the actuator. The two others recorded the horizontal deflections at 1/2 diameter (8.25 in. or 210 mm) and 1 diameter (16.5 in. or 420 mm). The actuators internal LVDT was also used to record the movement of the pile, which was fed to the data acquisition system through the MTS controller. This value was supplemented by the 12 in. (300 mm) LVDT taking a deflection reading at the same height. The exact placement of instruments varied slightly from specimen to specimen, and this detailed information is available elsewhere [Graff, 2001 and Soderstrom, 2001].

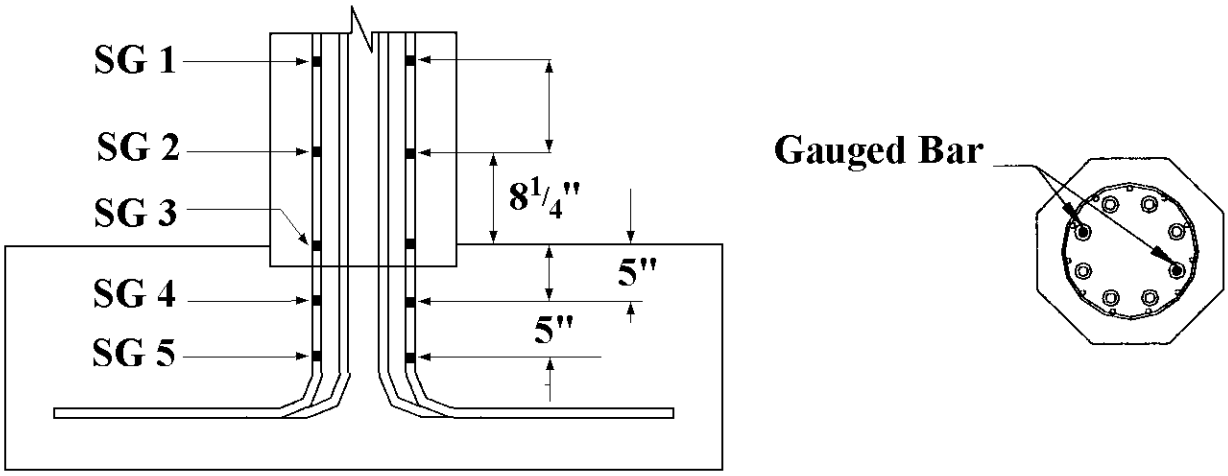

Fig. 3.17 Strain Gauges on Dowel Reinforcing

The potentiometers were powered externally by a Hewlett Packard DC power supply, model E3611A. The power supply voltage was measured and recorded along with the test data to determine if any change occurred during testing since voltage change requires an additional data correction. The data acquisition system scanned the channels 50 times per second, and recorded data according to three triggers. The three instruments used to trigger the system were the actuator load cell, actuator deflection, and horizontal deflection at one pile diameter up the pile. Each trigger compared the current instrument measurement with the last recorded value to determine whether or not to record. The value used for each trigger was changed manually throughout the test to ensure recording a minimum of 80 data points per cycle while attempting to record less than 6000 points for the entire test.

3.6 LOAD HISTORY

The specimens were subjected to lateral and axial loading. The axial load was intended to remain nearly constant during testing, and this load simulated the dead load on the prototype piles. The lateral loading was a displacement-controlled cyclic load history. The lateral load history used does not replicate any one earthquake; rather it covers a wide range of drift levels that could be expected during a strong seismic event.

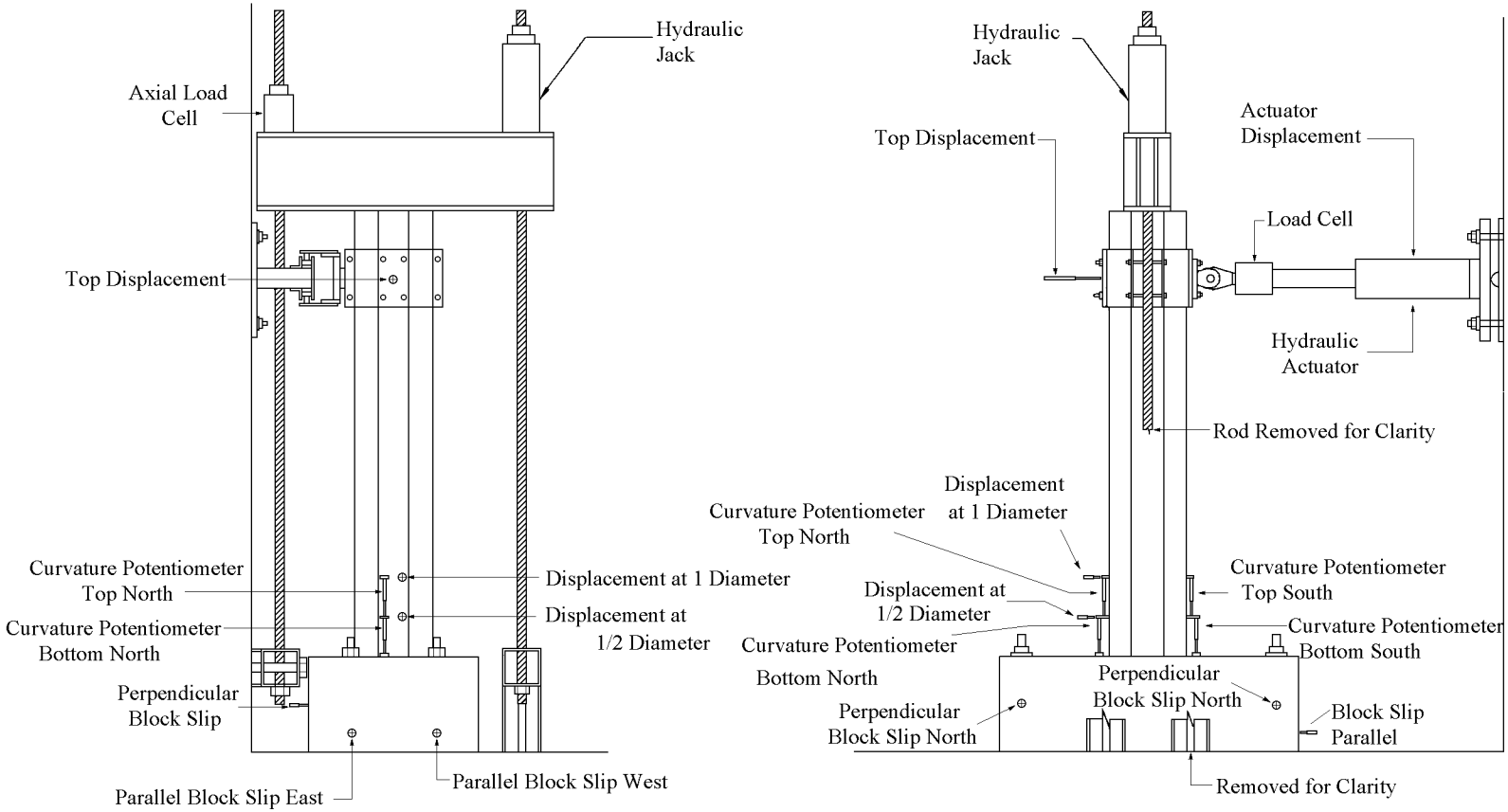

Fig. 3.18 Instruments for Deflection, Deformation, and Movement

All tests followed a predetermined deflection history with minor modifications for each individual test due to test set-up conditions. The planned deflection history was based upon the ATC-24 protocol, and it is illustrated in Figure 3.19. The predicted deflections required to obtain cracking, first yield, and plastic hinge formation were calculated for Specimens 1 and 2 as 0.055 in., 0.952 in., and 3.80 in. (1.0, 24.2, and 96.5 mm), respectively. These estimated deflections established the deformation history for all later tests.

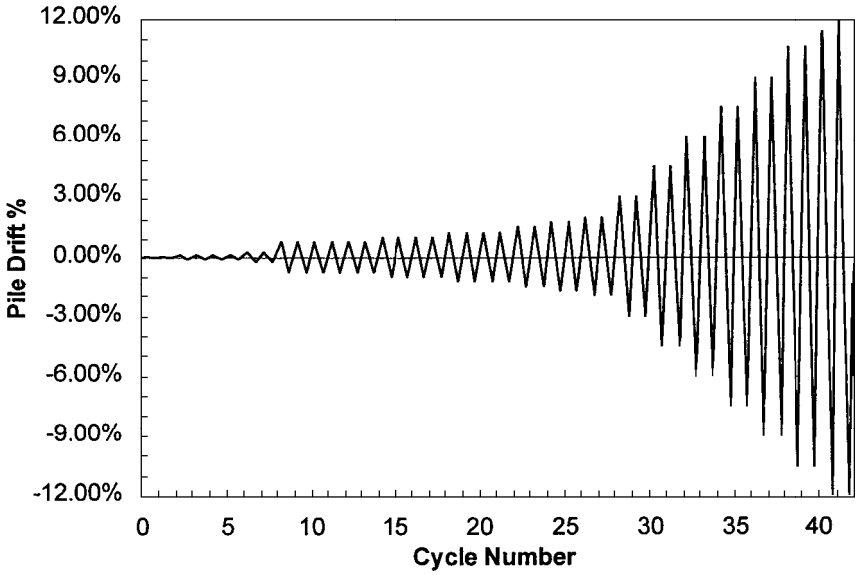

Fig. 3.19 Load Program

4 Experimental Results

4.1 INTRODUCTION

The experiments were started in August 2000 and were completed in February 2001. This chapter provides an overview and general discussion of the eight tests and an initial evaluation of the test results.

The actuator load and lateral deflection were measured directly. For specimens with no axial load, the actuator force provides an accurate indicator of the lateral resistance of the specimen and the moment resistance of the connection. However, Specimens 3–8 had axial loads applied through the load apparatus illustrated in Figures 3.17 and 3.18. This axial load travels with the horizontal actuator as can be seen in the figures. As a result of this movement, the axial load contains both a vertical and a horizontal component as illustrated in Figure 4.1. This horizontal component of force opposes the actuator force when the specimen is forced to larger deformations, and it provides a misleading estimate of the effective lateral resistance of the wharf connection. As a result, this horizontal component of the applied axial load must be deducted from the measured lateral load to produce a true load vs. deflection response. The corrected lateral load, H_c, was calculated using equation 4.1:

$$H_c = H - P_x \qquad \text{(Eq. 4.1a)}$$

where

$$P_x = P \sin\theta_2 \qquad \text{(Eq. 4.1b)}$$

$$\theta_2 = \tan^{-1}\left(\frac{\Delta 2}{L2}\right) \qquad \text{(Eq. 4.1c)}$$

$$\Delta 2 = \frac{L3\ \Delta 1}{L1} \qquad \text{(Eq. 4.1d)}$$

H is the lateral load measured by the actuator, P is the inclined axial load, and P_x is the horizontal component of P. Figure 4.1 shows the geometry used to define the correction given in the equation.

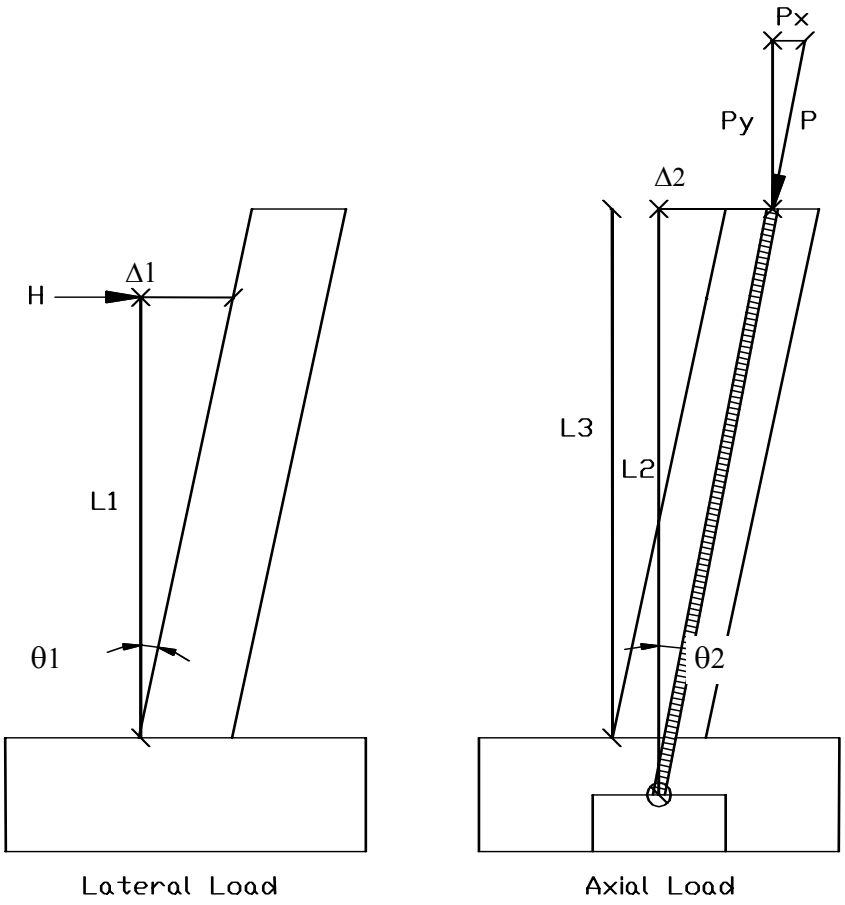

Fig. 4.1 Lateral Load Correction

The horizontal displacement of the actuator, Δ1, was measured from two independent sources. The MTS actuator contains an internal LVDT, which monitors this displacement and was used to provide the displacement control to the test. However, a separate potentiometer also recorded this displacement as illustrated in Figure 3.18. This potentiometer was used for displacement measurements reported in the load-deflection graphs that follow because the actuator's LVDT may include deformation of the actuator. However, this potentiometer was sometimes removed at large deflections to prevent damage to instruments, and the internal LVDT data were used under these circumstances. These lateral force-deflection curves are shown and discussed in this chapter. The lateral load plots do not provide an accurate indication of the actual moment resistance provide by the connections because the connection moment capacity is partly consumed by the P-Δ moments induced by axial load. As a result, moment-rotation curves are provided and discussed in Chapter 5.

4.2 SUMMARY OF EXPERIMENTS

The following is a brief summary of the eight tests. Reinforcing bars were tested from each lot purchased. The yield strength and ultimate tensile strength of reinforcing bars used for Specimens 1, 2, 3, and 4 were 62.3 ksi and 104 ksi, respectively. The reinforcing bars used for dowels in Specimens 5 and 8 had yield stress and ultimate tensile strength of 71.3 ksi and 119. ksi, respectively. Finally, reinforcing bars used for dowels in Specimens 6 and 7 had 73.4 ksi and 103 ksi yield strength and tensile strength, respectively.

Specimens 3–8 employed precast concrete piles manufactured by Concrete Technology Corporation. These piles had a concrete strength of 4,445 psi at the time of release of the prestress. The strength at 21 days was 9,810 psi, and the concrete strength at the time of testing exceeded 10,100 psi. The strength of concrete in the deck section and the grout strength varied with each test specimen and are provided in the following descriptions.

4.2.1 Specimen 1

Specimen 1 evaluated a pile extension with the outward bent dowel connection. The specimen was tested on August 21, 2000, 53 days after the concrete in the pile and deck was placed. No axial load was applied. By that date the strength of the concrete for the pile extension and the deck section was 8790 psi (60.6 MPa). Figures 4.2 and 4.3 show the crack patterns and photos of damage level observed at various drift levels. Figure 4.4. shows the corrected lateral load-deflection behavior of the specimen. The specimen developed small cracks at the base of the pile during the 0.10% drift cycle when the bending moment was 300 kip-in. (33.9 kN-m) at the pile-deck interface, and distribution and length of cracking grew with increasing deformation levels. The bending moment at the connection interface reached 1420 kip-in. (160.5 kN-m) by the 1.0% drift cycles, and the cracked region extended approximately 65 in. (1.65 m) from the interface. Small cracks were observed in the deck. Figure 4.3a shows the connection at this drift level. Vertical cracks in the side of the deck were noticed at 1.25% drift and are shown in Figures 4.2 and 4.3b. Small vertical cracks were also present on the north and south faces of the pile, which are not shown in the figures.

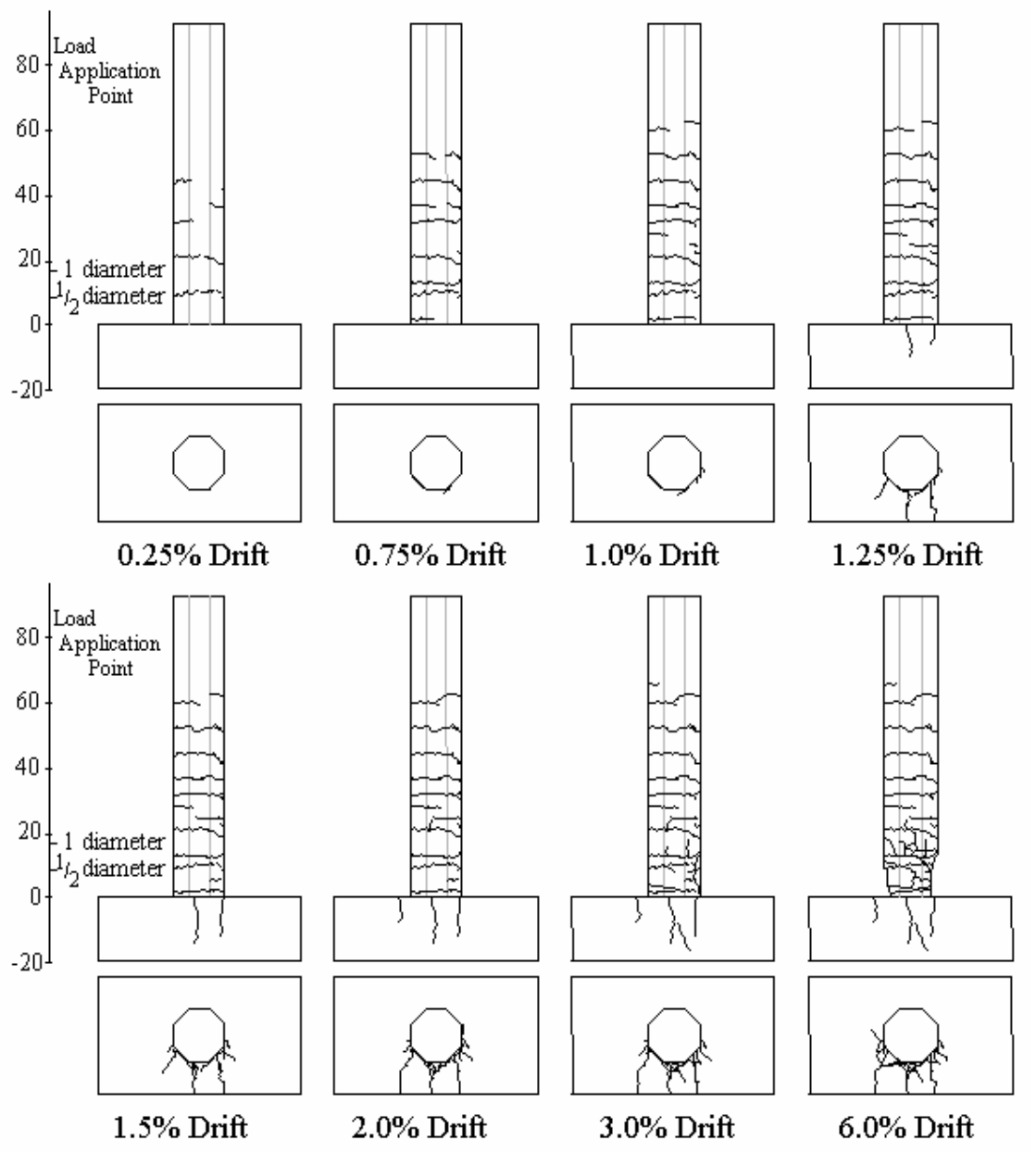

Fig. 4.2 Crack Patterns Observed in Specimen 1

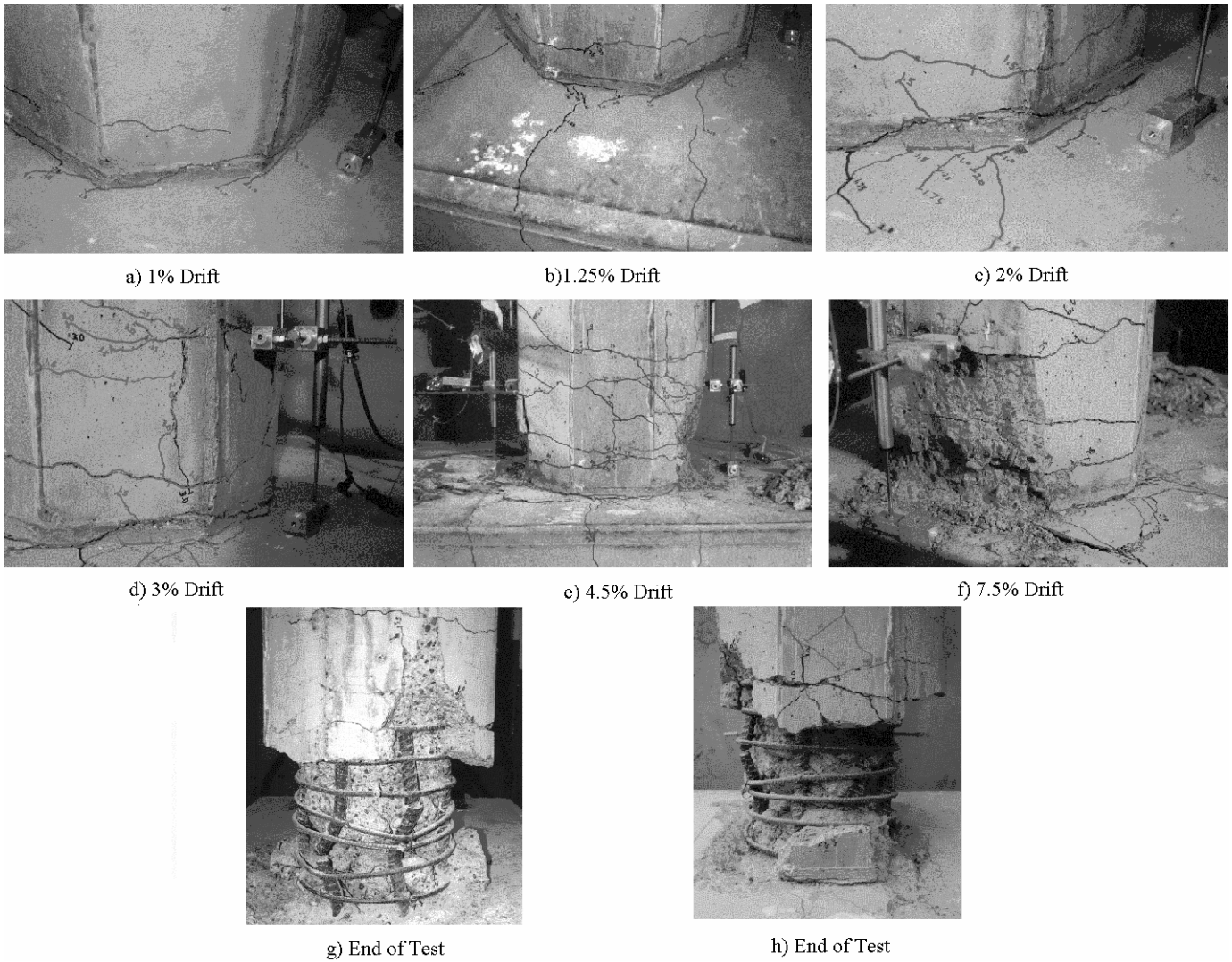

Fig. 4.3 Photographs of Specimen 1 at Various Drift Levels

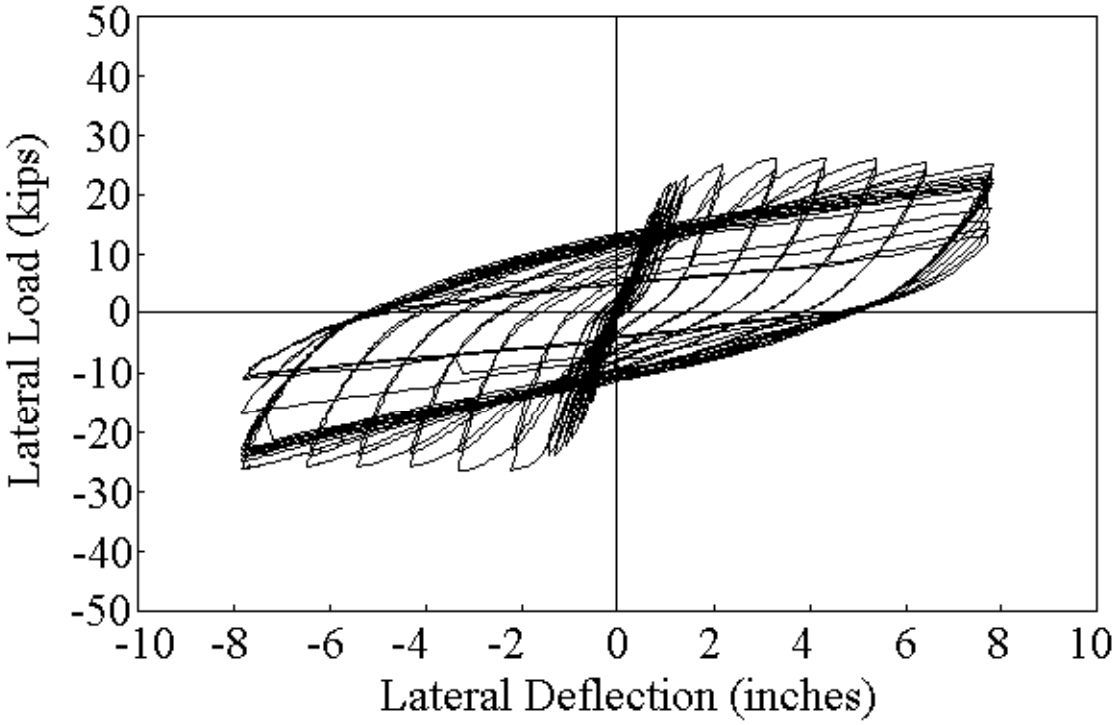

Fig. 4.4 Corrected Load-Deflection History for Specimen 1

Slight spalling, which is just visible in the Figure 4.3c photograph, first occurred at the base of the pile at 2.0% drift and continued to increase throughout the rest of the test, as shown in Figures 4.3d and 4.3e. Figure 4.3e clearly shows spalling extending approximately 1/2 pile diameter from the interface at 4.5% drift. Also visible in this photograph is a piece of the deck slab that began to break off on the pile's northwest side during the 4.5% drift cycles. At 7.5% drift the spiral in the pile was exposed, as shown in Figure 4.3f, and at 9.0% drift the pile reinforcement was visible on the north side.

After the predetermined loading plan was completed, the deflection was increased to the 10.6% drift level and 14 loading cycles were performed. This was the maximum deflection the setup and positioning of the specimen allowed. The test was stopped after the two north reinforcing bars had fractured in the 12^{th} and 14^{th} cycles and the load capacity dropped by 50%. Figure 4.2 shows the cracks in the pile and deck at the conclusion of the test, and Figures 4.3g and h shows the fractured rebar at this point.

Specimen 1 had very good distribution of inelastic deformation as noted in the broad distribution of cracking in the photos of Figures 4.2 and 4.3. A large number of inelastic cycles

were required to ultimately fracture the steel reinforcement. The hysteretic behavior was stable with only modest deterioration in resistance at larger drift levels. The behavior was typical of that expected in flexural yielding of beams.

4.2.2 Specimen 2

Specimen 2 was identical to Specimen 1 except that spiral reinforcement was continued into the deck section as illustrated in Figure 3.8. No axial load was applied. The specimen was tested on September 7, 2000, 70 days after the concrete in the pile and deck was placed. The concrete strength for the pile extension and the deck section was 9080 psi (62.6 MPa) by that date.

Specimen 2 first developed small cracks at the base of the pile during the 0.10% drift cycle, when the bending moment reached 200 kip-in. (22.6 kN-m) at the pile-deck interface. Upon further loading, cracking in the pile increased — initially at intervals of approximately 9 in. (225 mm) along the pile length as shown in Figure 4.5. At 0.25% drift, Figure 4.5 shows that the cracked region extended approximately 68 in. (1.73 m) from the pile-deck interface by 1.0% drift. Cracking in the deck was first observed at 0.75% drift, when the interface bending moment was 1100 kip-in. (124.3 kN-m). Figures 4.5 and 4.6a show the deck cracks at 1.0% drift.

Spalling started at 1.75% drift and increased during each cycle as shown in Figure 4.6. Figures 4.5 and 4.6d show extensive cracking and spalling extending 1/2 pile diameter from the interface at 6.0% drift. In the 4.5% and 6.0% drift cycles, 45° cracks appeared in the center of the deck as pictured in Figs 4.5 and 4.6e. The spiral reinforcement was exposed during the 7.5% drift cycles and is visible in Figure 4.6e. Figure 4.6f shows the deck concrete beginning to separate and break off at 9.0% drift.

As was done in the testing of Specimen 1, additional cycles were added after the end of the predetermined loading plan. Two cycles were completed at the 10.6% drift level then seven were completed at a nominal 11.6% drift. The actuator had difficulty operating at this extreme stroke. This occurs because of geometric changes that occur at large deformations of the pile. The erratic behavior of the actuator is visible in the load-deflection plot in Figure 4.7. As a result, this large deformation was not employed in the other seven experiments. The vertical reinforcement was first exposed on the north side of the pile during the 3rd cycle of the 11.6% drift level. Testing was concluded after one south reinforcing bar fractured in the 4th cycle and

the two north reinforcing bars fractured in the 5th and 7th cycles. Figures 4.6g and h show the pile and fractured north rebar at the conclusion of the test. The final load capacity was 45% of the peak load capacity.

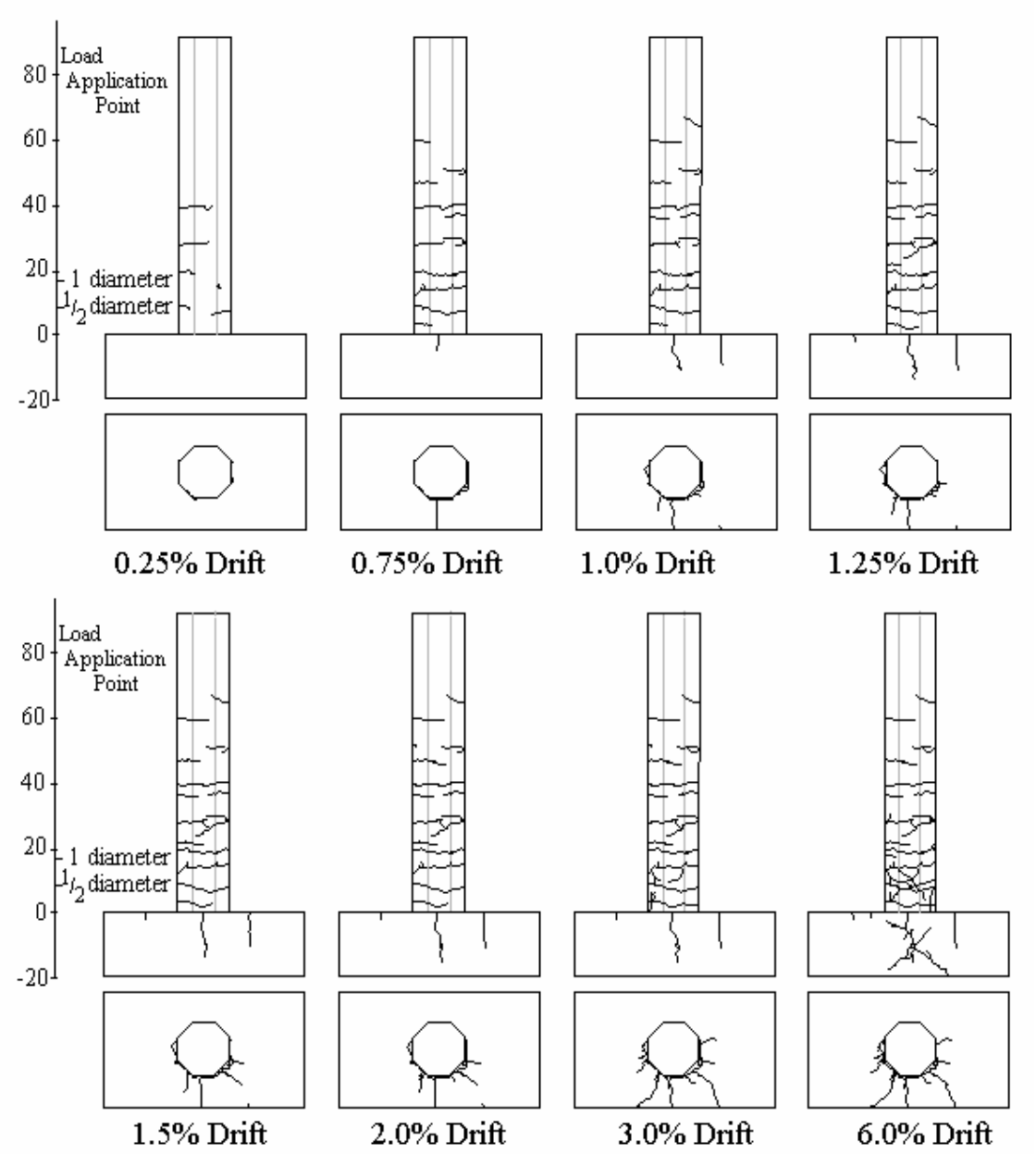

Fig. 4.5 Crack Patterns Observed in Specimen 2

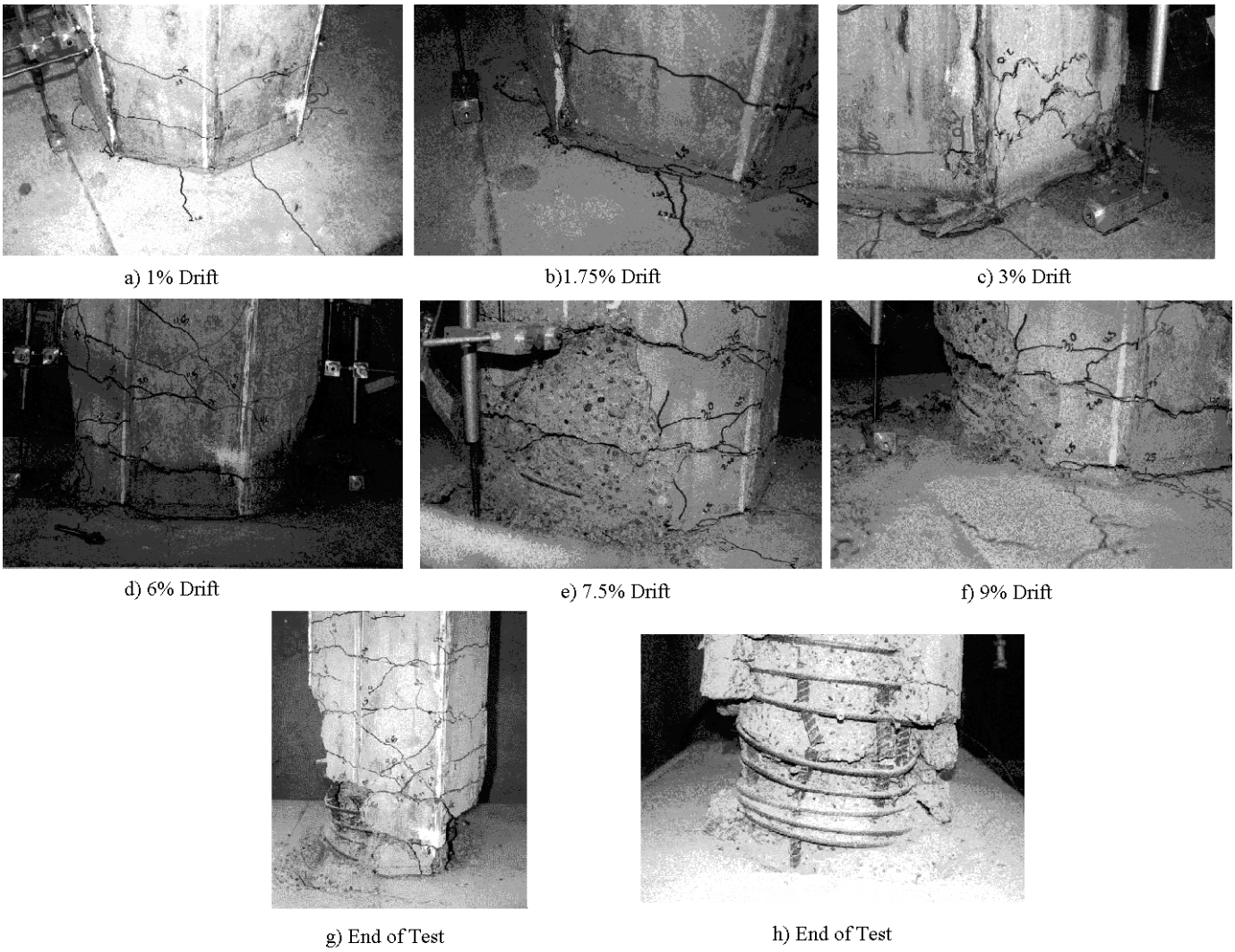

Fig. 4.6 Photographs of Specimen 2 at Various Drift Levels

Specimen 2 also had very good distribution of inelastic deformation over the height of the pile extension as noted in broad distribution of cracking in Figure 4.5 and the photos of Figure 4.6. Comparison of Figures 4.5 and 4.2 shows that the effect of continuing the spiral reinforcement into the deck section was primarily to induce earlier cracking of the deck section and to increase the extent of the deck section cracking. A number of inelastic cycles again were required to ultimately fracture the steel reinforcement. The hysteretic behavior was stable with only modest deterioration in resistance at larger drift levels as shown in Figure 4.7. The behavior was typical of that expected in flexural yielding of beams.

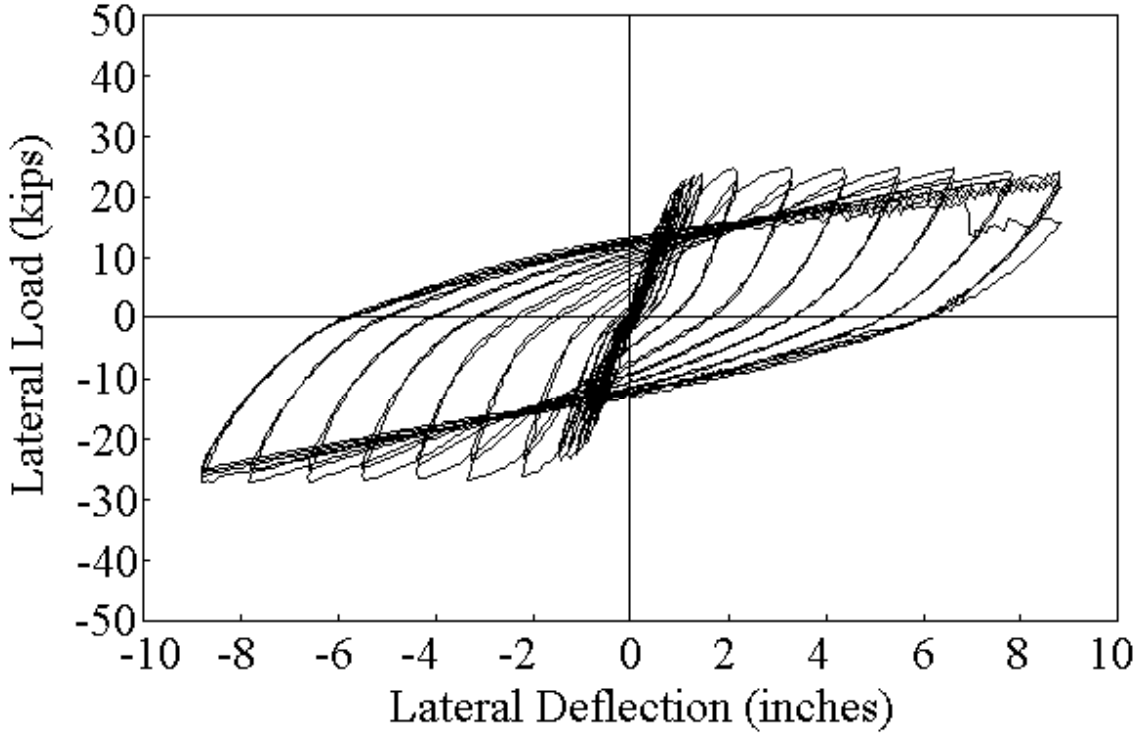

Fig. 4.7 Corrected Load-Deflection History for Specimen 2

4.2.3 Specimen 3

Specimen 3 evaluated a precast concrete pile with an outward bent dowel connection. Figure 3.9 illustrates the design of this specimen. The specimen was tested on October 24, 2000. This was 32 days after the deck concrete was placed. The concrete strength for the deck section and the grout strength were 7,680 psi and 8710 psi (52.9 and 60 MPa), respectively. The specimen had no axial load during testing. Cracking was first visible around the pile base during

the 0.10% drift cycle, and the moment at the pile-deck interface prior to cracking was 380 kip-in. (41.8 kN-m). This initial cracking moment was greater than the moment that initiated cracking in Specimens 1 and 2. Pile cracking increased upon further loading, extending approximately 36 in. (900 mm) from the base at 1.25% drift, as illustrated in Figure 4.8, though the cracks in the piles were concentrated in the bottom 12 in. (300 mm). Cracking in the deck was observed at 0.75% drift when the interface bending moment reached 1690 kip-in. (233 kN-m). Again, this moment was larger than the moment at which cracks formed in the decks of Specimens 1 and 2. Diagonal cracks appeared in the deck at 1.00% drift, as shown in Figs 4.8 and 4.9a. Figures 4.8 and 4.9b, c, and d show that limited additional pile cracking occurred between 1.25% and 3.0% drift, although existing cracks lengthened during that period. After 3.0% drift, a widening of the crack around the base of the pile was apparent. This crack is clearly visible in the photograph of Figure 4.9d. Spalling, which began at the 2.0% drift level, is also visible in this photo.

Figure 4.9e shows the significant increase in damage to the deck section on the south side of the specimen that occurred during the 4.5% drift cycles. Spalling continued through the 6.0% and 7.5% drift cycles. Some spalling occurred in the end segment of the pile section, but comparison of Figures 4.3, 4.6, and 4.9 shows that Specimen 3 had greater spalling in the deck section and less spalling in the pile than noted in Specimens 1 and 2. The steel driving ring in the base of the precast pile was first visible at 6.0% drift and almost completely exposed by 9.0% drift as shown in Figure 4.9g and h.

As was done with both Specimens 1 and 2, cycles of 10.6% drift were added after completion of the original loading plan. The actuator had difficulty performing at this large deflection, in part because the specimen was placed slightly closer to the wall than the other two specimens, and because of binding due to vertical deflection of the pile. After two cycles at 10.6% drift, the deflection was decreased and two more cycles of 9% drift were performed. In the first of these cycles, one of the north reinforcing bars fractured. The spiral in the pile was exposed on the north face as was the top layer of deck reinforcement on the south side. Figure 4.9h shows the connection at the conclusion of the test. Neither the prestressing strands nor the ducts containing the rebar were exposed and there was much less pile spalling than in the pile extension tests.

Only cracks in the west side of the pile and deck were recorded in Figures 4.9g and h, but it was noticed after the test that cracking of the east side of the deck was even more severe than that of the west side. A large section of the east deck seemed to be loosening, though no concrete had fallen off yet.

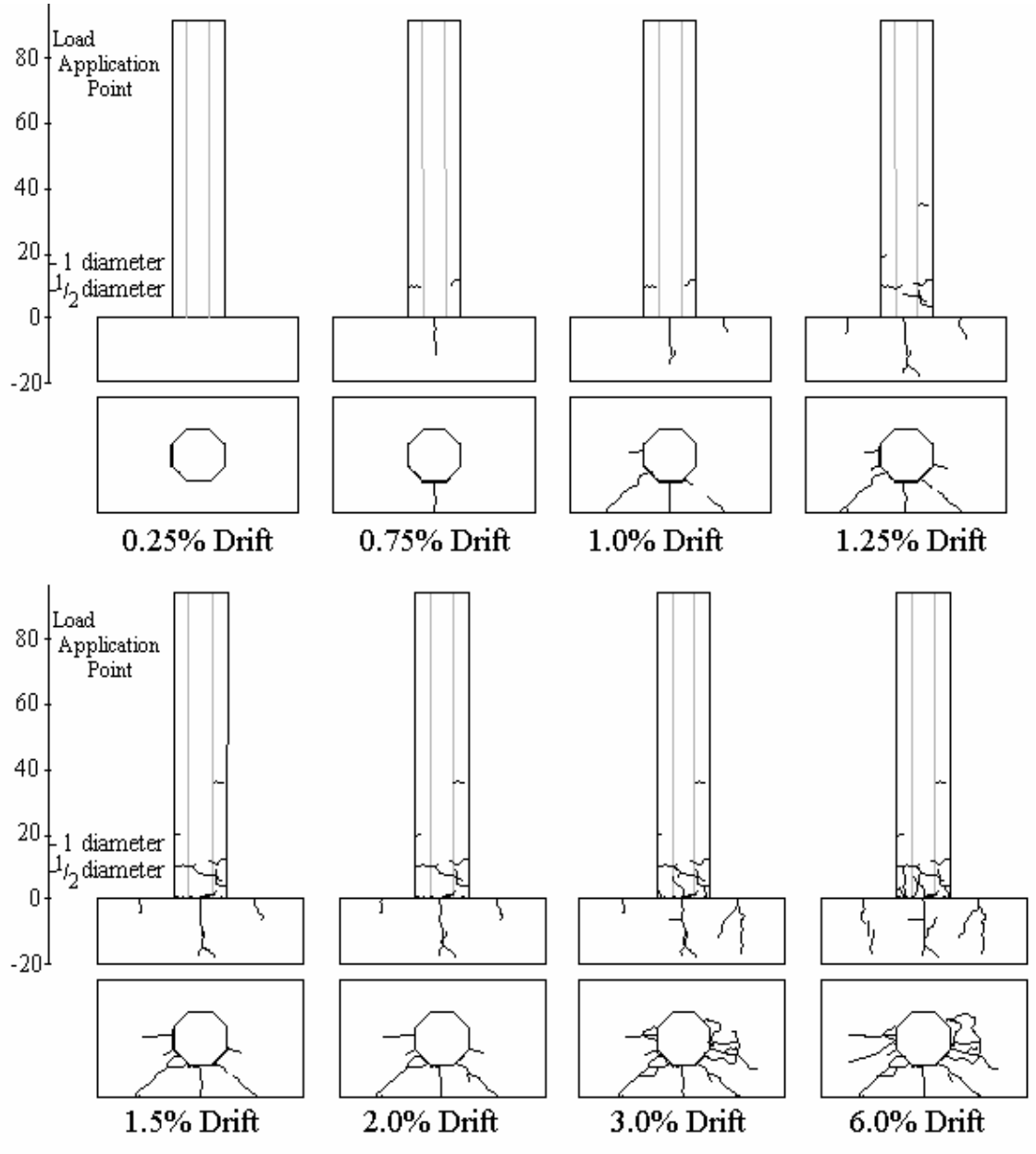

Fig. 4.8 Crack Patterns Observed in Specimen 3

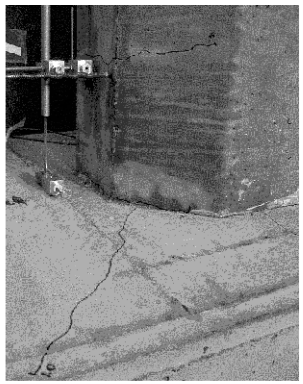

a) 1% Drift

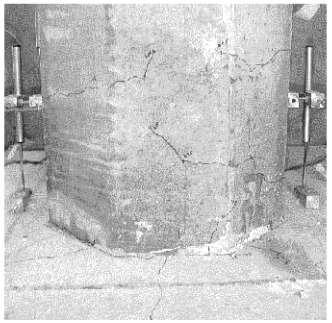

b)1.5% Drift

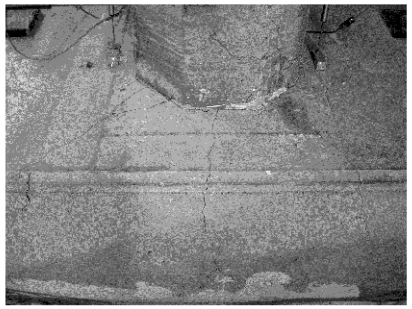

c) 1.5% Drift

d) 3% Drift

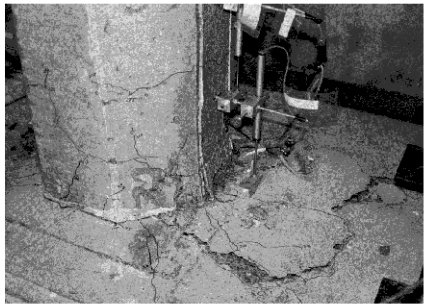

e) 4.5% Drift

f) 6% Drift

g) 9% Drift

h) End of Test

Fig. 4.9 Photographs of Specimen 3 at Various Drift Levels

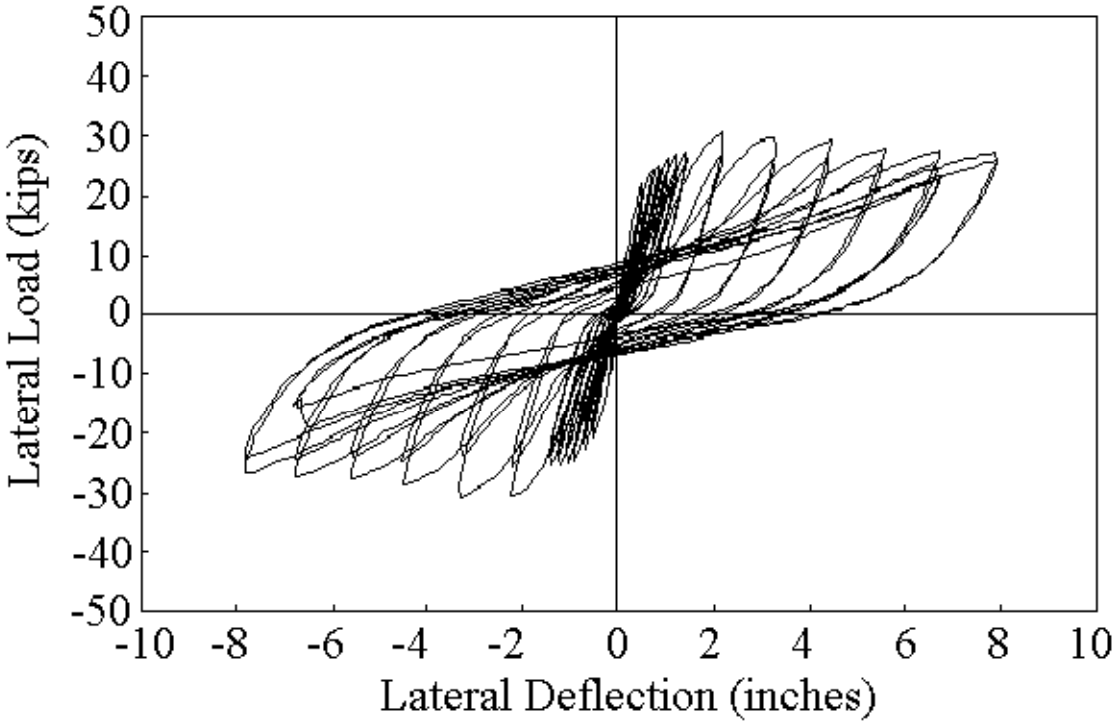

Fig. 4.10 Corrected Load-Deflection History for Specimen 3

Figure 4.10 shows the load-deflection behavior for Specimen 3. A number of large inelastic cycles again were sustained with moderate deterioration in lateral resistance. The hysteresis curves are somewhat pinched with smaller energy dissipation than noted for Specimens 1 and 2. Comparison of crack patterns and photos of damage from Specimen 3 with Specimens 1 and 2 suggests that Specimen 3 had greater concentration of damage during the inelastic deformation. The precast piles sustained only modest cracking and yielding, and this pile damage was concentrated at the end of the pile. There was greater spalling and cracking of concrete in the deck section. This suggests that the precast piles tend to concentrate the inelastic deformation into the deck section and the pile-deck interface. The precast concrete pile is commonly embedded into the deck section by approximately 2 in. (50 mm), and the limited damage to the pile results in the pile wrenching the concrete out of the deck section. The precast pile connection is somewhat stronger than the pile extension connection. This appears to be caused by the fact that the pile has both prestressing strand and dowel reinforcement. The prestressing strand is not fully developed at the ends of the pile, but it serves to strengthen the

pile in that region. This reduces the cracking and spalling of the pile section, increases the damage in the deck section, and increases the apparent resistance of the connection itself.

4.2.4 Specimen 4

Specimen 4 was of identical design to Specimen 3, but axial loads were applied during testing. The target axial load was 222 kips (988 kN), since this is approximate 10% of the ultimate capacity of the pile and an approximate scaling of the service loads in the prototype structures. The specimen was tested on January 12, 2001, 112 days after the concrete in the deck was placed. The concrete strength for the deck section was 9,880 psi (68 MPa). The grout strength was 9350 psi (64.4 MPa). Specimen 4 first developed visible cracks around the pile base during the 0.25% drift cycle when the bending moment reached 1390 kip-in. (157 kN-m) at the interface. This moment was more than 1000 kip-in. (113 kN-m) greater than the moment at which cracks were first seen in Specimens 1, 2, and 3. The later occurrence of visible cracking is not surprising because the presence of axial load increased the expected moment resistance of the connection. Cracking of the pile increased with additional loading, and while cracks extended approximately 24 in. (600 mm) from the deck, they were concentrated in a region 10 in. (250 mm) from the interface. This crack progression is illustrated in Figures 4.11 and 4.12. Cracking of the deck, first observed in the 1.0% drift cycles, is shown in the figures.

Just visible in the photograph of Figure 4.12b is the crushing and slight spalling that began at 1.50% drift. Long vertical cracks that appeared in the pile at 3.0% drift can be seen in Figure 4.12c. These cracks increased in size on both the north and south faces, shown at 4.5% drift in Figure 4.12d, until large pieces of concrete broke off in the 6.0% drift cycles. Figure 4.12e shows the area of spalling of the pile extending approximately 24 in. (600 mm) from the pile-deck interface. The pile driving ring, spiral, and prestressing strands were exposed at this point and are shown at 9.0% drift in Figure 4.12f. Cracking of the deck was much less severe than that of Specimen 3.

The lateral loading history of Specimen 4 was identical to that of Specimen 3. After the original loading plan was completed, two 10.6% drift cycles and two additional 9% drift cycles were added. Flexural bending of the axial load rods (see Fig. 3.17) was noted during these large deformation cycles. The conical washers at the base of the rods had been improperly installed and the rods were not pivoting freely. Because of the axial load system design, the axial load

applied to the pile increased as deflection magnitude increased and decreased as the pile returned to its starting position. The measured inclined axial load and its vertical component were nearly identical, because θ2 shown in Figure 4.1 was generally fairly small. The resulting variation in axial load was as much as 32% larger and 26% smaller than the target value, but the average axial loads were closer to the desired 222 kips (988 kN) at large drift angles.

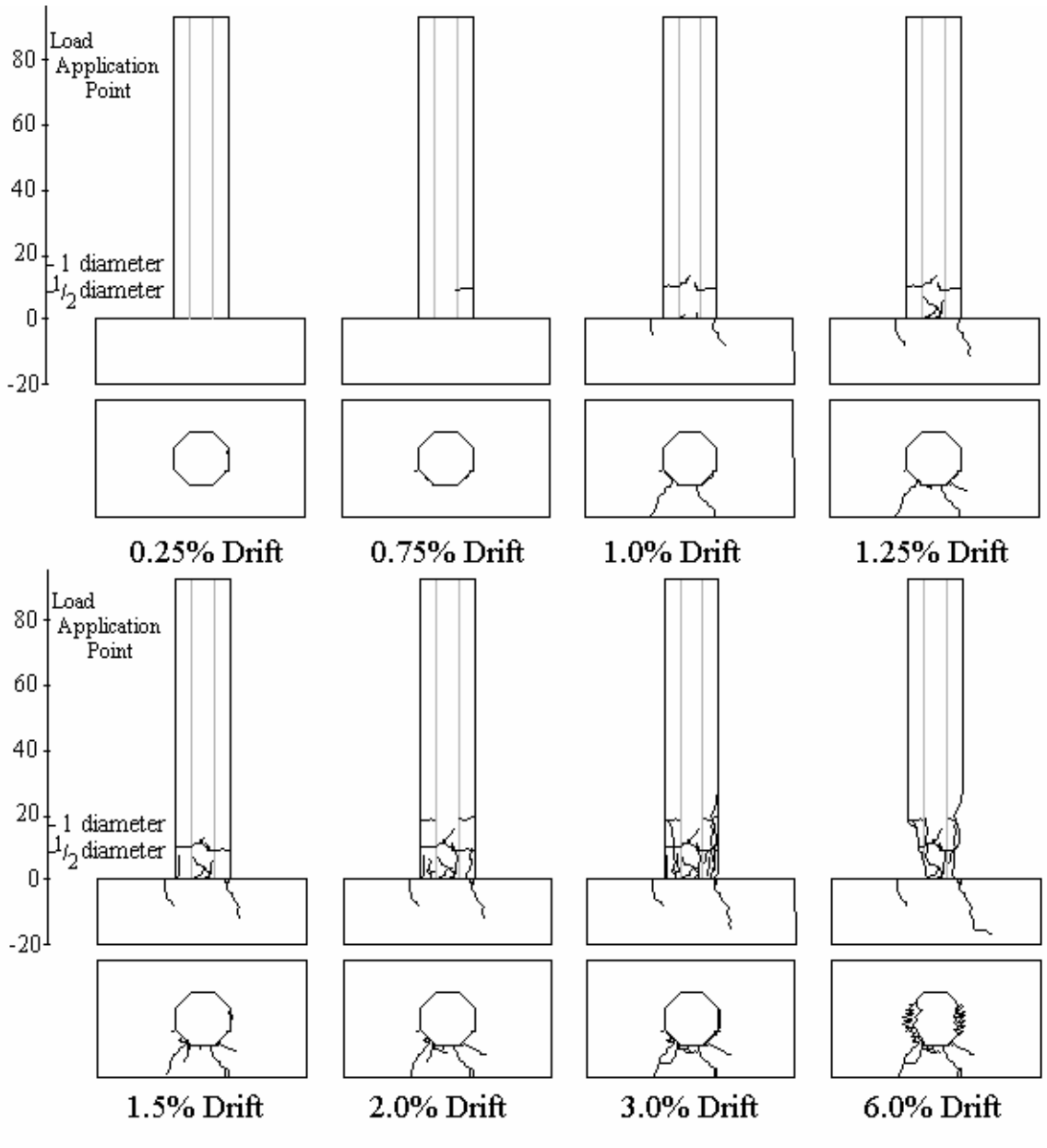

Fig. 4.11 Crack Patterns Observed in Specimen 4

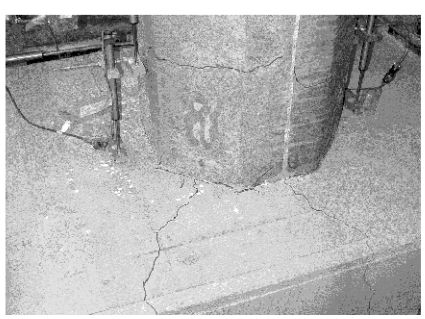

a) 1% Drift

b)1.5% Drift

c) 3% Drift

d) 4.5% Drift

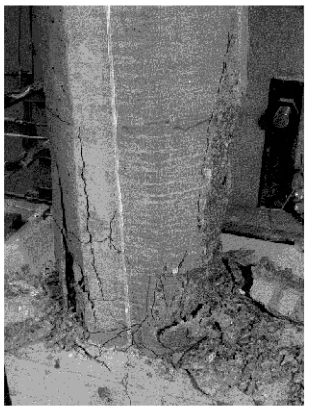

e) 6% Drift

f) 9% Drift

Fig. 4.12 Photographs of Specimen 4 at Various Drift Levels

Figure 4.13 shows the load-deflection behavior for Specimen 4. A number of large inelastic cycles again were sustained. The hysteretic behavior was stable but considerable deterioration in resistance was noted at larger drift levels. The deterioration in resistance is largely caused by the P-Δ effect, since this added moment to the pile-to-wharf connection reduces the resistance available to resist lateral loads. However, as will be shown later in this report a significant portion of this reduced resistance is caused by deterioration induced by the axial load and the concentration of damage caused by the precast concrete pile. The axial load also increases the initial connection moment resistance because of the contribution of the axial load acting through its moment arm to the neutral axis in bending. Comparison of crack patterns and photos of damage from Specimen 4 with Specimens 1, 2, and 3 suggests that Specimen 4 had significantly greater damage to both the pile and the deck section during the inelastic deformation. This greater damage also appears to be caused by the axial load because the added compressive stress due to the axial load causes greater spalling and surface damage to the pile. The precast piles sustained only modest cracking and yielding due to tension, and the results again suggest that the precast pile concentrated the inelastic deformation into the deck section.

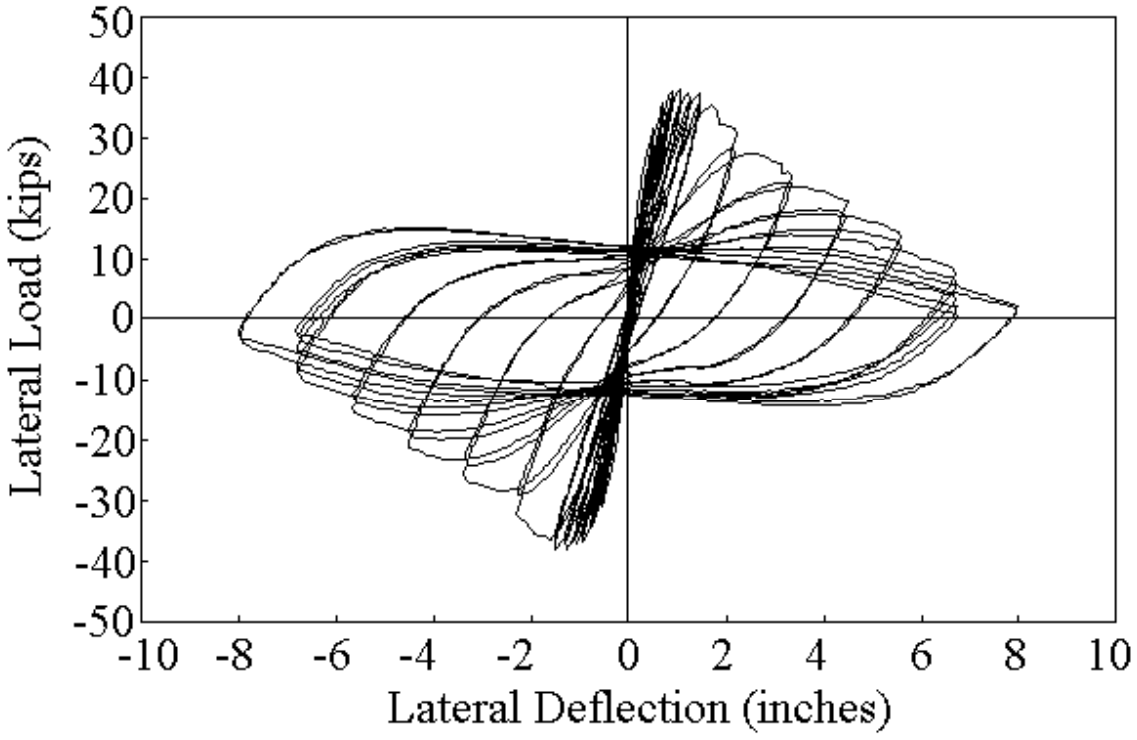

Fig. 4.13 Corrected Load-Deflection History for Specimen 4

4.2.5 Specimen 5

Specimen 5 was tested on January 22, 2001. This was 68 days after casting of the concrete deck section. The specimen had a precast concrete pile with an inward bent dowel connection. The specimen was tested under axial load, and the design of this specimen is illustrated in Figure 3.10. The deck concrete strength and the grout strength were 6,900 psi and 8,850 psi (47.5 and 61 MPa), respectively, on the day of testing. Specimen 5 first showed cracking around the base of the pile at 0.25% drift. At a drift of 0.75%, cracking occurred away from the pile-deck interface as illustrated in Figure 4.14, but most cracking was concentrated within a short distance of this interface. At 1.0% drift it was discovered that several cycles at 0.75% and 1.0% drift had been inadvertently skipped, but this should not have had a big impact on the specimen performance. Spalling on the north side of the specimen and cracking in the deck on the south side occurred at 1.25% drift as shown in Figures 4.14 and 4.15a. At 1.75% drift spalling greatly increased from previous drift levels as shown in Figure 4.15b. Additional cracking in the deck and higher up the pile began at 2.0% drift. After the first cycle of 3.0% drift the curvature LVDTs were removed and crack drawings were stopped. Larger portions of concrete began spalling at 3.0% drift, and this spalling was concentrated between the deck surface and 1/2 diameter up the pile. The axial load system suddenly released the entire axial load on the specimen at 4.5% drift. The effect of this load reduction can be seen in the load-deflection curve of Figure 4.16. Recovery of this axial load required considerable work on the load frame, and it was decided to complete the test without any axial load on the specimen. Specimen 5 also showed delamination of the deck immediately after the loss of axial load, and this suggests that the axial load may suppress delamination.

Immediately after resuming the test the north side of the deck began to delaminate as seen in Figure 4.15c. Once 6.0% drift was reached a smaller delamination occurred on the south side of the deck. The actuator began making noise once a drift of 9.0% had been reached. This noise appeared to be caused by binding of the actuator induced by the large deflections. At this drift level additional cracks were seen in the side of the deck. The test was then completed with 2 cycles at 10.61% drift.

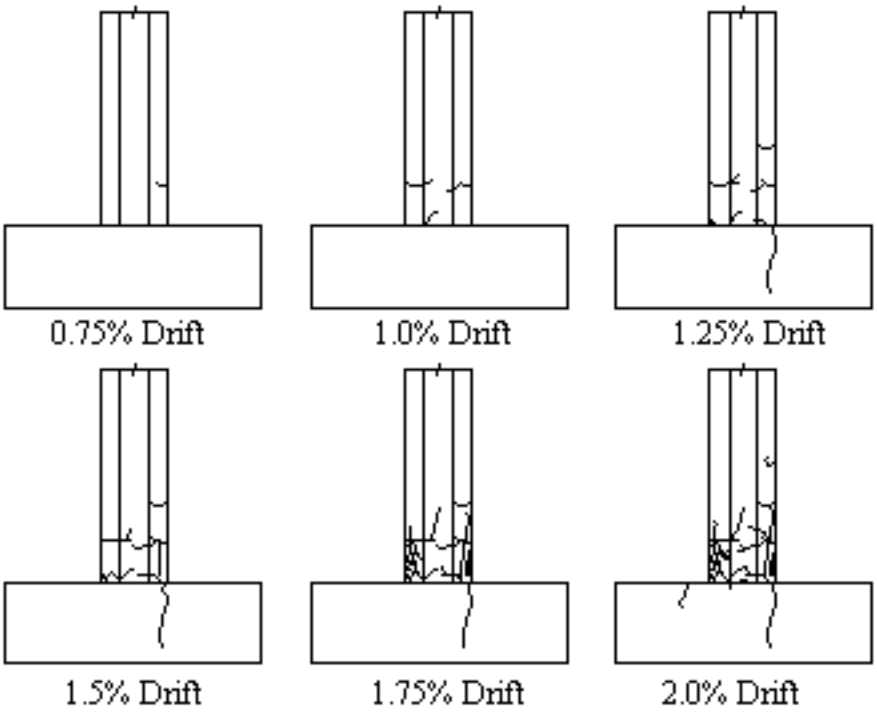

Fig. 4.14 Crack Patterns Observed in Specimen 5

The load-deflection curves of Specimens 4 and 5 (Figs. 4.13 and 4.16) are not directly comparable at very large deformations because Specimen 5 had lost its lateral load capacity at fairly large deformations. However, the performance up to the 4.5% drift level is nearly identical as can be seen by comparing Figures 4.13 and 4.16. The cracking and spalling patterns are also very similar for Specimens 4 and 5, and therefore there does not appear to be a significant difference in behavior noted with the outward bent dowel and inward bent dowel connections. Figure 4.16 shows a significant loss of resistance at large deformations even though no axial loads (and resulting P-Δ moments) are present. Comparison of this reduced resistance with that noted for Specimen 3 in Figure 4.10 at these same large deformations indicates that the axial load applied during smaller deformation cycles caused increased deterioration and damage to the connection at larger deformations. A number of large inelastic cycles again were sustained by the specimen. The hysteretic behavior was reasonably stable with slight deterioration in resistance with repeated cycles. Specimen 5 also had significantly

greater damage to both the pile and the deck section during the inelastic deformation than the pile extension connections and specimens without axial load.

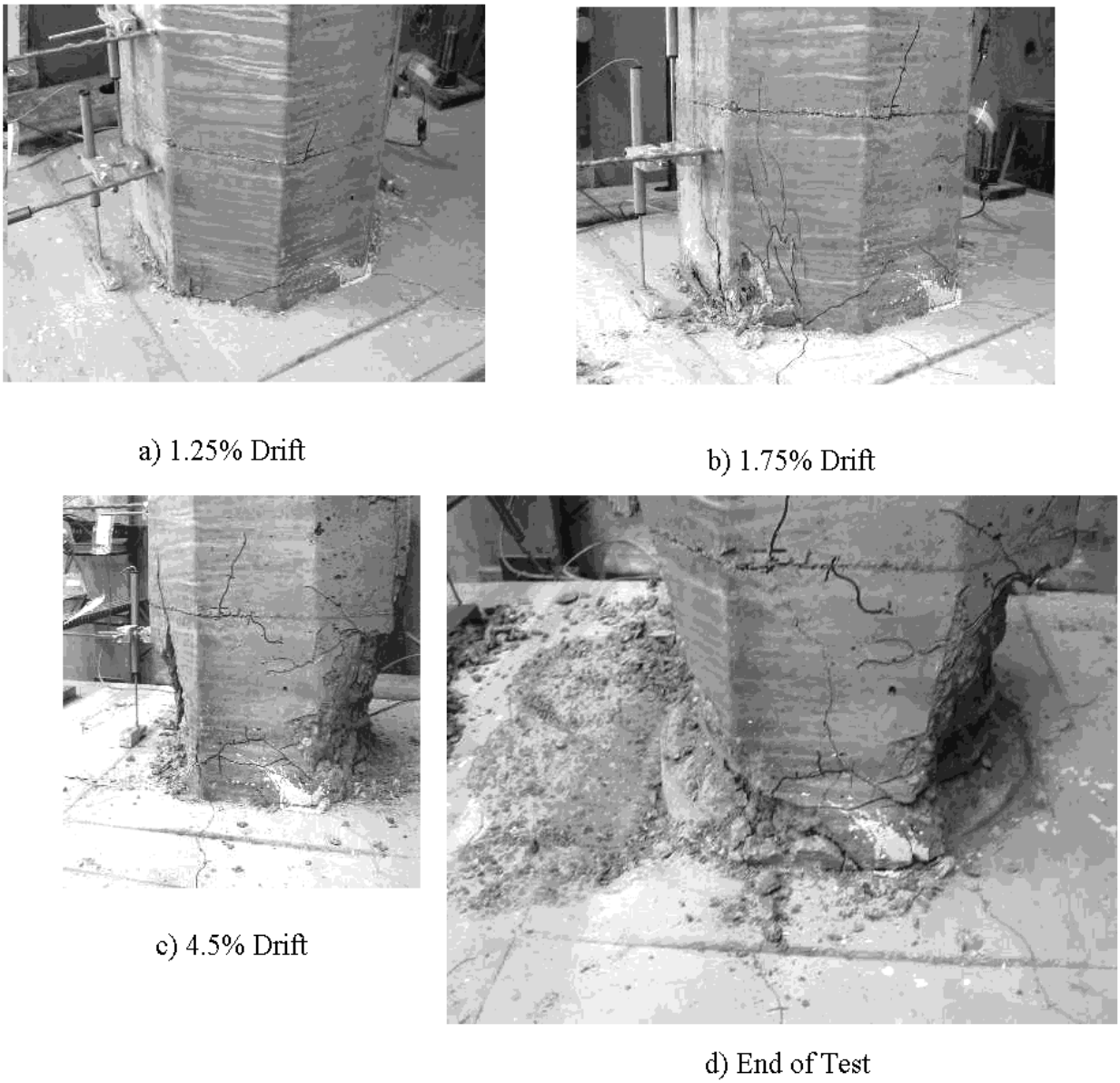

Fig. 4.15 Photographs of Specimen 5 at Various Drift Levels

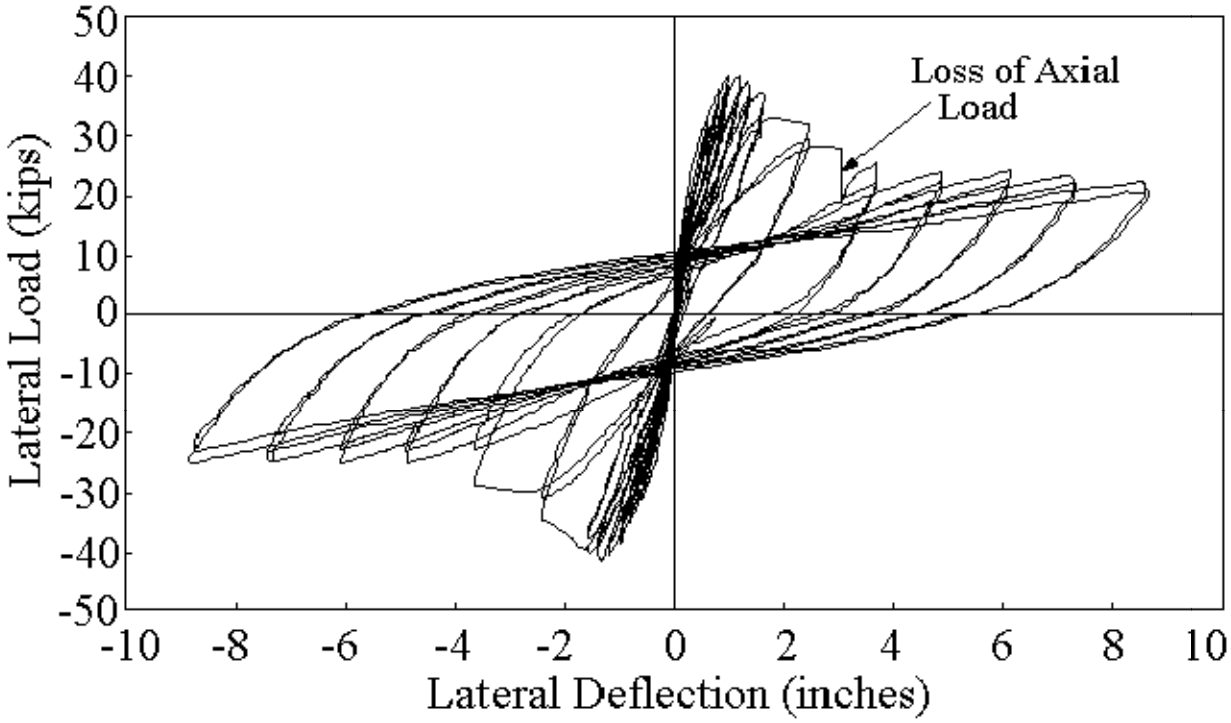

Fig. 4.16 Load-Deflection History for Specimen 5

4.2.6 Specimen 6

Specimen 6 was a T-headed bar connection with details as shown in Figure 3.11. This specimen was tested on February 6, 2001. This was 82 days after casting of the deck section, and the concrete and grout strengths were determined to be 6,800 psi and 7,650 psi (46.8 and 52.7 MPa), respectively. The specimen first showed cracking around the pile-deck interface at 0.75% drift (see Fig. 4.17). Once a drift of 1.25% drift was reached cracking in the base had begun and crushing on the north side of the pile was observed as shown in Figures 4.17 and 4.18a. The east side of the deck showed cracks indicating that the deck surface was delaminating at this drift. By a drift level of 1.75% the crushing on the north side had increased and crushing on the south side had begun. In addition the deck on the south side began to delaminate. Once 3.0% drift was reached spalling had started and additional signs of delamination were seen on the south side of the deck. The curvature LVDTs were removed and crack drawings were stopped at 3.0% drift. At 4.5% significant spalling of the concrete at the end of pile and delamination or separation of the deck section concrete were visible as shown in

Figure 4.18c. Increased spalling and the exposure of the spiral and prestressing strands occurred at 6.0% drift. The final state of the specimen can be seen in Figure 4.18d.

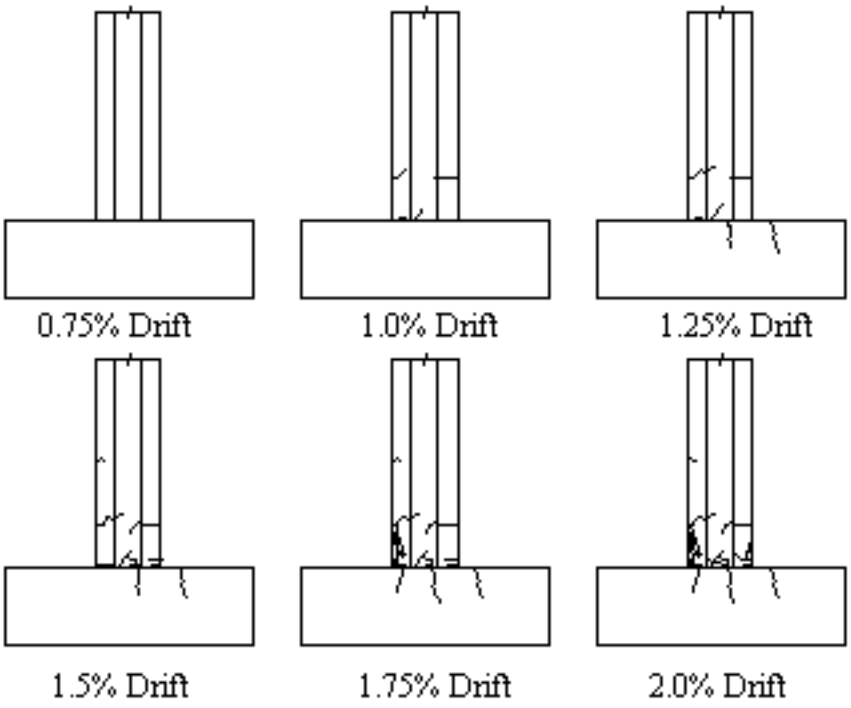

Fig. 4.17 Crack Patterns Observed in Specimen 6

Specimen 6 showed cracking similar to that noted for Specimens 4 and 5. Cracking was concentrated at the pile-deck interface, but the severity of the cracking in this specimen was less than was seen in the other specimens. Specimen 6 also showed practically no cracking above one diameter up the pile, while the other specimens had numerous cracks above this point.

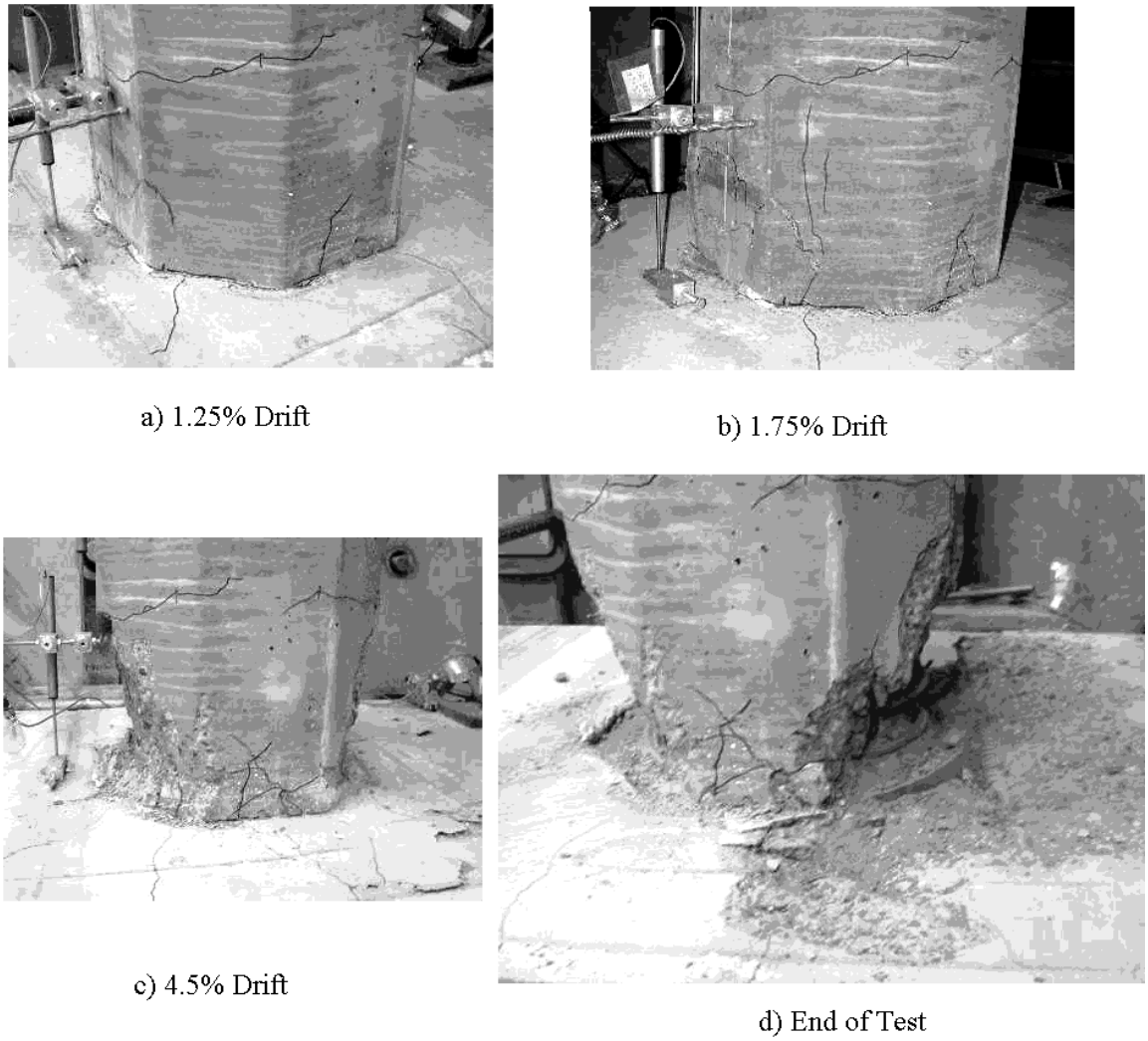

Fig. 4.18 Photographs of Specimen 6 at Various Drift Levels

Figure 4.19 shows the load-deflection curves of Specimen 6. The deterioration in resistance at large deformations is great. Part of this loss of resistance is caused by the P-Δ moments, but a significant portion is caused by damage to the pile and connection cause by the large cyclic deformations combined with the axial load. Nevertheless, the specimen tolerated quite large connection rotations and deformations.

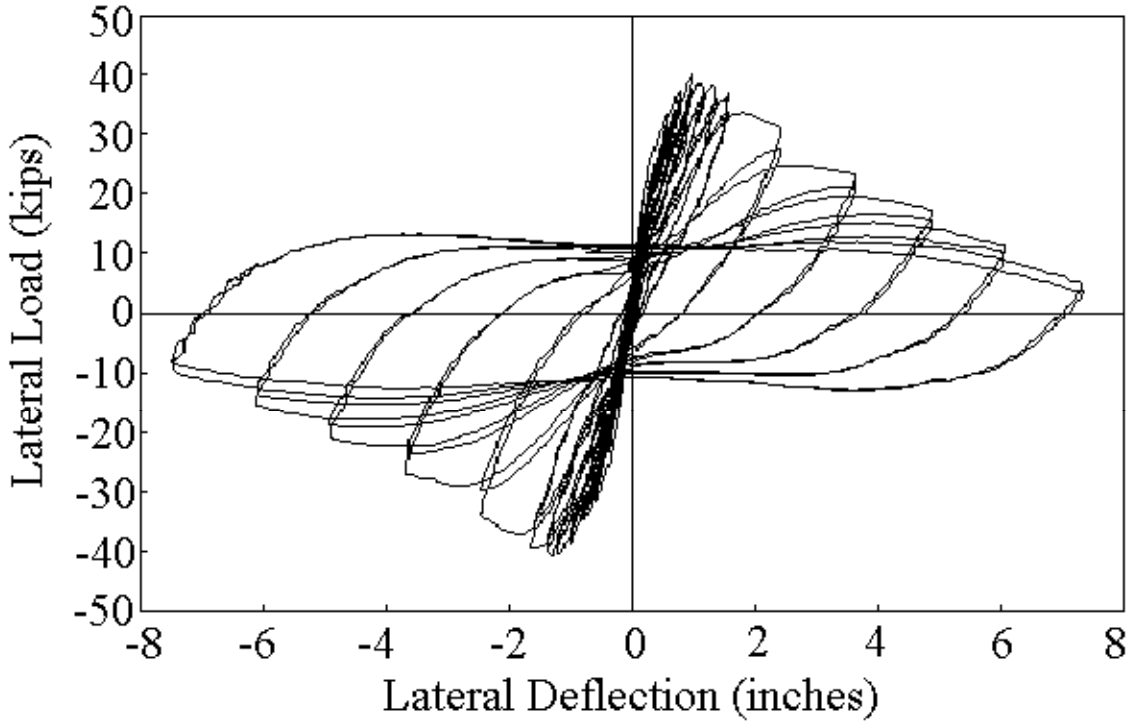

Fig. 4.19 Load-Deflection Curves for Specimen 6

4.2.7 Specimen 7

Specimen 7 was the bond bar connection with design as illustrated in Figure 3.12. The specimen was tested on February 12, 2001. This test was 63 days after the concrete was cast, and the strengths of the deck concrete and dowel grout were 8,900 psi and 8,650 psi (61.3 and 59.6 MPa), respectively. The first cracks in the specimen occurred at 0.75% drift at the pile-deck interface and up the length of the pile on the north side as shown in Figure 4.20. At a drift of 1.0% cracks appeared along the length of the pile on the south side. Once 1.25% drift was reached spalling of the deck on the north side had begun as seen in Figures 4.20 and 4.21a. Additional cracking of the deck occurred at 1.5% drift. Spalling of the pile was seen on both sides by 1.75% drift. During the first half cycle at 3.0% drift the hydraulic pump overheated, and the system shut down. This caused the pile to return to the zero position. After recovery of the pumping system, the test was resumed with no loss of test data. At this drift level, the top displacement LVDT was removed and the last crack drawings were done. At 4.5% drift the curvature LVDTs were removed along with the 1/2 diameter displacement LVDT. The spiral

within the pile became visible at 6.0% drift. The final state of the specimen can be seen in Figure 4.20d.

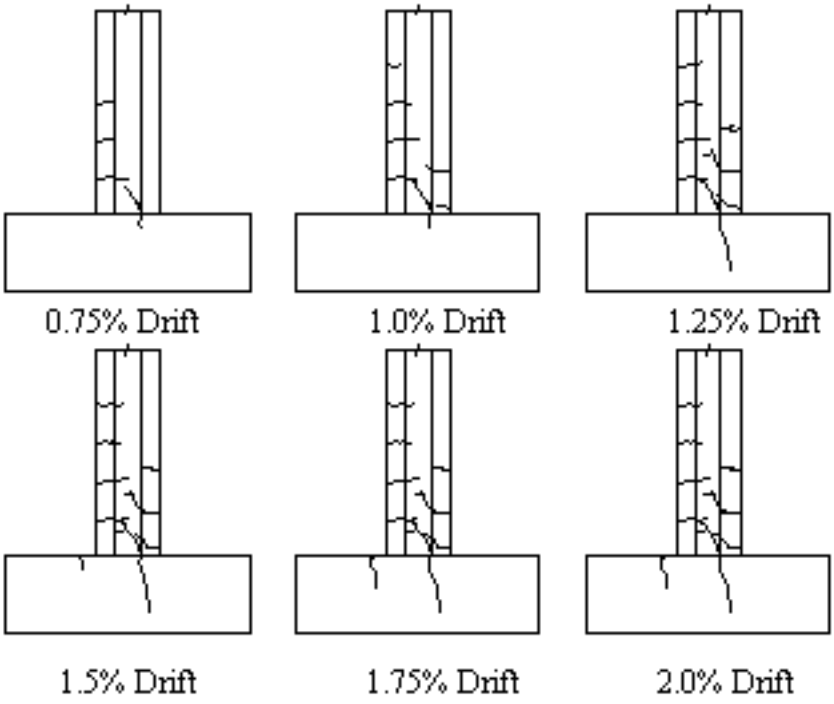

Fig. 4.20 Crack Patterns Observed in Specimen 7

The primary concrete cracking occurred at or very near to the pile-deck interface, but comparison of Figure 4.21 with crack patterns of Specimens 5 and 6 suggests that Specimen 7 sustained more cracking over the entire pile length than the other specimens. Further, comparison of the photo of the final damaged state in Figure 4.21d with photos of Specimens 5 and 6 shows that spalling occurred along a greater length of the pile in Specimen 7. Specimen 7 also showed no signs of delamination of the deck, which appeared in all the other specimens. Figure 4.22 is the lateral load-deflection curve for Specimen 7. Comparison of Figures 4.13, 4.19, and 4.22 suggests that the overall load-deflection behavior for Specimens 4, 6, and 7 are similar. Specimen 7 showed the smallest resistance of the specimens, but the difference was not large. As with the other specimens, Specimen 7 shows great loss of effective lateral resistance at large lateral deformation. Some of this loss is caused by the moments required to resist P-Δ

moments, but a considerable portion of this loss in resistance is caused by deterioration of the connection due to concrete spalling and other damage.

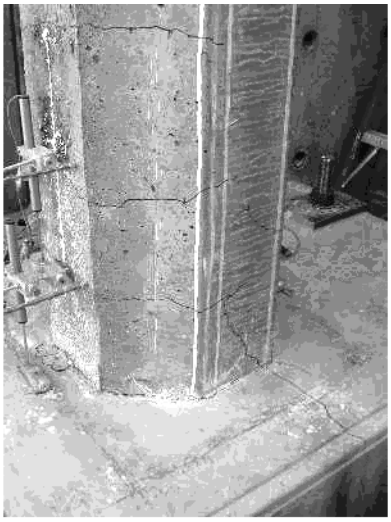

a) 1.25% Drift

b) 1.75% Drift

c) 4.5% Drift

d) End of Test

Fig. 4.21 Photographs of Specimen 7 at Various Drift Levels

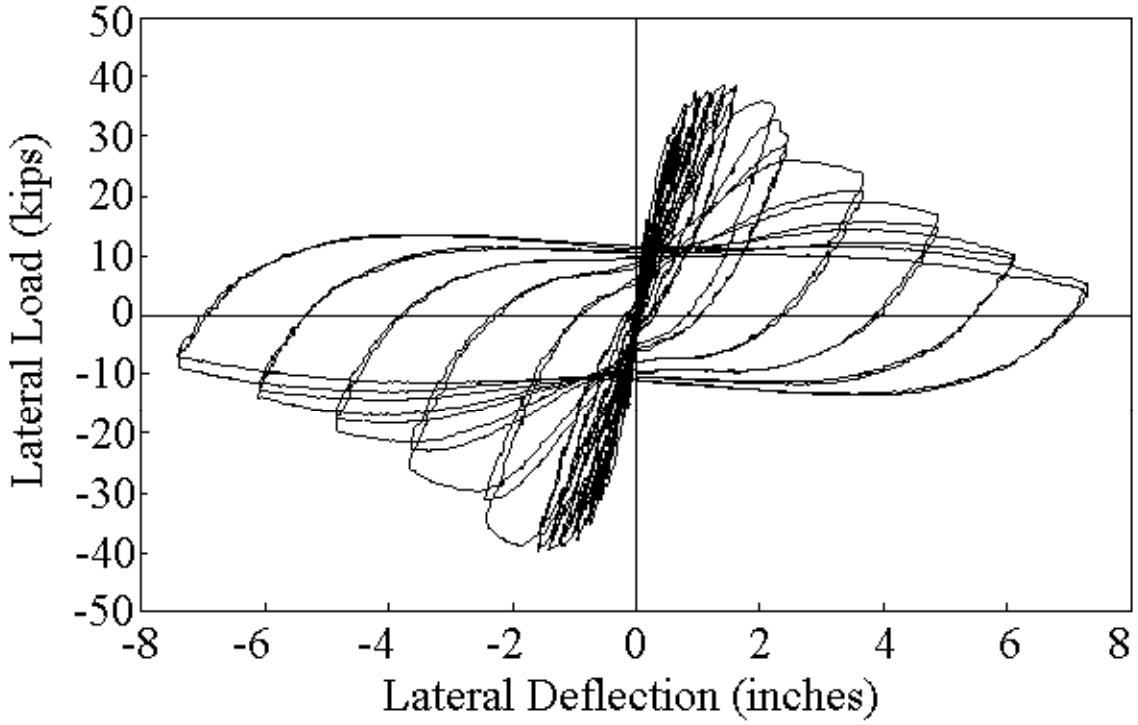

Fig. 4.22 Load-Deflection Curve for Specimen 7

4.2.8 Specimen 8

Specimen 8 was tested on February 2, 2001. This specimen was identical to Specimen 4 except that reduced confinement of the deck section concrete was provided as illustrated in Figure 3.6. The strengths of the deck section concrete and the grout were 8860 psi and 6370 psi (61 and 43.9 MPa), respectively. At 0.75% drift, the first cracks appeared around the pile-deck interface as shown in Figure 4.23. Cracks away from the pile-deck interface first occurred at a drift of 1.0%. Spalling of the pile began at a drift of 1.5%. Delamination of the deck was noticed on the south side at 1.75%, while few cracks appeared in the pile as shown in Figures 4.23 and 4.24b. Cracks oriented at approximately 45° were seen in the side of the deck section at 2.0% drift. At 3.0% drift spalling on both sides occurred exposing the spiral on the north side. Curvature LVDTs were removed at this drift level. Prestressing strands were exposed by 4.5% drift as shown in Figure 4.24c. Delamination of the south side of the deck occurred at 6% drift. At 7.5% drift cracks widened and the strands on the north side were visibly buckling. The final state of the specimen can be seen in Figure 4.24d.

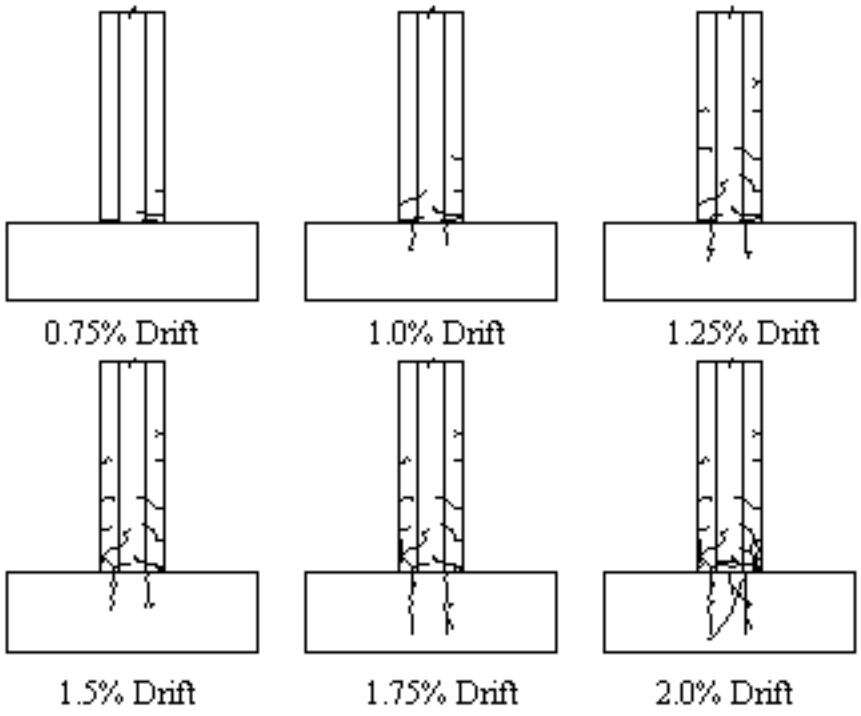

Fig. 4.23 Crack Patterns Observed in Specimen 8

The specimens showed the onset of cracking at or very near to the pile-deck interface after the first cycle at a drift of 0.75%. By a drift of 1.00% cracks had developed away from the pile-deck interface. At drifts of 1.75% the cracking began to concentrated in the lower portions of the pile. Larger portions of concrete began spalling at 3.0% drift between the deck surface and 1/2 pile diameter from the pile-deck interface. By the end of the test, spalling was noted for distance approximately one diameter up the pile, and significant spalling and delamination of the concrete on the deck section were observed as shown in Figure 4.24d. Specimen 8 had cracks in the side of the deck at approximately 45º indicating the beginning of a shear failure. This cracking pattern was not seen in the other specimens and is likely due to the reduction in shear reinforcement in this specimen.

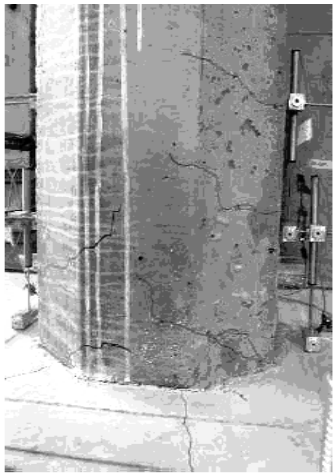

a) 1.25% Drift

b) 1.75% Drift

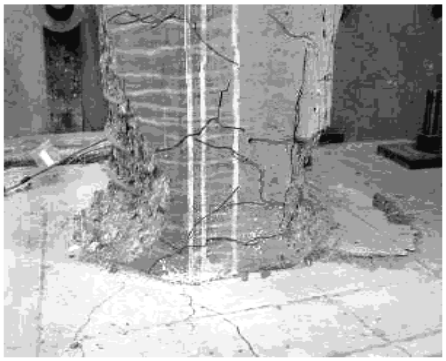

c) 4.5% Drift

d) End of Test

Fig. 4.24 Photographs of Specimen 8 at Various Drift Levels

Figure 4.25 provides the lateral load-deflection curve for Specimen 8. Comparison of this curve to Figure 4.13 suggests that there were not large differences in the performance of these specimens. As with previous specimens, there was significant deterioration in resistance with Specimen 8. However, Specimen 8 was slightly stronger than the other specimens.

Examination of the crack patterns in Figure 4.23 and comparison to Figures 4.11, 4.14, 4.17, and 4.20 suggest that the reduced confining reinforcement in the deck section led to greater cracking in the deck section. Further, significant delamination and spalling of the concrete occurred on the deck section. Comparison of Figure 2.24d with 4.12e, 4.15d, 4.18d, and 4.21d suggests that this deck spalling is among the more severe noted in these tests. In view of these combined observations, it is unlikely that the added confinement provided to Specimens 1–7 played a major role in the performance of any of these connections.

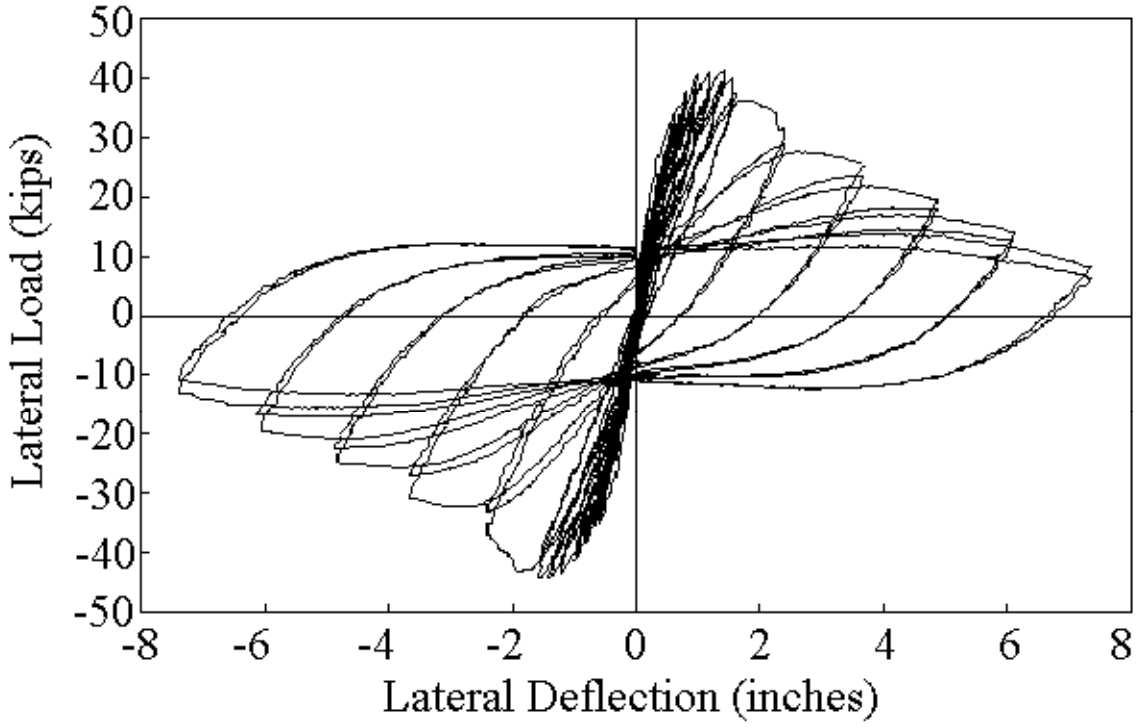

Fig. 4.25 Load-Deflection Curves for Specimen 8

5 Further Analysis of Experimental Results

5.1 MOMENT-ROTATION BEHAVIOR

Chapter 4 provided an overview of the test results. All specimens sustained large inelastic deformations, but connections with precast concrete piles behaved differently than the extended pile connections. The extended pile connections were able to distribute their plastic deformation over a greater pile length and this resulted in less concentration of damage and less deterioration of stiffness and resistance. The precast concrete piles all developed uplift from the deck at large deformations, and most of their inelastic deformation occurred as tensile yield and debonding of the dowel reinforcement in the deck section. The addition of axial load increased the connection deterioration at large inelastic deformations. These general observations are clear from the past discussion and they are important observations of connection performance. However, it is not possible to accurately quantify these effects based upon the results discussed in Chapter 4. Moment-rotation behavior provides better insight into this behavior, and it also aids in further interpreting and understanding the experimental results.

The instrumentation described in Chapter 3 and illustrated in Figures 3.17 and 3.18 provide 3 different methods for establishing moment-rotation or moment-curvature behavior. Curvature and rotation are directly related, because rotation is the integration of curvature over length. First, global moment-rotation behavior can be determined from the measured load and the lateral deflection, Δ_1, illustrated in Figure 4.1. The drift angle, θ_1, can be determined from Δ_1, and the moment at the face of the column can be determined from equilibrium with the applied loads shown in the figure. Because the axial load is nearly directed through the center of the connection, the connection moment can be determined with good accuracy by multiplying the actuator force by the length L_1 as illustrated in Figure 4.1. A second form of moment-rotation behavior can be determined by using the two pairs of curvature potentiometers (shown in Fig. 3.18) to obtain the measured rotation. These potentiometers measure the relative axial elongation or shortening over a 1/2 diameter length from the pile-deck interface and over the length from the 1/2 diameter point to the full diameter point of the pile. These elongations can

be translated into rotation, by dividing the difference between the elongation measurements by the separation distance. The rotations can be translated into average curvatures by dividing the rotations by the length over which the measurements are taken. These rotation measurements permit separation of the curvature or rotation developed at the pile-deck interface and within the last two 1/2 pile diameter lengths from the pile-deck interface. These moment-average curvatures, or moment-rotation curves, provide a measure of the distribution (or concentration) of inelastic deformation along the length of the specimen. These measurements clearly show the degree of pile participation in the inelastic deformation. However, these instruments are seldom available throughout the test, because they must be removed as spalling and extreme damage to the concrete occurs. Third, the strain gauges illustrated in Figure 3.17 are placed in pairs along the length of the dowel within the pile and the deck section. Curvatures at various locations are determined by the differences between the strain pairs. This third curvature, or rotation measure, provides an even better indication of the distribution of inelastic activity throughout the pile-wharf connection. This distribution information is provided both within the pile and within the deck section. This third measure is also unlikely to be effective throughout the experiment, because strain gauges fail or become less reliable when subject to large inelastic strains.

The global moment-rotation curves do not provide the detailed information that is desirable, but they are available throughout the test for all test specimens. As a result, these global moment-rotation curves are provided for the 8 test specimens in Figures 5.1–5.8. The moment-curvature information provided by the other two methods are extremely useful for defining connection behavior, but they are not available at all inelastic deformation levels. Nevertheless, these data are valuable and are discussed in subsequent sections.

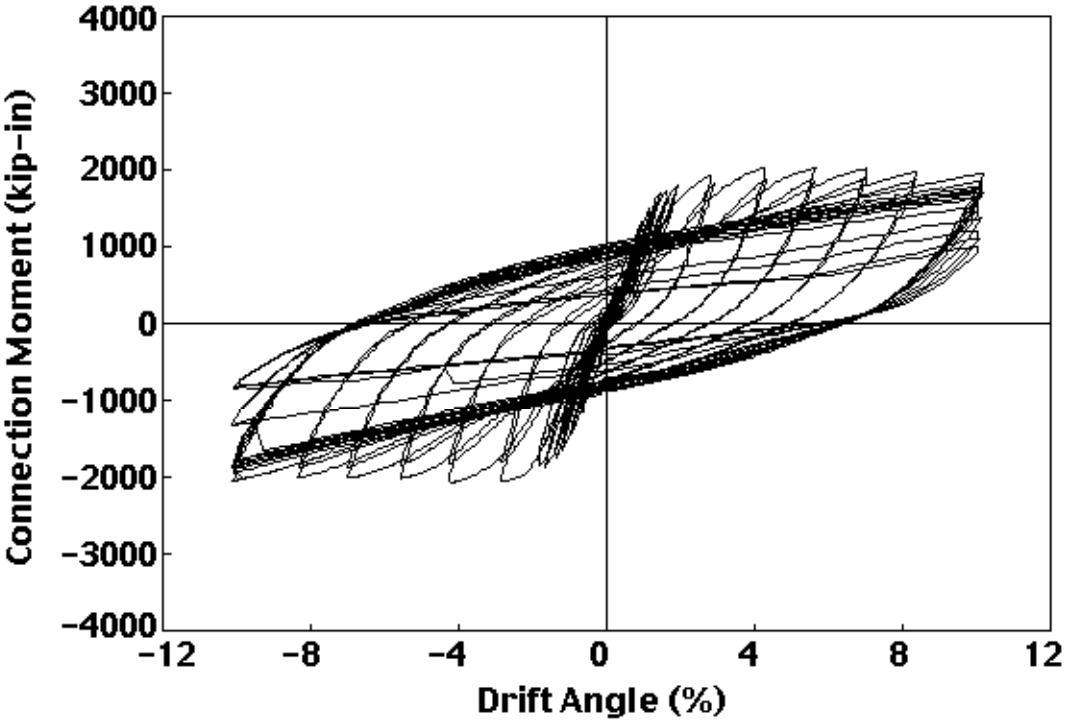

Fig. 5.1 Global Moment-Rotation Curve for Specimen 1

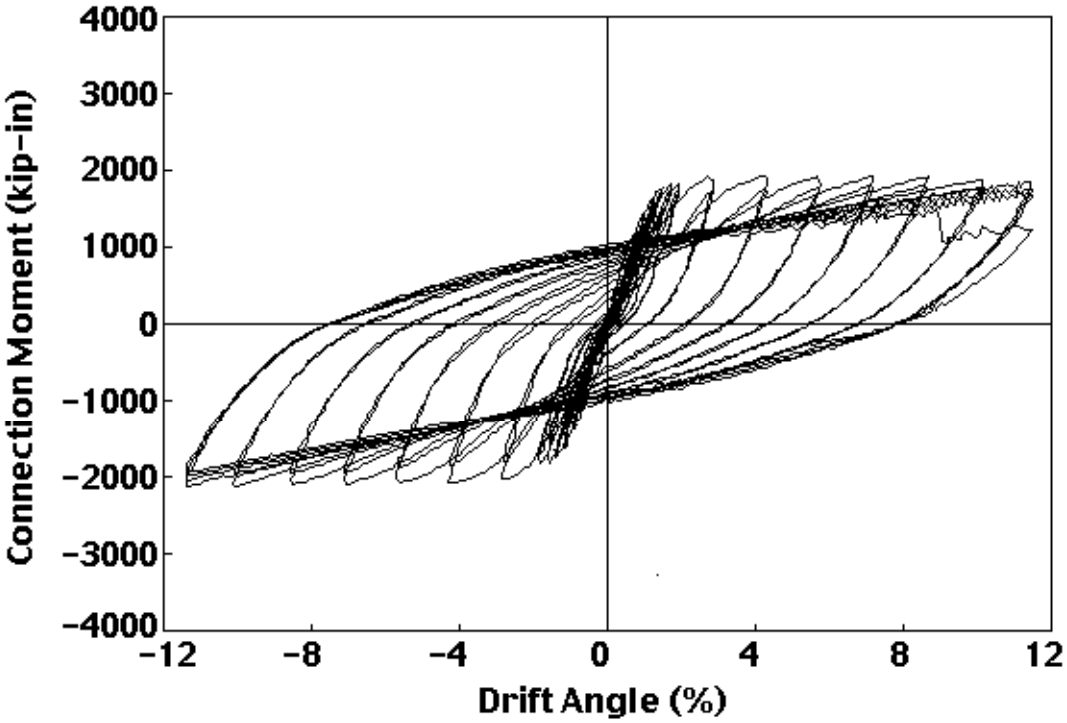

Fig. 5.2 Global Moment-Rotation Curve for Specimen 2

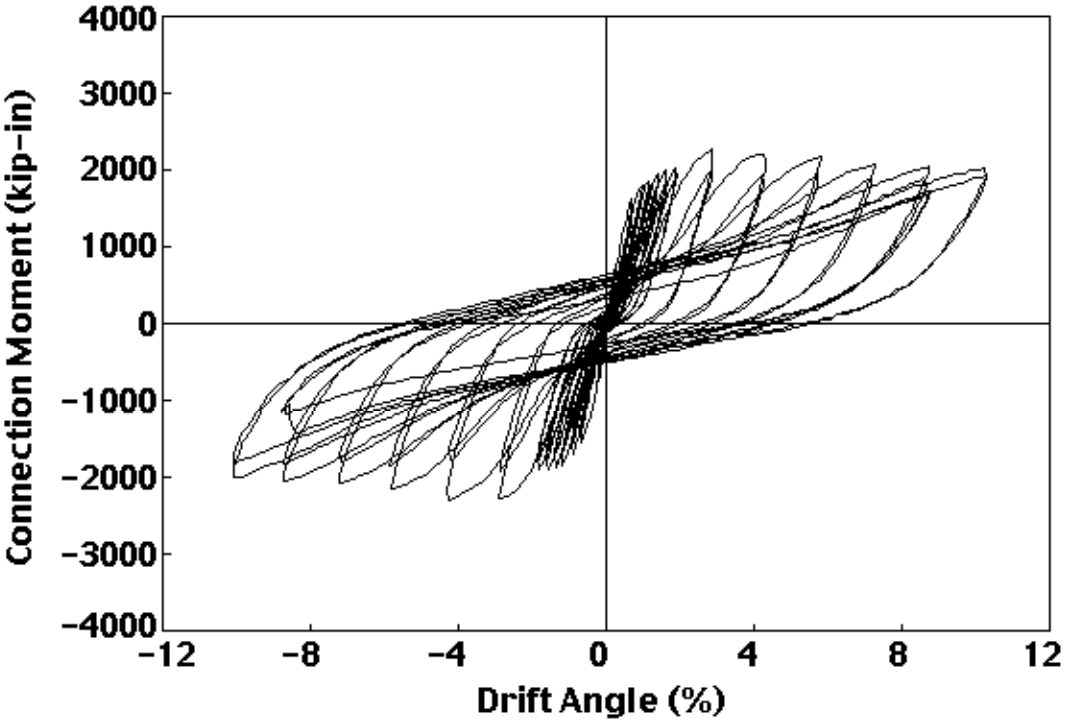

Fig. 5.3 Global Moment-Rotation Curve for Specimen 3

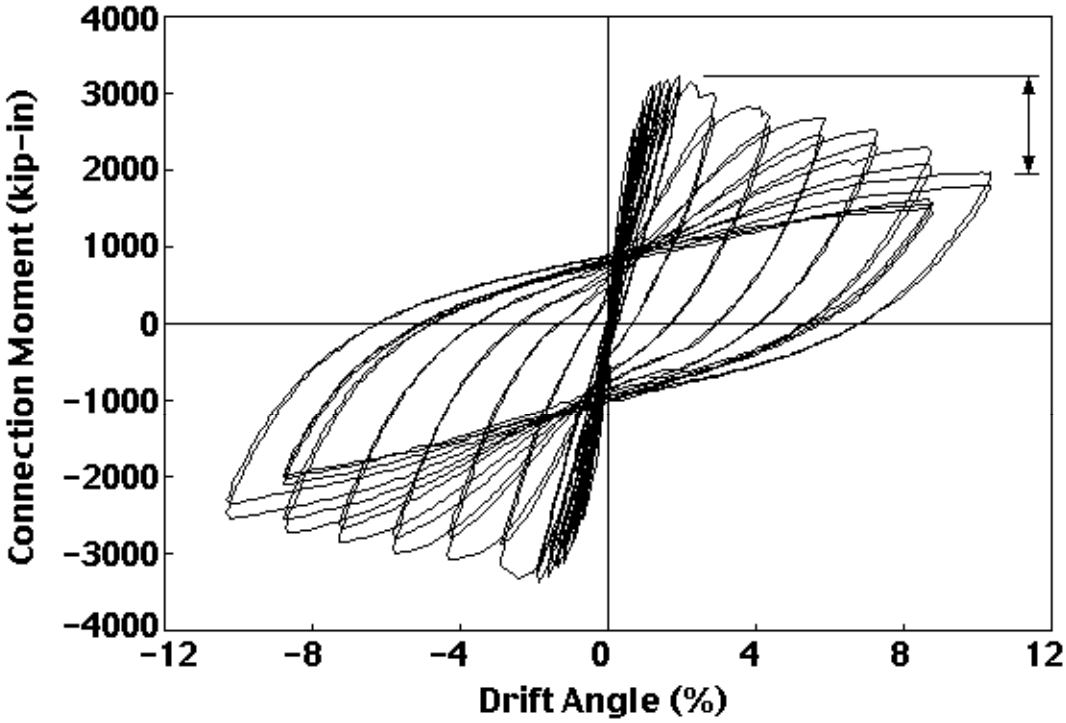

Fig. 5.4 Global Moment-Rotation Curve for Specimen 4

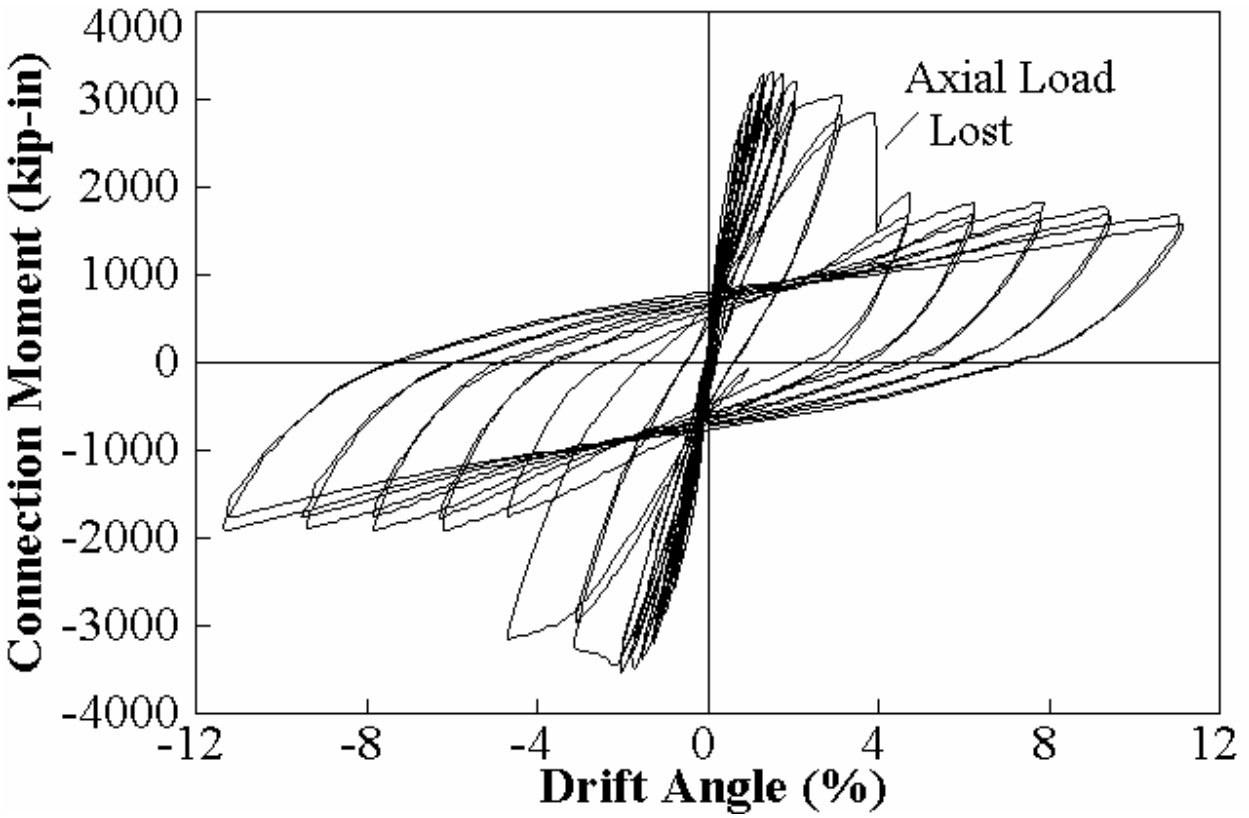

Fig. 5.5 Global Moment-Rotation Curve for Specimen 5

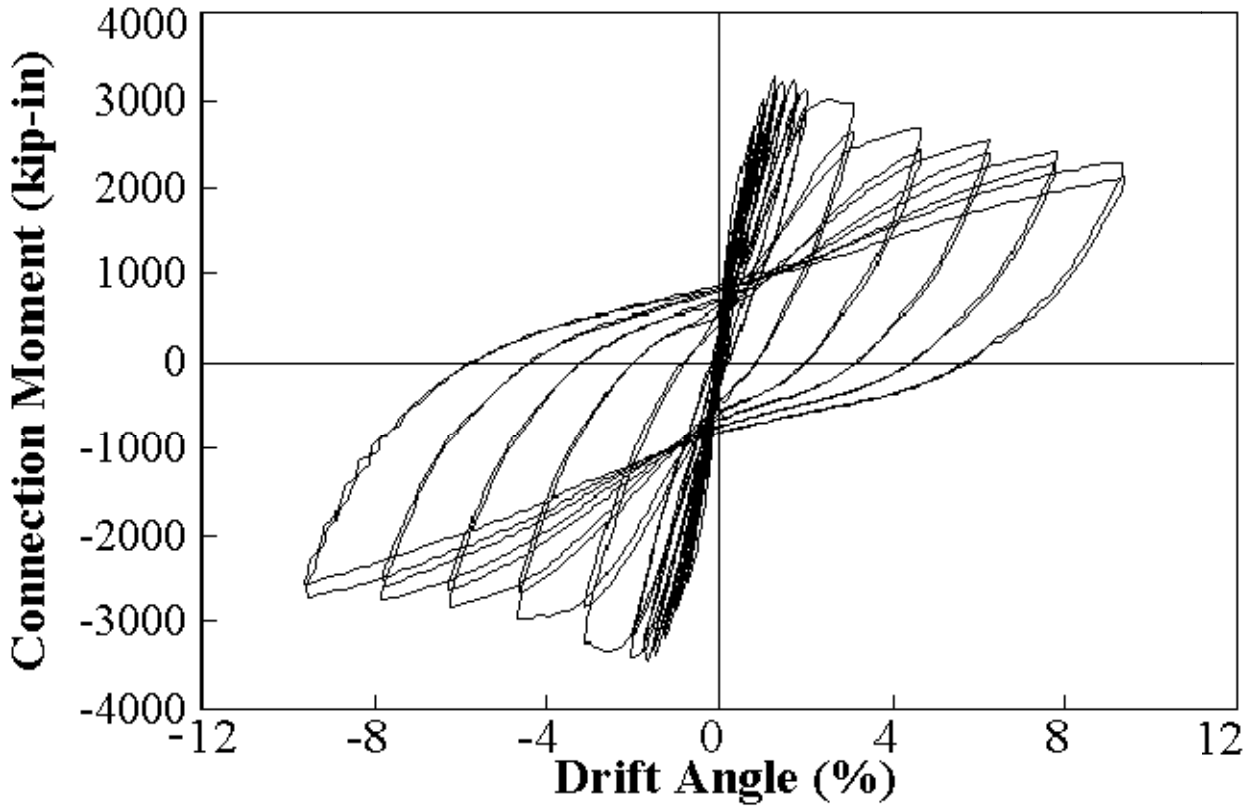

Fig. 5.6 Global Moment-Rotation Curve for Specimen 6

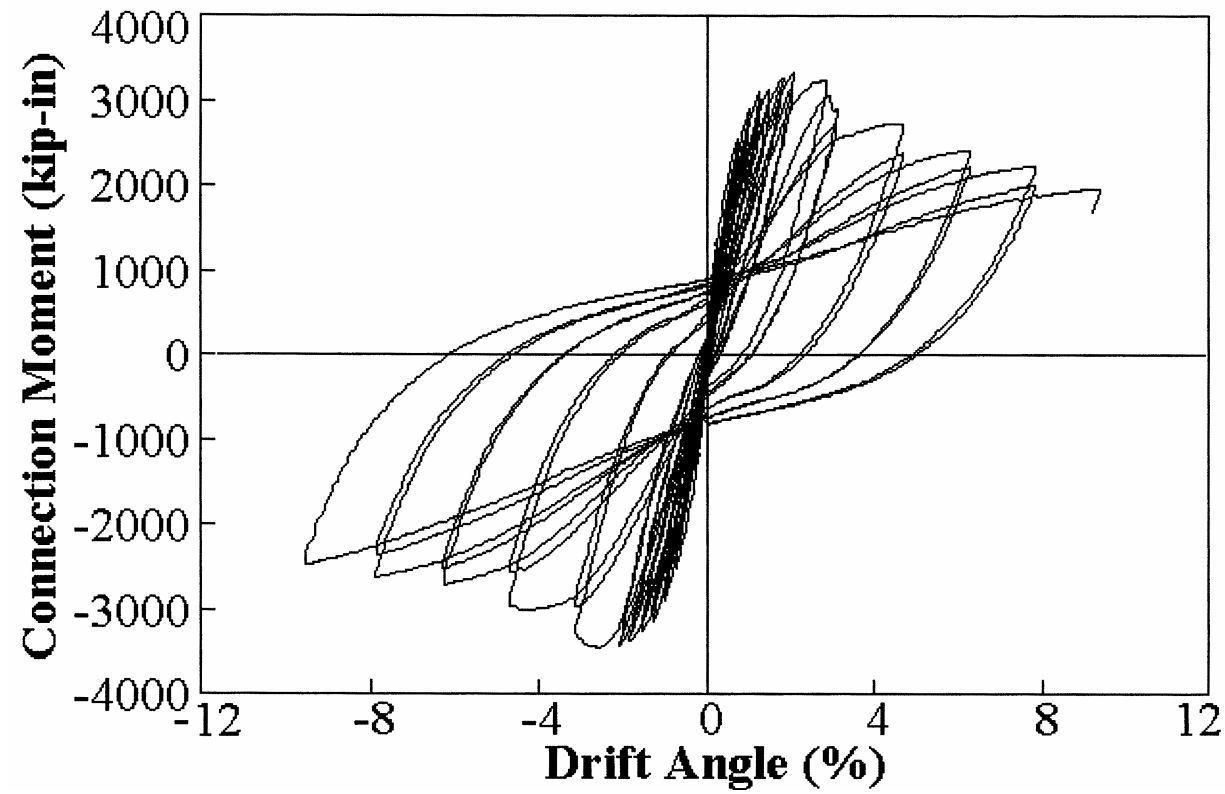

Fig. 5.7 Global Moment-Rotation Curve for Specimen 7

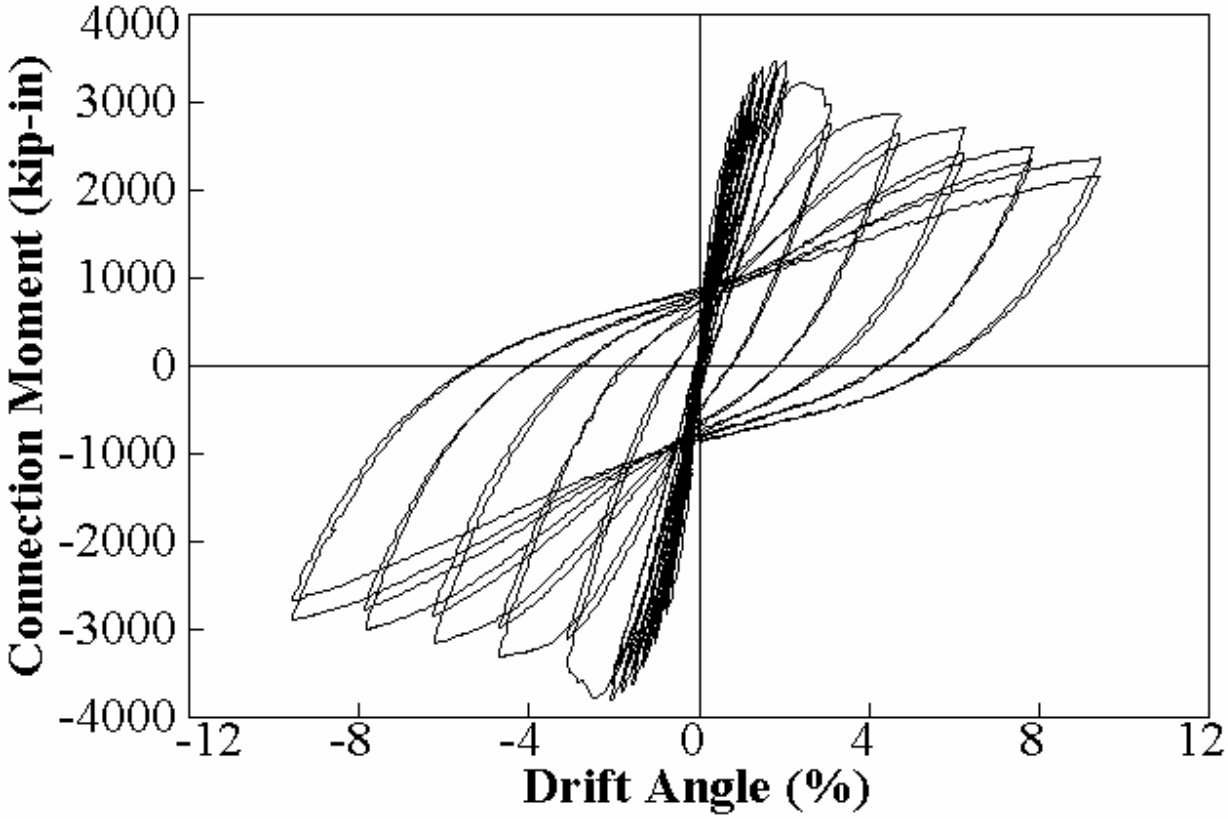

Fig. 5.8 Global Moment-Rotation Curve for Specimen 8

5.2 GLOBAL MOMENT-ROTATION BEHAVIOR

Figures 5.1–5.8 show the global moment-rotation behavior. Most of these figures show a reduction in moment resistance at large deformation. This reduction in moment resistance reflects a true deterioration in resistance in the connection because the full moment capacities (including the moment consumed in resisting P-Δ effects) are included in these curves. Figures 5.1 and 5.2 are the moment-rotation curves for Specimens 1 and 2. These specimens had a normal reinforced concrete pile, since they examined extended pile connections. They were tested without axial load, and only modest deterioration is noted in these specimens. The maximum moment resistance developed at drift angles between 4% and 8% for these specimens, and the moment resistance in initial cycles at 10% or 11% drift angle was never more than 5% smaller than the maximum resistance. There was slight deterioration in resistance for repeated cycles at given inelastic deformation levels, but this reduction was typically no greater than 10%.

Comparison of Specimen 3 to Specimens 1 and 2 shows the effect of the use of precast pile connections as opposed to extended pile connections. The use of precast piles results in a significant increase in the deterioration of the resistance. The precast pile connections are invariably stronger than the reinforced concrete extended pile connections even though the dowel reinforcement and rebar have the same size and spacing for all 3 connections. The maximum moment capacity is in the range of 20% to 25% larger than that observed in Specimens 1 and 2. This increased resistance appears to be caused by the delayed yielding in the pile caused by the added reinforcement of the prestressing strand The stress in the prestressing strand at the end of the pile would not normally be predicted by design calculations. As a result, this added resistance was not predicted by the ACI design calculations. The resistance for the first excursion to the maximum drift had deteriorated approximately 16% from maximum resistance. The deterioration associated with repeated cycles at given deformation levels was also significantly larger than Specimens 1 and 2, since these were also commonly another 15% to 20% smaller than the initial excursion. Thus, it can be clearly stated that the use of precast concrete piles results in more rapid deterioration than expected with reinforced concrete members.

Specimen 4 had a precast concrete pile connection and was subjected to axial load. Comparison of Figure 5.4 with Figures 5.1, 5.2, and 5.3 shows that the addition of axial load further increases the deterioration in resistance of pile-wharf connections. The maximum resistance was about 30% to 35% stronger than noted in Specimens 1 and 2. Much of this

strength increase is caused by the axial compressive load and its contribution to bending moment caused by its eccentricity to the member neutral axis, and so much of this increase is predicted by normal design resistance calculations. The maximum resistance is also attained at smaller inelastic deformation, since the maximum occurred at drift angles of approximately 2%. The resistance for the first excursion to the approximately 10% drift level was 25% to 40% smaller than the maximum resistance. The deterioration noted for repeated cycles at a given inelastic deformation level is similar to that noted for Specimen 3. This deterioration in resistance due to axial compressive load is quite important, because the axial loads on the piles were approximately 10% of the compressive load capacity of the pile. This load level simulated the deadweight of the wharf structure. Larger axial loads will occur if the wharf is fully loaded during an earthquake, and much greater deterioration will likely result.

Specimens 4–8 examined a range of different connection details for precast concrete pile-wharf connections. Comparison of Figures 5.4–5.8 suggests that there is not a big difference in the performance of these connections. In general they all show increased resistance because of the axial load and use of precast piles. The maximum resistance is similar for all connections. All specimens achieved their maximum moment resistance at approximately a 2% drift angle, and they all exhibited similar deterioration. That is, the resistance for the first excursion to the approximately 10% drift level was 25% to 40% smaller than the maximum resistance in all cases. Specimen 7 was a bond bar connection, and it had slightly greater deterioration than other specimens. Specimen 8 employed the reduced confinement detail for the deck section, but it was a bit stronger than other specimens. Examination of Figure 5.5 would suggest that this specimen had greater deterioration than noted for other specimens, but the specimen was tested without axial load for large deformations. Therefore, the moment resistance of Specimen 5 lacks the increased resistance caused by this compression load at large deformations. However, comparison of this large deformation resistance to that of Specimen 3 shows significantly greater (approximately 20%) deterioration because of the earlier applied axial load.

Bond bar connections were tested in earlier research [Sritharan and Priestley, 1998]. The earlier test noted no deterioration with the bond bar connection and full hysteresis loops (see Fig. 1.6). As a result, the behavior observed for Specimen 7 appears to contradict this earlier work. However, there is no contradiction in these results. The earlier research examined connections with reinforced concrete piles (that is, extended pile connections), and the specimens were tested without axial load. Therefore, the earlier work is more comparable to the results noted for

Specimens 1 and 2. The behavior noted for Specimens 1 and 2 are comparable to Figure 1.6 both in the characteristics of the moment-rotation curves and the deterioration that results. The adverse effects of deterioration of the pile-wharf connections are associated with the use of precast pile connections and the application of axial compressive load.

The maximum resistance obtained from each connection was compared to that predicted by the ACI analysis procedure. In all cases, the maximum moment capacity obtained in the experiments was larger than that predicted by the ACI procedure. The difference was small for Specimens 1 and 2 because these specimens were essentially reinforced concrete beams with no axial load. The difference was quite large for all precast pile connections, since the measured resistance was 12% to 18% larger than computed value in all cases. This difference occurs because of the added resistance provided by the prestressing strand at the pile-deck interface as noted earlier.

5.3 OTHER MOMENT-CURVATURE MEASUREMENTS

Moment-curvature obtained from the rotation potentiometers and the dowel strain gauges were evaluated for each specimen. This data provided further insight into the moment transfer between the pile and the wharf deck. It showed the locations of nonlinear deformation of the connection, and the relative magnitude of the inelastic deformation. These curves are repetitive and only selected curves are provided here. Additional comparisons are provided elsewhere [Graff, 2001 and Soderstrom, 2001].

The prior discussion notes a remarkable difference between the behavior noted for the extended pile connections and the precast pile connections. Specimens with precast piles developed nearly all of their connection rotation through tensile yielding of rebar within the deck section. Much of this rotation was observed as rocking of the end of the pile at the precast pile-deck interface. Specimens with extended pile details developed much of their nonlinear deformation through inelastic flexure of the columns. This was further verified in the detailed moment-curvature evaluation, and is illustrated by comparing Figures 5.9 and 5.10. These figures show the moment-curvature results obtained from strain gauge measurements of Specimens 2 and 4, respectively. These measurements are included only for deformation cycles up to a 3% drift angle, because some gauges malfunctioned at larger deformation cycles. Figure 5.9 shows that the extended pile connections sustained some yielding of the reinforcement throughout the pile and deck section, but the largest plastic strains occurred at the pile-deck

interface and within the pile itself. Very little plastic strain occurred within the pile body for Specimen 4. Relatively large strains occurred in Specimen 4 at the pile-deck interface, and the very largest strains occurred within the body of the deck section. This verifies that the inelastic deformation in the precast pile connections occurs through tensile yield of dowel bars and slip or debonding between the steel and concrete.

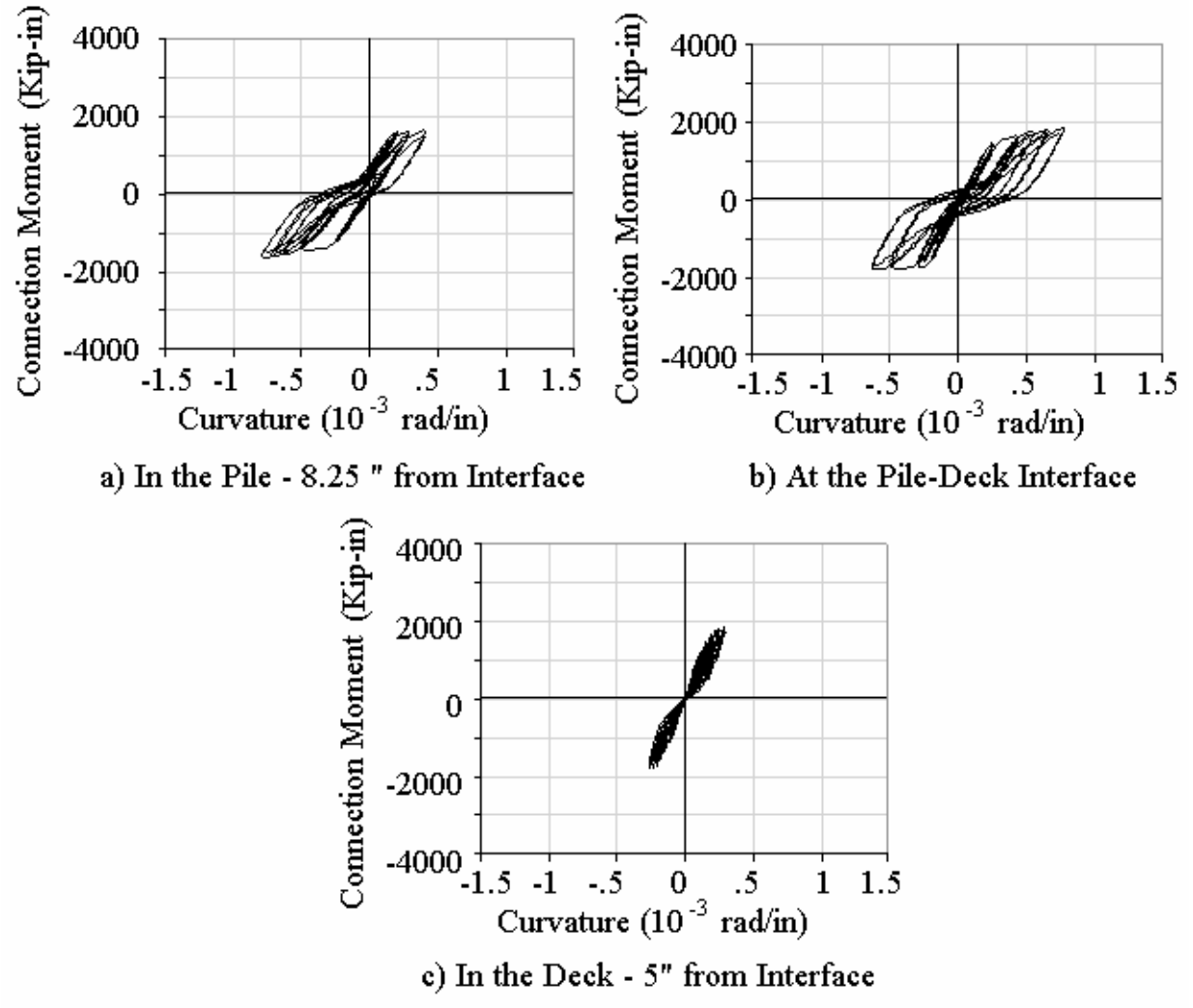

Fig. 5.9 Moment-Curvature from Strain Gauge Data of Specimen 2

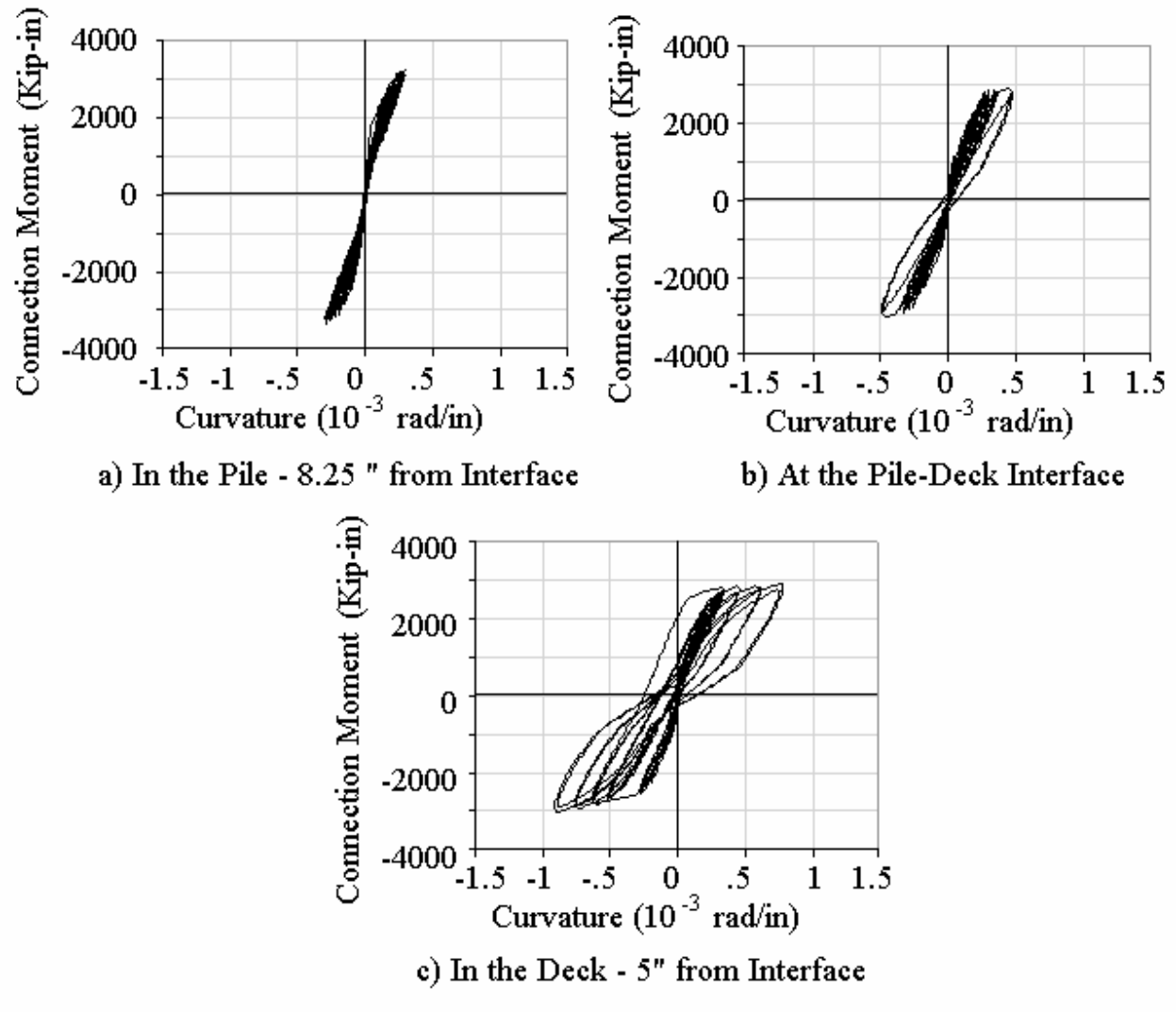

Fig. 5.10 Moment-Curvature from Strain Gauge Data of Specimen 4

Similar observations were made for all precast pile connections. However, Specimens 6 and 7 had slightly better transfer of stress between the steel and concrete within the deck section. They had slightly smaller inelastic strains in this region than Specimens 5 and 8. The difference was not large, but the reason for this difference is not clear from the research results.

5.4 SPECIMEN STIFFNESS

The stiffness of the specimens was determined at various deformation levels so that deterioration of stiffness and differences in performance for each connection type could be noted. For small deformations, the definition of connection stiffness is precise and there can be little variation in the stiffness definitions obtained from the experimental data. At large

deformations, the tangent stiffness, secant stiffness, or other definitions produce different results. A secant modulus may be used to establish stiffness, but at large deformations this stiffness definition becomes a measure of the resistance (and deterioration in resistance) as a function of deformation level. Resistance and deterioration in resistance have already been discussed. As a result, a tangent stiffness based upon the unloading cycles at a given deformation level was used to define specimen stiffness as illustrated for a given cycle in Figure 5.11. This stiffness will converge on the normal elastic stiffness at small elastic deformations, and it is probably the best indication of the elastic characteristics of the specimen after large deformations. The corrected lateral load-deflection curves of Chapter 4 were used to obtain these stiffness estimates. Table 5.1 provides estimates of the initial elastic stiffness and the deterioration at various deformation levels for all eight specimens. The stiffness calculations are average stiffness values determined from the two estimates shown in the figure.

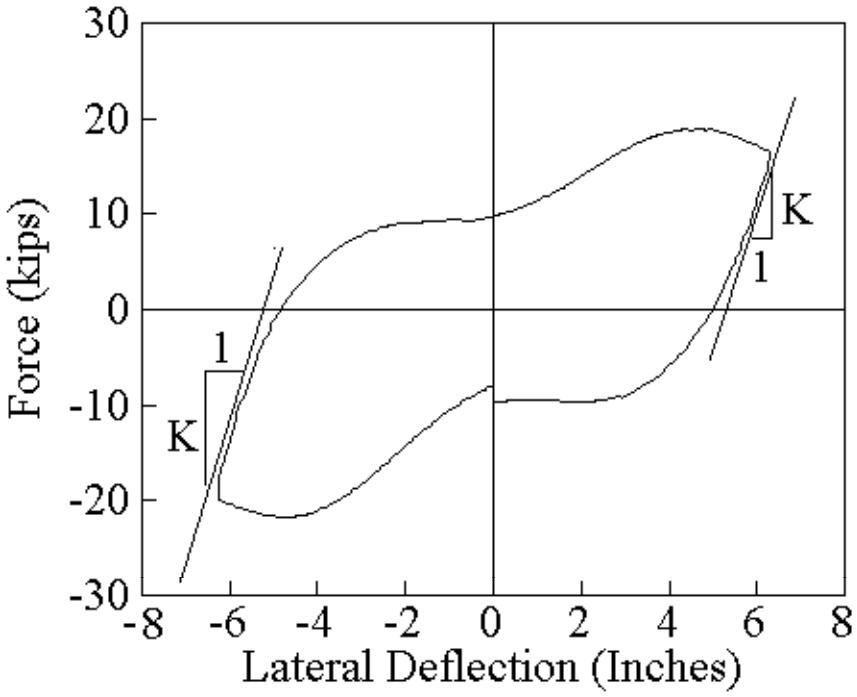

Fig. 5.11 Definition of Stiffness at Large Deformations

Table 5.1 shows that the average initial stiffness varied considerably. This should be expected because limitations in the accuracy of displacement measurements may affect this initial stiffness measurement. However, the precast pile connections were all stiffer than the extended pile connections, and connections with axial load were generally stiffer than

connections without axial compression. The initial stiffness approached the uncracked stiffness of the pile, since the measurements were taken at small deformations where cracking was limited to the local area around the pile-deck interface. The addition of axial load reduced the amount of cracking noted at these small deformation levels.

Table 5.1 Deterioration of Stiffness at Large Deformations

Specimen	Average Initial Stiffness (Kip/in)	Ratio of Stiffness at 0.75% Drift Angle to Initial Stiffness	Ratio of Stiffness at 2% Drift Angle to Initial Stiffness	Ratio of Stiffness at 9% Drift Angle to Initial Stiffness
1	61	50%	40%	21%
2	41	73%	60%	29%
3	70	60%	47%	19%
4	131	36%	22%	7%
5	84	62%	39%	26%
6	62	90%	51%	36%
7	79	70%	48%	28%
8	77	71%	42%	19%

All specimens had significant deterioration in stiffness with increasing deformation levels. Specimen 4 had the largest initial stiffness and it also had the largest relative deterioration levels. In general, specimens lost approximately 30% to 40% of their initial stiffness at drift angles smaller than 1%, and the specimens lost 70% to 80% of their initial stiffness at drift angles in the order of 10%.

5.5 EFFECT OF SPIRAL REINFORCEMENT AND CONCRETE CONFINEMENT

Some pile-wharf connections are designed with spiral reinforcement surrounding the dowels in the deck section as illustrated in Figures 2.2b, 2.2c, and 3.8. This is generally done to provide better confinement and stress transfer to the connection. Comparison of the performance of Specimens 1 and 2 provides a direct comparison of the consequence of this change. Comparison of the general behavior of these specimens in Figures 5.1 and 5.2 suggests that there is not a great difference in the behavior of these specimens. The strain in the reinforcement (see

Fig. 3.17) was compared for these specimens in some detail, and again only minor differences were noted in the ability of the two connections to transfer moment from the pile to the deck section. The largest difference in performance between these specimens can be seen by comparing the crack patterns in Figures 4.2 and 4.5. Specimen 2 had the spiral reinforcement continuing into the deck, and the figures suggest that this specimen developed cracking of the deck section earlier than Specimen 1. This cracking may be caused by the greater integrity and continuity of the concrete in the deck section over the pile. This concrete may be acting as an extension of the pile and the resulting rotations may be placing greater demands upon the concrete in the deck section. However, the differences observed are not great.

Additional insight into this issue may be provided by comparing Specimen 8 to Specimen 4. As noted earlier, Specimens 1–7 were believed to have greater confinement of the deck section than would be expected in most prototype structures. This greater confinement was caused by the details employed to insure development of the flexural reinforcement in the deck section. Specimen 8 was identical to Specimen 4 except that it was designed to eliminate the extra deck section confinement. Comparison of the performance of these two specimens in Figures 5.4 and 5.8 and in Figures 4.13 and 4.25 shows relatively small differences in performance. Specimen 8 had the reduced confinement, and it had somewhat larger resistance and less deterioration in resistance at large deformations than Specimen 4. Comparison of the crack patterns in Figures 4.11 and 4.23 shows slight differences. Specimen 8 had less confinement in the deck section than Specimen 4 and so it sustained earlier cracking into the deck section. The results of this comparison suggest that the addition of more confining reinforcement within the wharf deck or the use of spiral extensions into the deck will not have a large beneficial effect on the pile-wharf connection performance. On the other hand, spirals extending into the deck and increased deck reinforcement would complicate construction.

6 Consequences of Observed Behavior

6.1 OBSERVED BEHAVIOR

This research has examined a wide range of pile-wharf connections with precast concrete piles and moment-resisting connections as required for the system illustrated in Figure 1.1. The research has shown that a wide range of connection details have been used in past engineering practice. These connections were analyzed and experimentally evaluated. Connections with piles driven to an elevation below the bottom of the wharf deck require extended pile connections, and analyses and experiments show that the behavior of precast pile connections and extended pile connections are fundamentally different. Precast pile connections have higher initial resistance, but they have greater deterioration in the resistance at large inelastic deformation. Precast concrete pile connections develop their yield deformation within the deck section and at the pile-deck interface. They concentrate the large strains and deformation, and most rotational capacity occurs at the pile-deck interface and within the deck section. Extended pile connections behave more like reinforced concrete elements. They distribute the yield deformation over a significant length of the pile section. They have significantly less deterioration in resistance at large inelastic deformation, and they distribute the inelastic strains throughout the pile member.

Wharfs support large gravity loads, and the axial load in the pile further increases the moment resistance and the deterioration of this resistance in pile-wharf connections. While a wide range of connections have been commonly used in seismic resistance construction of these wharf structures, the experiments show that there are not great differences in the seismic performance of these various connections. In all cases, the connections held together through large drift angles although substantial deterioration in resistance and stiffness was noted. The large drift angles normally suggest a very beneficial performance. However, as shown in Figure 1.1, the pile lengths vary widely in this structural system, and therefore the vast majority of both the force and deformation demands are concentrated into a very few short piles. These short piles may sustain large drift angle demands with even relatively small wharf deck movements.

As a result, it is desirable to assess how the connection performance observed in this study relates to the overall seismic performance of the wharf structural system.

In considering the performance of the structural system, it is important to recognize that there are several seismic risks. First, the wharf rests on a man-made embankment, and the potential for movement due to lateral spreading of the soil, slope stability, or liquefaction are serious concerns. These effects will have a major impact upon the wharf structure. If this large soil mass moves, the structure will also move and deform, and it is unlikely the pile-wharf connections will have a big impact on the final position or deformation of the structure because the mass of the soil is huge compared to the mass of the structure. This soil movement issue is considered in another study in the PEER research program, and will not be considered here. A second category of concern, however, is the structural vibration that results from the ground shaking. The soil embankment may remain stable during this shaking if the soil has adequate stiffness and resistance. Under these conditions, the structure will vibrate, and the strength, stiffness, and ductility of the pile-wharf connections will have a major impact upon the structural performance. This later behavior was considered in an analytical study [Yoo, 2001].

6.2 CORRELATION OF EXPERIMENTAL RESULTS TO WHARF BEHAVIOR

The experiments described in this report were 69% scale models of prototype structures, and there are inherent limitations in the ability of any experimental investigation to simulate true full-scale structural behavior. It is important to recognize these limitations before attempting to correlate the experimental results to expected seismic performance of wharf structures. Two issues are of particular importance in this evaluation, and these are illustrated in Figures 6.1 and 6.2.

The test specimens all had approximately a 77 in. (1.96 m) moment arm between the pile-deck interface and the actuator loading. This length was chosen to represent a 69% scale of the distance between the pile inflection point and the pile-deck section interface of the prototype structure. Figure 1.1 shows that pile lengths vary widely, and this experimental length was an intermediate length estimate noted for shorter piles. As noted in earlier chapters, the shortest piles contribute the largest lateral resistance and stiffness to the wharf structural system. However, the length of these short piles depends upon the geometry of the wharf, the stiffness of the soil embankment, and numerous other factors. Figure 1.1 shows that the geometry alone will

assure that these lengths vary dramatically, and Figure 6.1 shows that this variation in length can have a significant effect on the ductility achieved in experiments on these pile-wharf connections.

The figure shows two piles with identical geometry and moment resistance, but the length of the two piles are different. The moment resistance, M_y and M_{max}, for the two specimens is identical. The moment diagram for the two piles will have the same general shape but will be affected by the specimen length as shown in the figure. Plastic deformation in the pile is a very desirable source of inelastic deformation as noted in the experiments, but this deformation can occur only within the region where the pile bending moment is larger than M_y. The length of yielding is then directly proportional to the length of the pile as shown in the figure. Therefore, pile-wharf connections with longer pile sections will develop larger inelastic deformations and connection rotations than shorter piles if strain levels in the steel and concrete are the same for both elements. Since crushing of the concrete and fracture of the reinforcement are at least partly related to the maximum strain levels in the concrete and steel, respectively, shorter piles typically will result in reduced connection ductility and deformation capacity. This observation will be particularly true for the extended pile connections (Specimens 1 and 2), since they develop most of their inelastic deformation in the pile. Precast concrete pile connections (Specimens 3–8) will be less strongly influenced by this observation, because most of their plastic deformation occurs within the deck section.

The experiments performed in this study provide a good indication of the yield mechanisms, failure modes, and general seismic performance of prototype wharf connections. However, as the pile length to the inflection point becomes shorter than the 77 in. (1.96 m) used in the research program, the ductility and rotational capacity of the connection will generally be reduced. As the pile length to the inflection point becomes longer than that used in this study, the ductility and rotational capacity of the connection will generally be increased.

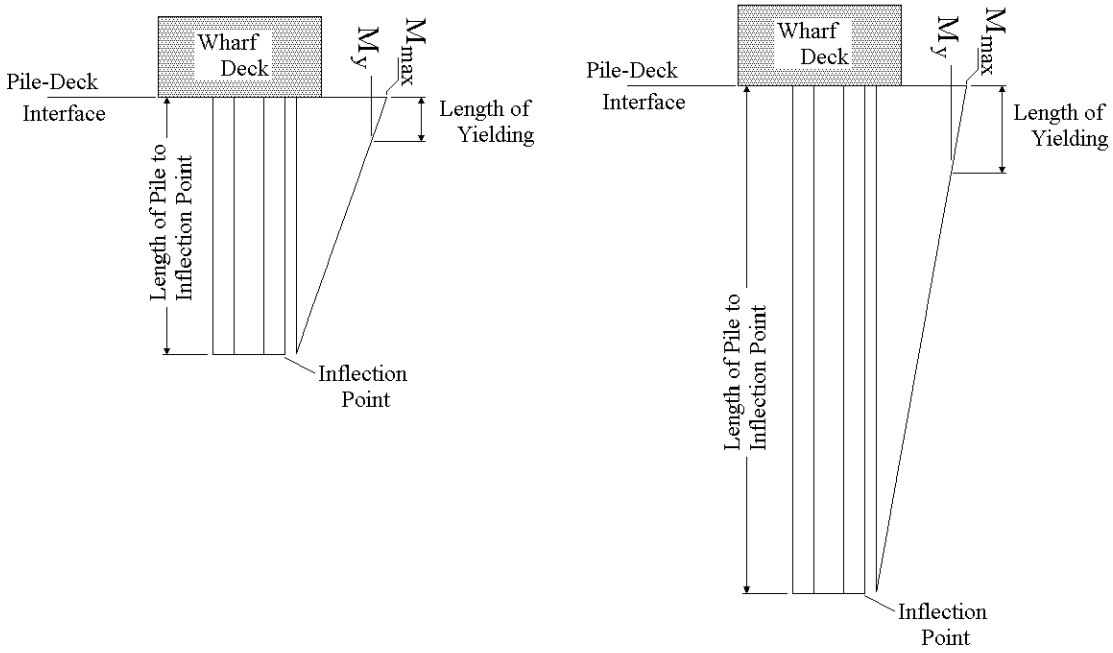

Fig. 6.1 Effect of Pile Length on Pile-Wharf Connection Performance

The 69% scale of the test specimens means that the pile diameters of the test specimens were reduced to 16.5 in. (420 mm) from the typical 24 in. (610 mm) octagonal pile, and the moment arm for the pile reinforcement was reduced by a similar amount. Figure 6.2 shows two octagonal piles with identical pile length, shape, and geometry, except that one pile has a larger diameter than the other. As noted earlier, inelastic rotation or deformation of the connection is an important measure of the seismic performance of the connection. Rotation is an integration of curvature over length, and if the length of the two piles are the same, the large diameter pile and the smaller diameter pile must have the same maximum curvature if they are to develop the same connection rotational capacity. However, Figure 6.2 shows that the strains in the steel and concrete are related to the curvature in the pile and the diameter of the pile. If the large diameter and small diameter pile have the same curvature, the large diameter pile will have much larger strains in both the steel and concrete as shown in the figure. Crushing of the concrete and fracture of the steel are again at least partially related to the strains in the concrete and steel, respectively. Therefore large diameter piles will in general develop crushing of the concrete and fracture of the reinforcement at smaller connection deformations and rotations than smaller diameter piles. As noted earlier, the experiments performed in this study provide a good indication of the yield mechanisms, failure modes, and general seismic performance of prototype wharf connections. However, the large 24 in. (610 mm) diameter piles used in most prototype

wharfs will in general have less inelastic deformation capacity, smaller rotation capacity prior to crushing of concrete or debonding of dowel bars, and reduced ductility than that noted in these experiments. The reduction should be approximately proportional to the ratio of their diameters. Therefore, 24 in. (610 mm) piles of identical length should provide approximately 70% of the inelastic deformational capacity noted in these experiments. This observation is valid for both precast pile connections and extended pile connections.

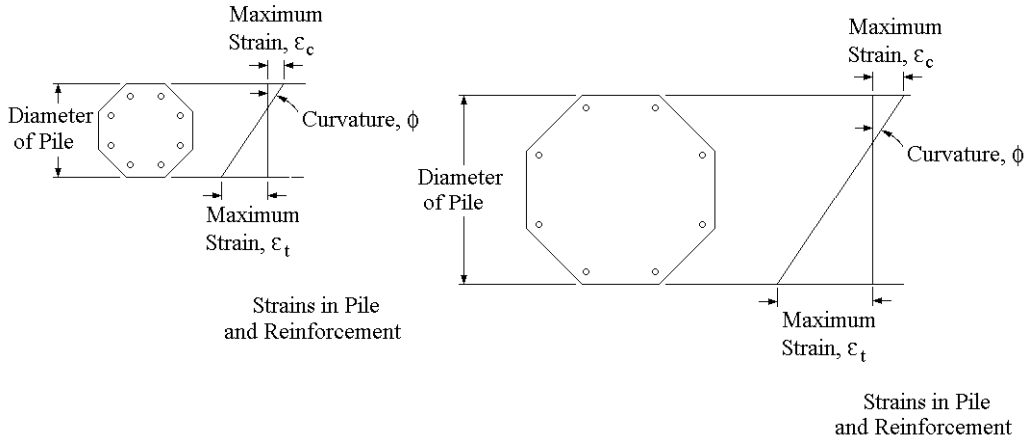

Fig. 6.2 Effect of Pile Diameter on Pile-Wharf Connection Performance

These observations are important in understanding the evaluation of structural response that follows.

6.3 ANALYTICAL STUDY

A model of a typical precast concrete pile-wharf structure was developed using the two-dimensional nonlinear analysis program, RUAUMOKO [Carr, 1996]. RUAUMOKO is designed to produce a time-history response of a nonlinear general two-dimensional framed structure to ground acceleration or time-varying force excitation. The prototype wharf typifies a number of structures built on the West Coast of the U.S., but variations in dimensions can be observed on different facilities as noted earlier. Typical wharf structures consist of a reinforced concrete deck supported on vertical octagonal prestressed concrete piles along the length. The piles are spaced at 15–20 ft as part of transverse frames such as illustrated in Figure 6.3. These transverse frames are spaced longitudinally along the wharf structure in 18–20 ft intervals as depicted in Figure 6.4. A plane frame model was used to model the transverse deformation of a single bay of the deck structure as illustrated in Figure 6.4.

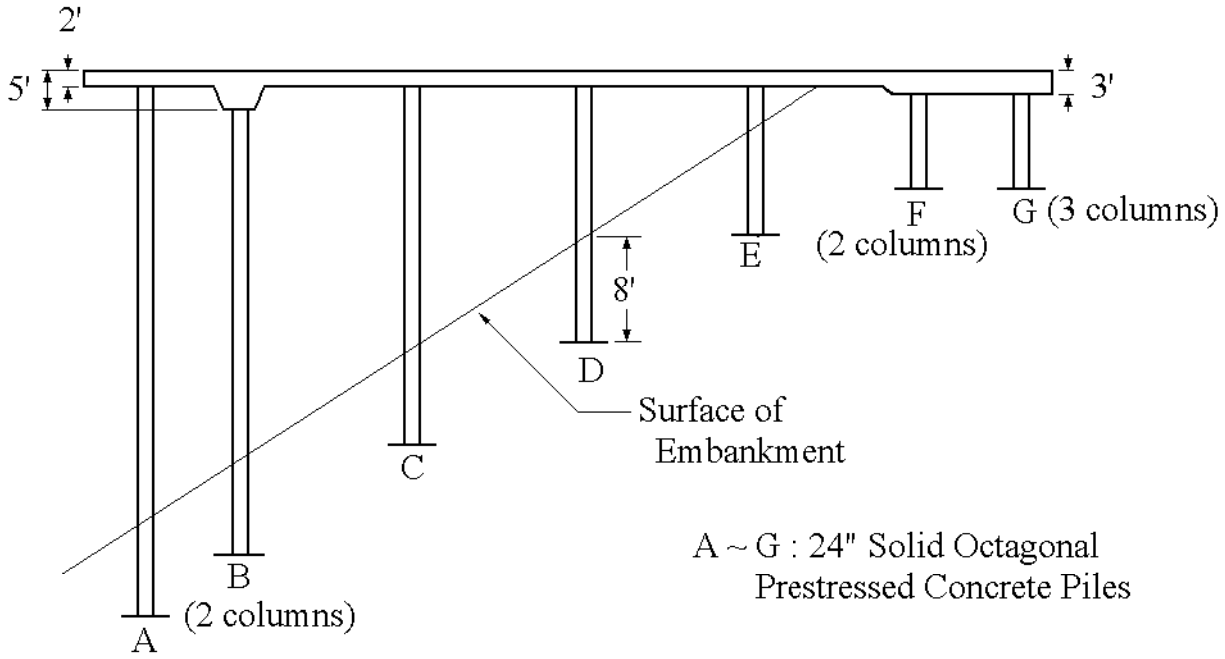

Fig. 6.3 Transverse Frame of Prototype Los Angeles Wharf

Berths 308-312 of the Port of Los Angeles were used as the prototype for this analysis. The concrete deck is 124.25 ft (37.9 m) long and 2 ft (.61 m) thick (3 ft or .9 m thick for columns F and G) as shown in the figures. Each transverse section is supported vertically by seven rows, A–G, of 24 in. (610 mm) solid octagonal prestressed concrete piles. The 24-in. octagonal piles are reinforced longitudinally with eight #10 welded headed bars which are grouted into metal ducts for the pile connection, and sixteen 0.6 in. (15.2 mm) diameter prestress strands which end at the end of the pile at the bottom of the wharf deck. Transverse reinforcement is W11 spirals with a pitch of 3-in.

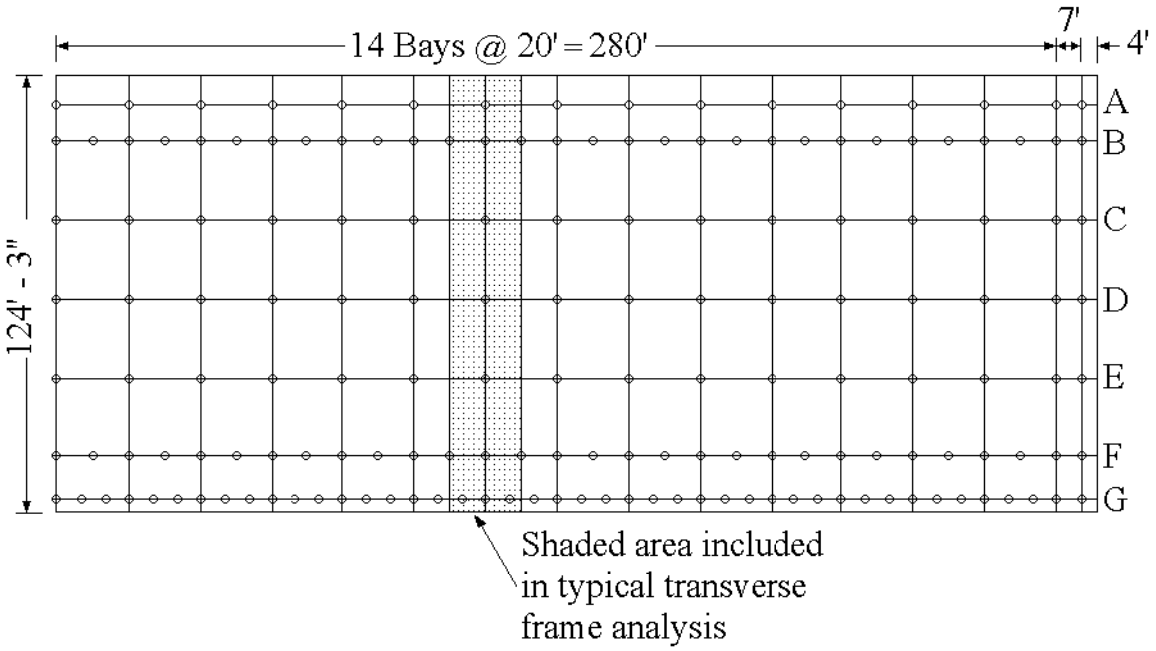

Fig. 6.4 Plan of Prototype Wharf Structure

The piles are driven into the soil until refusal. The boundary condition of the pile at the soil interface is an important variable in the analysis. The basic model placed all piles 8 ft (2.44 m) into the soil with a pinned or fixed support at the base. Other analyses employed p-y curves to model the soil stiffness and pile performance, since these curves employ a load-deflection stiffness of the soil bearing on the pile as a function of pile depth. The results of the p-y curve analyses were compared to the fixed and pinned base pile analyses. The p-y curve analysis would ordinarily be the preferred procedure. However, the stiffness of the soil due to the inclined surface of the embankment is important to the p-y curve analysis, and this stiffness is not known for the prototype structures. The soil stiffnesses used in the p-y curve analysis were measured on another wharf site, but they were not the specific properties for the particular structures analyzed in this study. As a result, limit analyses were performed to bound the solution. That is, fixed base pile analysis would invariably provide smaller displacements and ductility demands than the p-y curve analysis, and pinned base pile analysis would typically be larger than the p-y analysis results. As a result, the basic analysis shown here used a fixed support at this point 8 ft (2.44 m) into the soil, since this provided reasonable evaluation of the structural performance and was a lower-bound estimate of the maximum wharf response and

ductility demands. Other prototype structures from the Port of Oakland and Port of Seattle were analyzed with similar results to those noted here, but these analyses are not discussed here.

The modified bilinear Takeda hysteresis rule was used to represent the inelastic behavior of the piles and pile-wharf connections [Yoo, 2001]. The connection of the vertical piles to the concrete wharf deck was modeled as fully restrained, but rigid end segments were employed between the centerline and the bottom surface of the deck. P-Δ effects were included in the analysis, but the gravity load on the wharf was limited to the self weight of the wharf deck and the pile. The moment of inertia of the piles were based upon the uncracked section, but a slight reduction was made in recognition of the local cracking that was expected near the pile-wharf connection and at the plastic hinge location under the soil. The bi-linear strain hardening ratio was taken as 0.01, and no deterioration in resistance was included in this initial model. The ultimate resistance of the piles and pile-wharf connections, respectively, was computed by normal ACI methods, since the research showed that ultimate resistance was a conservative estimate of the maximum resistance. Experiments showed that the ultimate resistance estimates were quite accurate for pile extension connections, but they were 11% to 15% smaller than the maximum resistance obtained in experiments for precast pile connections. Rayleigh damping proportional to the tangent stiffness matrix was used, and the damping was modeled as 5% of critical for the first mode of vibration.

The prototype structure (and other comparable structures in Oakland and Seattle) was stiff and strong. The fundamental period of the Los Angeles prototype structure was computed to be 0.22 sec, and the lateral resistance of this transverse section based upon elasto-plastic analysis with nominal material properties was 34% of the weight of the structure. However, because of the variable lengths of the piles, this plastic resistance is achieved only after deck deflections of approximately 6 in. (150 mm) were attained. The shortest piles carry the largest lateral load, and these piles sustain large connection rotations by this 6 in. (150 mm) deflection level. Experiments show significant deterioration of resistance by this deformation level, but deterioration was not considered in the initial calculations. The natural period and lateral resistance were computed with the computer model, but they were also computed by hand methods with good comparison, because this provided some verification of the validity of the model.

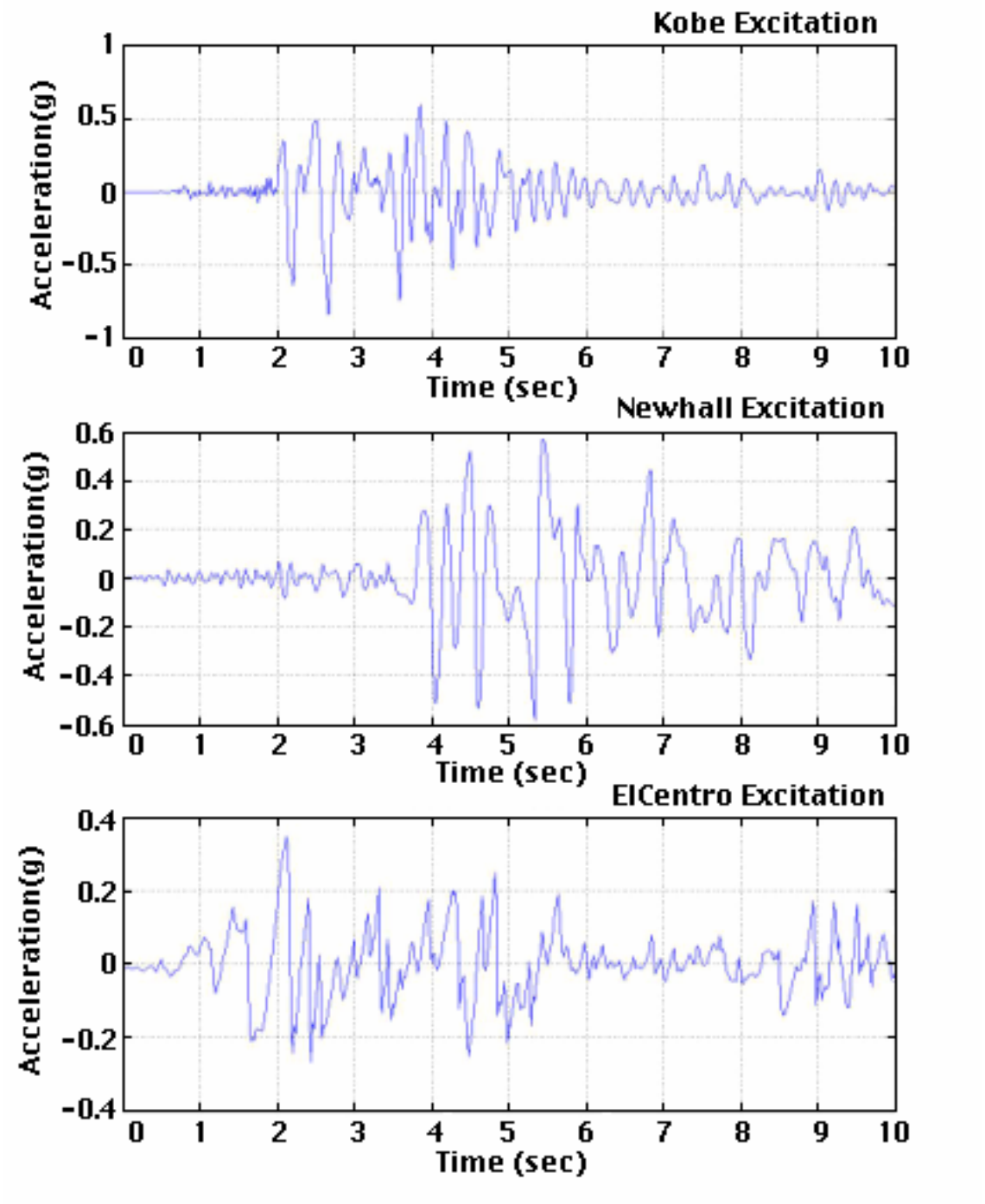

Fig. 6.5 Earthquake Acceleration Records

Elastic and inelastic time-history analyses were completed for several earthquake excitations that appeared to be appropriate seismic risks for the prototype structure. The acceleration records used for the Los Angeles prototype analyses were

- Kobe acceleration record from JMA observation, January 17, 1995,
- Newhall acceleration record from Northridge earthquake, January 17, 1994, and
- El Centro acceleration record from May 18, 1940, earthquake.

These acceleration records all reflect plausible seismic demands on a Los Angeles port facility, but they also reflect a wide range of possible seismic demand levels for that site. These acceleration records are all illustrated in Figure 6.5.

Elastic and inelastic dynamic analyses were performed for each of these acceleration records. Figures 6.6, 6.7, and 6.8 show the elastic dynamic response for the El Centro, Newhall, and Kobe acceleration records, respectively. The maximum displacements for the El Centro acceleration record were quite small because of the relatively small acceleration demands of this record and the relatively strong structure. The maximum deck displacements were 0.32 in. and 0.61 in. for the elastic and inelastic cases, respectively. The maximum rotations of the top of the shortest piles were 0.0038 rad and 0.0059 rad for the elastic and inelastic cases, respectively. The experimental results would suggest that the pile-wharf connection would at most be modestly damaged by this event, since they will sustain only modest inelastic rotation at a few connections.

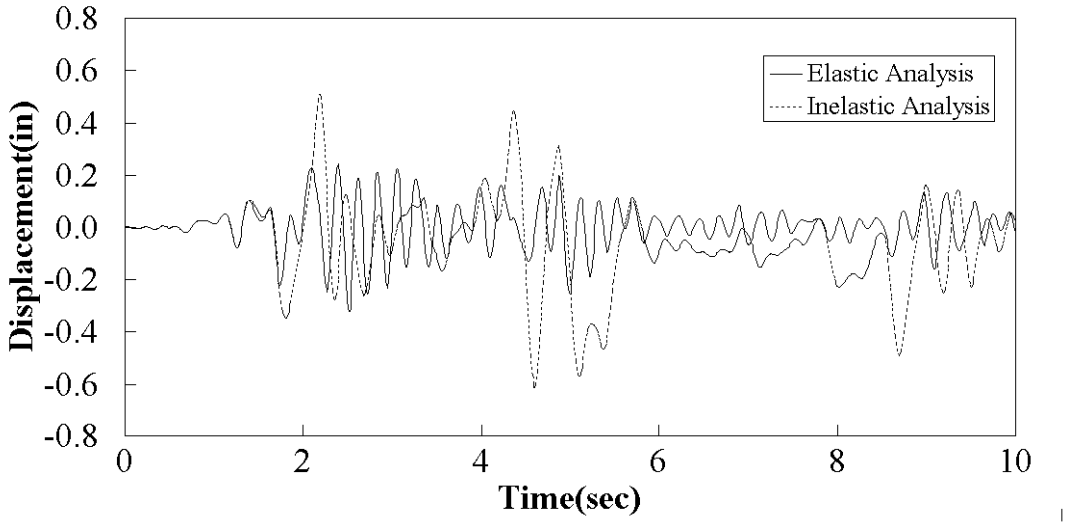

Fig. 6.6 Elastic and Inelastic Response of Prototype Wharf due to 1940 El Centro

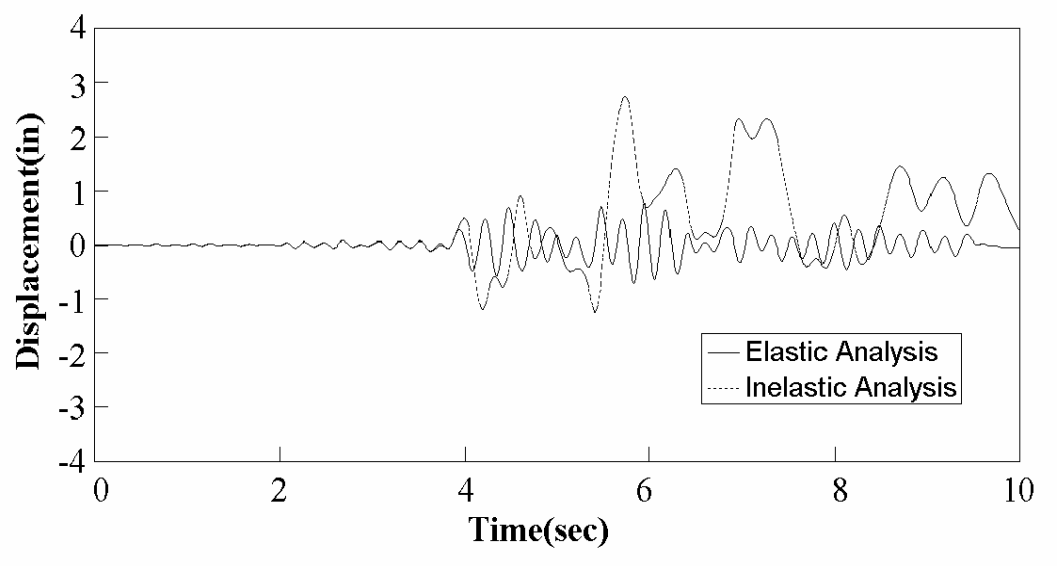

Fig. 6.7 Elastic and Inelastic Response of Prototype Wharf due to 1994 Newhall

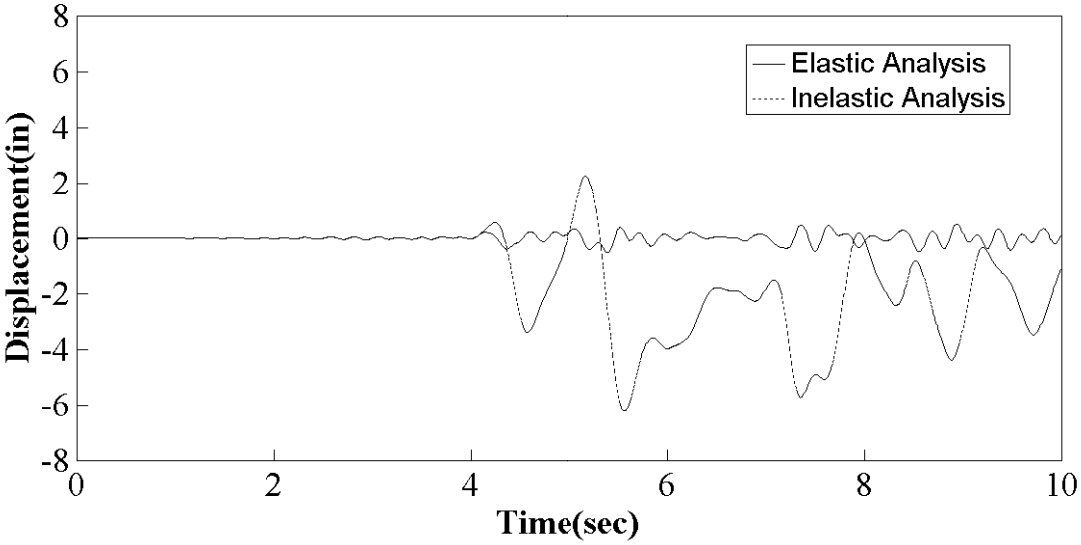

Fig. 6.8. Elastic and Inelastic Response of Prototype Wharf due to 1995 Kobe

The Newhall acceleration record placed significantly greater inelastic demands on the structure. The maximum computed displacement of the wharf deck was 0.79 in. and 2.75 in. for the elastic and inelastic cases, respectively. The maximum rotations of the pile-wharf connection were approximately 0.03 rad with this excitation. Comparison of this deformation level to the experimental results suggests that the connections considered in this study would tolerate this deformation level, but it would sustain significant structural damage. The scaling discussion of Section 6.2 would suggest that this computed rotation is equivalent to a rotation of

approximately 0.045 rad in the experimental program. All specimens tolerated this rotation level, but the precast concrete pile connections sustained significant deterioration of resistance and stiffness by this deformation.

For the Kobe earthquake record, the maximum displacements of the wharf deck were 0.512-in. and 6.22-in. for the elastic and inelastic cases, respectively. This is a large difference between the peak elastic and inelastic response. Several analyses were completed with scaled versions of the Kobe earthquake excitation record to examine the validity of this difference. These analysis scaled the peak acceleration to 25%, 50%, 75%, and 100% of the recorded value. The analysis showed that this acceleration record caused significant yielding of the structure even at the small acceleration levels. At these smaller acceleration levels, the maximum elastic and inelastic response was similar, but the difference became much larger as the amplitude of the acceleration increased. This is consistent with general observation that the inelastic response of short period structures with low yield resistance have increasing difference between elastic and inelastic displacements as the strength decreases. The maximum connection rotations would be in the order of 0.06 rad. When scaling considerations of Section 6.2 are applied to this connection rotation, the state of the prototype connection should be equivalent to that noted at 0.09 rad in the test specimens. The experiments show that this deformation may be attainable, but that severe damage to the pile-wharf connection must be expected. The resistance would have deteriorated significantly, and impact of this deterioration on the computed demands was not considered in the prior analysis.

6.4 EVALUATION OF EFFECT OF CONNECTION DETERIORATION ON SEISMIC DEMANDS

The computer model was revised to better simulate the deterioration in resistance at large inelastic deformations. The basic properties of the model were retained as described earlier, but deterioration in resistance was input to better simulate the performance of the wharf at large deformations. The degree of deterioration in the model was empirically chosen to fit the experimental results of Specimen 4 in the test program. The resulting fit of this deteriorating model is illustrated in Figure 6.9. In this figure, the moment-rotation behavior of Specimen 4 is shown, and the envelope of maximum resistance as used in the computer model is shown as a heavy shade line. It can be seen that this model is a relatively good representation of the measured performance. This model was then used to recompute the prototype wharf response.

Calculations were made as both pushover analyses to examine the effect on the computed resistance and deformability of the structure as well as inelastic time-history analysis.

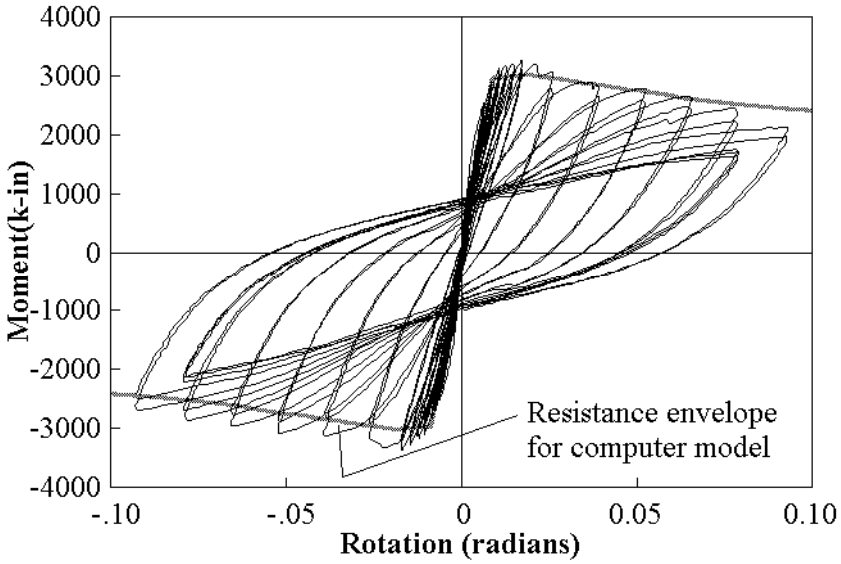

Fig. 6.9 Comparison of Connection Deterioration Model with Specimen 4 Test Results

Figure 6.10 shows a comparison of the pushover resistance of the Los Angeles prototype wharf with elastic–perfectly plastic analysis, with the computer model employing strain hardening without deterioration in resistance, and with the computer model including deterioration of resistance. As noted earlier, the elastic–perfectly plastic resistance of the structure based upon the nominal material properties of the structure is approximately 460 kips or 34% of the deadweight of the structure. However, as shown in the figure, this resistance is developed only at very large deflections. This occurs because the long piles develop their full plastic resistance only after large lateral deflections. These long piles contribute very little to initial resistance, but they provide a very positive post-yield stiffness even when the elastic–perfectly plastic model is employed. When strain hardening is employed, the resistance at large deformations and the post-yield stiffness increase dramatically as shown in the figure. When deterioration in resistance is included in the pushover analysis, the maximum resistance of the wharf section is only about 400 kips (1780 kN) or 24% of the deadweight of the structure. The reduction in calculated resistance is very significant and may have an adverse effect on the inelastic time-history analytical results.

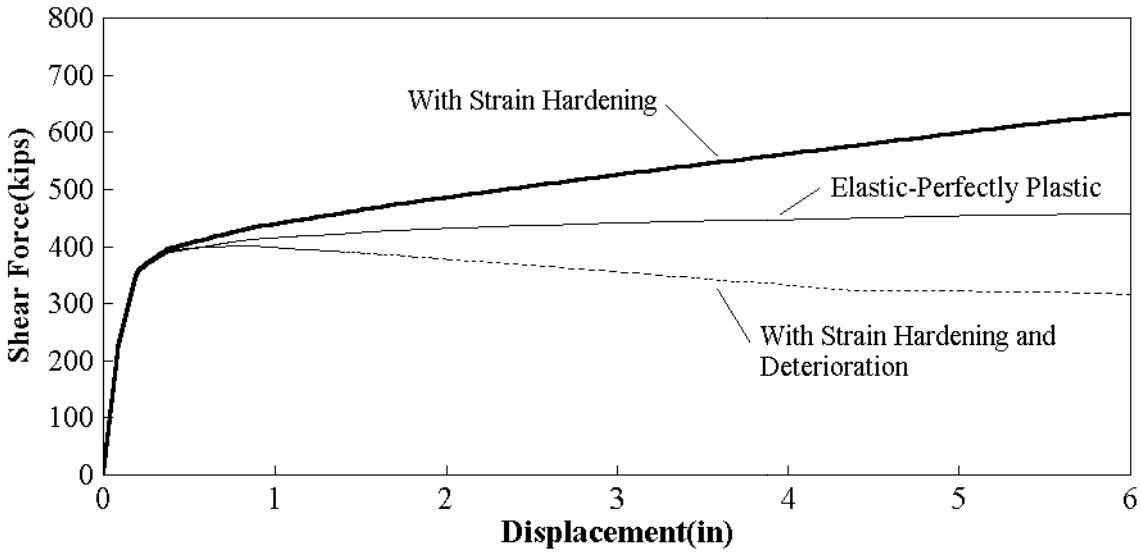

Fig. 6.10 Comparison of Pushover Resistance

The inelastic time-history response of the prototype structure was evaluated for Newhall and Kobe acceleration records. The 1940 El Centro record was not included because this record did not cause large inelastic deformations, and is therefore unlikely to produce dramatically different results when deterioration of resistance is considered. Figure 6.9 shows that the correlation between experimental and analytical result is generally good, and Figures. 6.11 and 6.12 show that displacements were about 40% larger than obtained in early analysis because of strength degradation. This is a significant increase because connection rotations are near the maximum tolerated in the connection experiments at these deformation levels. Severe damage to the connection would be noted with both of these acceleration levels. These analyses suggest connection rotations in excess of 0.08 rad for the shortest piles. When scaling considerations are added to the reasoning, the performance of the prototype structure must be expected to be equivalent to the test specimens after a .12 rad rotation after the Kobe acceleration record. The condition of the prototype structure is uncertain after this deformation level. The structure would probably be irreparable and clearly unserviceable after these events.

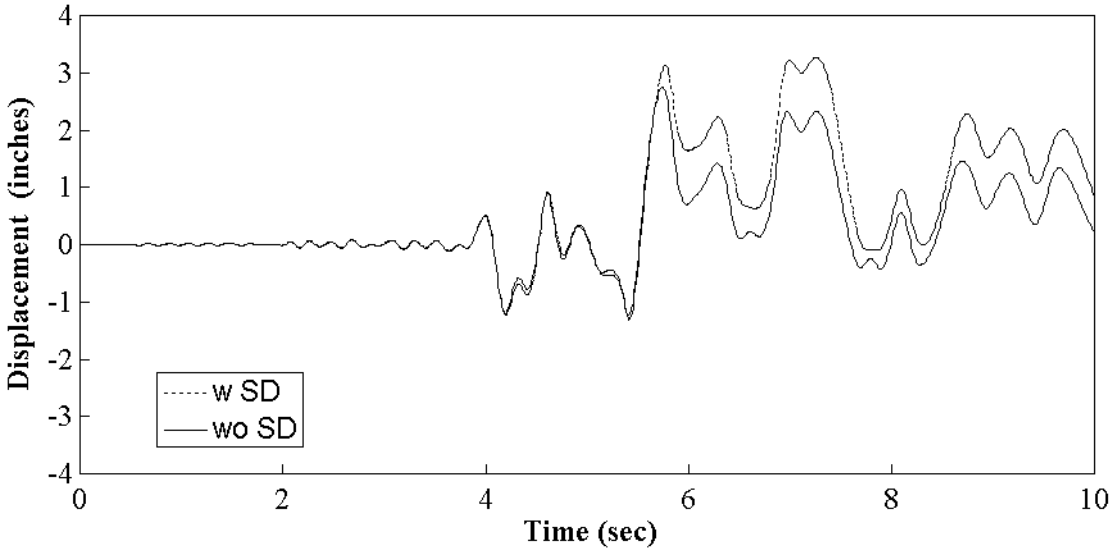

Fig. 6.11 Effect of Deterioration on Inelastic Response with Newhall Acceleration Record

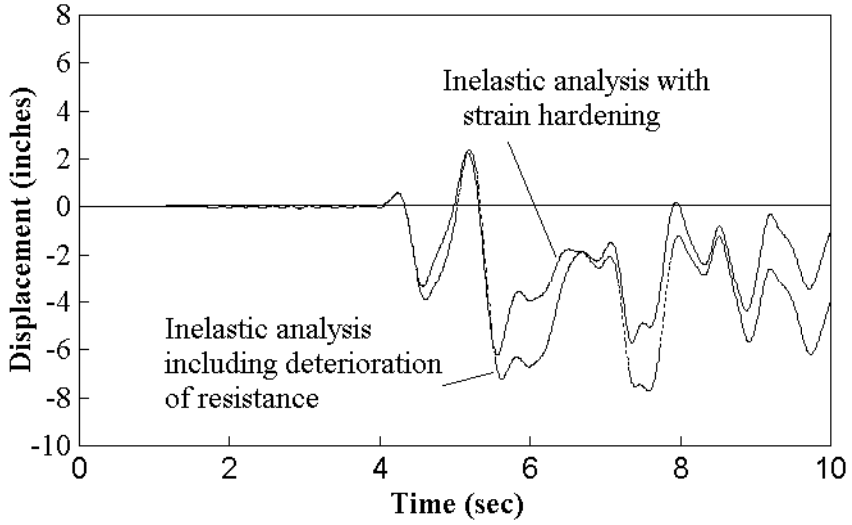

Fig. 6.12 Effect of Deterioration on Inelastic Response with Kobe Acceleration Record

7 Summary and Conclusions

7.1 SUMMARY

This research has examined the seismic performance of precast concrete pile-wharf connections. These connections are all moment-resisting connections with the general wharf geometry as illustrated in Figure 1.1. A review of existing literature was completed. The range of engineering practice was examined, and a wide range of pile-wharf connections was noted. The ramifications of this variation in design were discussed with practicing engineers, and recent designs were evaluated and compared. An experimental program was designed to evaluate the seismic performance of these connections, and consider possible improvements to the connections. Eight specimens were tested. The specimens were approximately 69% scale of the prototype structures, and they were fabricated by methods similar to those used in field construction. The tests included connections with reinforced concrete pile extensions as required when the pile is driven to a level below the bottom surface of the wharf deck and precast concrete pile connections as used for other applications. These later connections all employed dowel bars bonded into ducts in the prestressed piles. A wide range of reinforcement details and connection configurations were evaluated including outward bent dowel bar connections, inward bent dowel bar connections, bond bar connections, and T-headed bar connections. The tests evaluated the continuation of spiral reinforcing into the deck section, and they examined the effect of axial load on the pile and decreased confining steel in the deck section on the connection performance. The bent dowel bar connections simulate historic connection details, whereas the T-headed dowel and bond bar connections are recent innovations designed to improve the economy of wharf construction.

Upon completion of the testing, the experimental results were evaluated and analyzed. The experimental results were then correlated to the performance of prototype wharf structures. This was done through elastic and inelastic analysis of the wharf structures and their connections. Different modeling assumptions were employed to examine their effect on the

performance of the system. Finally, the computed results were compared to the experimental results to make predictions of the expected performance at different earthquake excitation levels.

7.2 CONCLUSIONS

A number of major conclusions were drawn from this research, and some of the more important observations are

1. The performance noted with precast concrete pile connections and reinforced concrete extended pile connections was fundamentally different. The extended pile connections developed most of their inelastic deformation as flexural yielding of the pile, and they had full hysteresis curves with little deterioration of resistance. The precast pile connections were inherently stronger than the extended pile connections, but they had greater deterioration of resistance and relatively pinched hysteretic behavior.
2. The axial load used in these tests simulated the deadweight of wharf only, and the piles were loaded to only about 10% of their ultimate capacity. The addition of axial load to the pile resulted in increased maximum resistance of the connection but much more severe and more rapid deterioration of resistance of the connection.
3. While significant deterioration in resistance was noted in these connection tests, all test specimens were able to tolerate large inelastic deformations while maintaining the basic integrity and compressive load capacity of the connection.
4. The various connection details exhibited significant differences in behavior. Precast pile connections yielded and dissipated energy primarily through yielding of the reinforcement and debonding of the reinforcement in the deck section. The extended pile connections yielded primarily within the pile section. The extended pile connections, therefore, had better distribution of plastic deformation and smaller maximum local strains than the precast pile connections.
5. Additional confinement of the reinforcement dowels into the deck section influenced the connection performance somewhat. It primarily influenced cracking patterns of the concrete and the distribution of inelastic deformation in the connection. However, it did not have a visible impact on the overall performance or ductility of the connection.

6. The bond bar connection and T-headed bar connection were developed to permit more economical wharf construction. In general, these connections provided comparable performance to other connection types.

7. Computer analyses of prototype wharf structures from Oakland, Los Angeles, and Seattle showed that these structures are relatively stiff and strong. The shortest piles develop the largest amount of lateral strength and stiffness for these prototype structures. Elastic–perfectly plastic hinge analysis of the Los Angeles prototype structure indicated that its ultimate lateral load capacity of the structure was approximately 34% of the deadweight of the structure if no deterioration in connection resistance is noted. The maximum resistance will only be approximately 24% of the deadweight of the structure if deterioration of resistance is considered.

8. Inelastic time-history analyses were performed, and very little inelastic deformation can be expected with many smaller seismic acceleration records because of the strength and stiffness of the structural system. However, more demanding acceleration records such the Newhall acceleration record from the 1994 Northridge earthquake or near fault acceleration records from the 1995 Kobe earthquake place large inelastic demands upon the connections. Because of the very short length of the piles, the connection demands are often very large even though the wharf movements are relatively small.

9. The limitations of the experimental results were evaluated. Decreased pile length and increased pile diameter decrease the expected connection ductility. Since the test specimens were 69% scale models of the 24 in. (610 mm) prototype pile, the expected ductility in the prototype structure should be only about 70% of that achieved in the experiments. Prototype structures with very short pile flexural lengths will have further reductions in connection ductility.

10. The deterioration found in the experimental study due to precast piles and axial compression loading of the piles was considered in the analytical results. When this deterioration is included the apparent lateral resistance of the wharf is reduced significantly. This occurs because the short piles have significant deterioration before longer piles develop their full lateral resistance. Pushover analysis indicated that the Los Angeles prototype structure will lose between 20% and 25% of its maximum resistance when this deterioration is considered. The inelastic time-history analysis also considered

this deterioration, and the results showed that the deterioration resulted in significant increases in inelastic response and ductility demand.

7.3 RECOMMENDATIONS FOR FURTHER STUDY

There have not been many studies of the seismic performance of pile-wharf connections, and this study cannot be regarded as definitive on many issues. In particular, several gaps in existing knowledge are apparent after examining these research results. These include

1. The deterioration with precast concrete pile connections subjected to axial load was significant. However, the axial load was relatively small, since it attempted to simulate only the axial load due to the deadweight of the wharf. Wharfs are commonly heavily loaded, and increased gravity load will likely increase the deterioration noted with these connections. Further, the increased mass associated with the added wharf loading will likely increase the seismic demands on the connections. The effect of this increased axial load requires further investigation.

2. Many engineers believe that steel batter piles are a better choice for seismic design of wharfs. These batter pile connections will be quite different than the precast pile connections studied here, but they were explicitly excluded from this study. Steel batter piles may economically provide much greater lateral stiffness and resistance than the moment-connection precast concrete piles studied here. Further, steel piles may provide greater ductility with less deterioration in the resistance because the yielding can be forced into the pile rather than into the deck section. This may be a very economical and practical way of improving the seismic performance of these structures and warrants further investigation.

3. The study shows that increased pile diameter and reduced pile length decrease the ductility and deformation capacity that should be expected from pile-wharf connections. Shorter lengths are clearly possible. Further, the test specimens were scale models of the prototype connections, and so larger diameters will also occur. Shorter pile lengths and increased diameter will increase the cost and complexity of these connection experiments. However, tests on shorter piles and larger pile diameters are needed to quantify these effects.

References

AASHTO. 1996. "Standard Specifications for Highway Bridges." 16th ed. American Association of Highway and Transportation Officials.

ACI Committee 318. 1995. "Building Code Requirements for Structural Concrete (ACI 318-95) and Commentary (ACI 318R-95)." American Concrete Institute, Farmington Hills, Mich.

Birdy, Jal N. and Lawrence L. Dodd. 1999. "Design of Wharves for Seismic Regions." *Concrete International*. Dec.: 28-32.

Carr, A. 1996. "RUAUMOKO: The Maori God of Volcanoes and Earthquakes, " Dept. of Civil Engineering, University of Canterbury, New Zealand.

EERI. 1990. "Lifelines," *Earthquake Spectra*, Supplement to Volume 6, Earthquake Engineering Research Institute, Oakland, CA, pg 290.

EQE International. 1995. "The January 17, 1995 Kobe Earthquake: An EQE Summary Report."

Graff, Robert. 2001. "Seismic Evaluation of Prestressed Pile-Wharf Connections." Thesis submitted in partial fulfillment of the Master of Science in Civil Engineering, University of Washington, Seattle, WA.

Landers, P. 2001. "Kobe Disaster Offers Clues on Rebuilding. " *Wall Street Journal*, October 9, 2001, New York, NY, pg A19.

Mander, J.B., M. J. N. Priestley, and R. Park. 1988. "Theoretical Stress-Strain Model for Confined Concrete." *Journal of Structural Engineering* 8: 1804-1826.

MIL-HDBK-1025/1. 1987. "Piers and Wharves". Naval Facilities Engineering Command. Department of the Navy.

Pam, Hoat Joen and Robert Park. 1990. "Simulated Seismic Load Tests on Prestressed Concrete Piles and Pile-Pile Cap Connections." *PCI Journal*. Nov-Dec: 42-61.

Pizzano, Barbara A. 1984. "Behavior of Prestressed Concrete Piles Under Seismic Loading". Thesis submitted in partial fulfillment of the Master of Science in Civil Engineering, University of Washington, Seattle, WA.

Roth, W. H., H. Fong, and C. de Rubertis. 1992. "Batter Piles and the Seismic Performance of Pile-Supported Wharves." *Proceedings of Ports '92*. ASCE 1992: 336-349.

Sritharan, Sri and M.J. Nigel Priestley. 1998. "Seismic Testing of a Full-Scale Pile-Deck Connection Utilizing Headed Reinforcement." Report. University of California, San Diego.

Soderstrom, J. 2001. "Seismic Evaluation of Prestressed and Reinforced Concrete Pile-Wharf Deck Connections." Thesis submitted in partial fulfillment of the Master of Science in Civil Engineering, University of Washington, Seattle, WA.

"Uniform Building Code (UBC)." 1997. International Conference of Building Officials.

Xiao, Y., J.B. Mander, H. Wu, and G. Martin. 1999. "Experimental Study on Seismic Behavior of Bridge Pile-to-Pile Cap Connections," Department of Civil Engineering, University of Southern California, Los Angeles.

Yoo, J.H. 2001. "Dynamic Analysis of Pile-to-Wharf Connections." Thesis submitted in partial fulfillment of the Master of Science in Civil Engineering, University of Washington, Seattle, WA.

PEER REPORTS

PEER reports are available from the National Information Service for Earthquake Engineering (NISEE). To order PEER reports, please contact the Pacific Earthquake Engineering Research Center, 1301 South 46th Street, Richmond, California 94804-4698. Tel.: (510) 231-9468; Fax: (510) 231-9461.

PEER 2002/07 *Seismic Performance of Pile-Wharf Connections.* Charles W. Roeder, Robert Graff, Jennifer Soderstrom, and Jun Han Yoo. December 2001.

PEER 2002/06 *The Use of Benefit-Cost Analysis for Evaluation of Performance-Based Earthquake Engineering Decisions*. Richard O. Zerbe and Anthony Falit-Baiamonte. September 2001.

PEER 2002/05 *Guidelines, Specifications, and Seismic Performance Characterization of Nonstructural Building Components and Equipment*. André Filiatrault, Constantin Christopoulos, and Christopher Stearns. September 2001.

PEER 2002/01 *Nonstructural Loss Estimation: The UC Berkeley Case Study. Mary C. Comerio and John C. Stallmeyer.* December 2001.

PEER 2001/16 *Statistics of SDF-System Estimate of Roof Displacement for Pushover Analysis of Buildings.* Anil K. Chopra, Rakesh K. Goel, and Chatpan Chintanapakdee. December 2001.

PEER 2001/15 *Damage to Bridges during the 2001 Nisqually Earthquake.* R. Tyler Ranf, Marc O. Eberhard, and Michael P. Berry. November 2001.

PEER 2001/14 *Rocking Response of Equipment Anchored to a Base Foundation.* Nicos Makris and Cameron J. Black. September 2001

PEER 2001/13 *Modeling Soil Liquefaction Hazards for Performance-Based Earthquake Engineering.* Steven L. Kramer and Ahmed-W. Elgamal. February 2001.

PEER 2001/12 *Development of Geotechnical Capabilities in OpenSees.* Boris Jeremic. September 2001.

PEER 2001/11 *Analytical and Experimental Study of Fiber-Reinforced Elastomeric Isolators*. James M. Kelly and Shakhzod M. Takhirov. September 2001.

PEER 2001/10 *Amplification Factors for Spectral Acceleration in Active Regions.* Jonathan P. Stewart, Andrew H. Liu, Yoojoong Choi, and Mehmet B. Baturay. December 2001.

PEER 2001/09 *Ground Motion Evaluation Procedures for Performance-Based Design.* Jonathan P. Stewart, Shyh-Jeng Chiou, Jonathan D. Bray, Robert W. Graves, Paul G. Somerville, and Norman A. Abrahamson. September 2001.

PEER 2001/08 *Experimental and Computational Evaluation of Reinforced Concrete Bridge Beam-Column Connections for Seismic Performance*. Clay J. Naito, Jack P. Moehle, and Khalid M. Mosalam. November 2001.

PEER 2001/07 *The Rocking Spectrum and the Shortcomings of Design Guidelines.* Nicos Makris and Dimitrios Konstantinidis. August 2001.

PEER 2001/06 *Development of an Electrical Substation Equipment Performance Database for Evaluation of Equipment Fragilities*. Thalia Agnanos. April 1999.

PEER 2001/05 *Stiffness Analysis of Fiber-Reinforced Elastomeric Isolators.* Hsiang-Chuan Tsai and James M. Kelly. May 2001.

PEER 2001/04 *Organizational and Societal Considerations for Performance-Based Earthquake Engineering.* Peter J. May. April 2001.

PEER 2001/03 *A Modal Pushover Analysis Procedure to Estimate Seismic Demands for Buildings: Theory and Preliminary Evaluation.* Anil K. Chopra and Rakesh K. Goel. January 2001.

PEER 2001/02 *Seismic Response Analysis of Highway Overcrossings Including Soil-Structure Interaction.* Jian Zhang and Nicos Makris. March 2001.

PEER 2001/01 *Experimental Study of Large Seismic Steel Beam-to-Column Connections.* Egor P. Popov and Shakhzod M. Takhirov. November 2000.

PEER 2000/10 *The Second U.S.-Japan Workshop on Performance-Based Earthquake Engineering Methodology for Reinforced Concrete Building Structures.* March 2000.

PEER 2000/09 *Structural Engineering Reconnaissance of the August 17, 1999 Earthquake: Kocaeli (Izmit), Turkey.* Halil Sezen, Kenneth J. Elwood, Andrew S. Whittaker, Khalid Mosalam, John J. Wallace, and John F. Stanton. December 2000.

PEER 2000/08 *Behavior of Reinforced Concrete Bridge Columns Having Varying Aspect Ratios and Varying Lengths of Confinement.* Anthony J. Calderone, Dawn E. Lehman, and Jack P. Moehle. January 2001.

PEER 2000/07 *Cover-Plate and Flange-Plate Reinforced Steel Moment-Resisting Connections.* Taejin Kim, Andrew S. Whittaker, Amir S. Gilani, Vitelmo V. Bertero, and Shakhzod M. Takhirov. September 2000.

PEER 2000/06 *Seismic Evaluation and Analysis of 230-kV Disconnect Switches.* Amir S. J. Gilani, Andrew S. Whittaker, Gregory L. Fenves, Chun-Hao Chen, Henry Ho, and Eric Fujisaki. July 2000.

PEER 2000/05 *Performance-Based Evaluation of Exterior Reinforced Concrete Building Joints for Seismic Excitation.* Chandra Clyde, Chris P. Pantelides, and Lawrence D. Reaveley. July 2000.

PEER 2000/04 *An Evaluation of Seismic Energy Demand: An Attenuation Approach.* Chung-Che Chou and Chia-Ming Uang. July 1999.

PEER 2000/03 *Framing Earthquake Retrofitting Decisions: The Case of Hillside Homes in Los Angeles.* Detlof von Winterfeldt, Nels Roselund, and Alicia Kitsuse. March 2000.

PEER 2000/02 *U.S.-Japan Workshop on the Effects of Near-Field Earthquake Shaking.* Andrew Whittaker, ed. July 2000.

PEER 2000/01 *Further Studies on Seismic Interaction in Interconnected Electrical Substation Equipment.* Armen Der Kiureghian, Kee-Jeung Hong, and Jerome L. Sackman. November 1999.

PEER 1999/14 *Seismic Evaluation and Retrofit of 230-kV Porcelain Transformer Bushings*. Amir S. Gilani, Andrew S. Whittaker, Gregory L. Fenves, and Eric Fujisaki. December 1999.

PEER 1999/13 *Building Vulnerability Studies: Modeling and Evaluation of Tilt-up and Steel Reinforced Concrete Buildings.* John W. Wallace, Jonathan P. Stewart, and Andrew S. Whittaker, editors. December 1999.

PEER 1999/12 *Rehabilitation of Nonductile RC Frame Building Using Encasement Plates and Energy-Dissipating Devices.* Mehrdad Sasani, Vitelmo V. Bertero, James C. Anderson. December 1999.

PEER 1999/11 *Performance Evaluation Database for Concrete Bridge Components and Systems under Simulated Seismic Loads.* Yael D. Hose and Frieder Seible. November 1999.

PEER 1999/10 *U.S.-Japan Workshop on Performance-Based Earthquake Engineering Methodology for Reinforced Concrete Building Structures.* December 1999.

PEER 1999/09 *Performance Improvement of Long Period Building Structures Subjected to Severe Pulse-Type Ground Motions*. James C. Anderson, Vitelmo V. Bertero, and Raul Bertero. October 1999.

PEER 1999/08 *Envelopes for Seismic Response Vectors.* Charles Menun and Armen Der Kiureghian. July 1999.

PEER 1999/07 *Documentation of Strengths and Weaknesses of Current Computer Analysis Methods for Seismic Performance of Reinforced Concrete Members.* William F. Cofer. November 1999.

PEER 1999/06 *Rocking Response and Overturning of Anchored Equipment under Seismic Excitations.* Nicos Makris and Jian Zhang. November 1999.

PEER 1999/05 *Seismic Evaluation of 550 kV Porcelain Transformer Bushings.* Amir S. Gilani, Andrew S. Whittaker, Gregory L. Fenves, and Eric Fujisaki. October 1999.

PEER 1999/04 *Adoption and Enforcement of Earthquake Risk-Reduction Measures.* Peter J. May, Raymond J. Burby, T. Jens Feeley, and Robert Wood.

PEER 1999/03 *Task 3 Characterization of Site Response General Site Categories*. Adrian Rodriguez-Marek, Jonathan D. Bray, and Norman Abrahamson. February 1999.

PEER 1999/02 *Capacity-Demand-Diagram Methods for Estimating Seismic Deformation of Inelastic Structures: SDF Systems*. Anil K. Chopra and Rakesh Goel. April 1999.

PEER 1999/01 *Interaction in Interconnected Electrical Substation Equipment Subjected to Earthquake Ground Motions.* Armen Der Kiureghian, Jerome L. Sackman, and Kee-Jeung Hong. February 1999.

PEER 1998/08 *Behavior and Failure Analysis of a Multiple-Frame Highway Bridge in the 1994 Northridge Earthquake.* Gregory L. Fenves and Michael Ellery. December 1998.

PEER 1998/07 *Empirical Evaluation of Inertial Soil-Structure Interaction Effects.* Jonathan P. Stewart, Raymond B. Seed, and Gregory L. Fenves. November 1998.

PEER 1998/06 *Effect of Damping Mechanisms on the Response of Seismic Isolated Structures.* Nicos Makris and Shih-Po Chang. November 1998.

PEER 1998/05 *Rocking Response and Overturning of Equipment under Horizontal Pulse-Type Motions.* Nicos Makris and Yiannis Roussos. October 1998.

PEER 1998/04 *Pacific Earthquake Engineering Research Invitational Workshop Proceedings, May 14–15, 1998: Defining the Links between Planning, Policy Analysis, Economics and Earthquake Engineering.* Mary Comerio and Peter Gordon. September 1998.

PEER 1998/03 *Repair/Upgrade Procedures for Welded Beam to Column Connections.* James C. Anderson and Xiaojing Duan. May 1998.

PEER 1998/02 *Seismic Evaluation of 196 kV Porcelain Transformer Bushings.* Amir S. Gilani, Juan W. Chavez, Gregory L. Fenves, and Andrew S. Whittaker. May 1998.

PEER 1998/01 *Seismic Performance of Well-Confined Concrete Bridge Columns.* Dawn E. Lehman and Jack P. Moehle. December 2000.